

A15 15393

N72-30854

**CASE FILE  
COPY**



Applied Dynamics Research Corporation

Final Report

Design, Develop, Fabricate, Assemble And  
Checkout An Advanced Active Damper  
System

Contract Nas8-26593 31 March 1972

Prepared By: C. S. Chang  
C. S. Chang



## FOREWORD

This final technical report is prepared by Applied Dynamics Research Corporation in partial fulfillment of MSFC Contract NAS8-26593, "Design, Develop, Fabricate, Assemble and Checkout an Advanced Active Damper System." The period of performance of this contract was from November 18, 1970 to March 31, 1972.

The program was conducted under the technical direction of S&E-AERO-AUU, Messrs. J. W. Poe and R. G. Beranek.

## SUMMARY

An active electromagnetic damper system was developed for and used in a 5.5% aeroelastic model of Saturn IB/SA206 launch configuration in wind tunnel tests to determine ground-wind-induced loads. Included in this report are detailed descriptions of the damper development program--approach, design analyses, fabrication, checkout, system calibration, wind tunnel test results, damper assembly and operating instructions, and trouble-shooting procedures. Conclusions and recommendations to improve the damper system for future applications are also presented.

Two complete sets of final design drawings, one of which is reproducible, have been forwarded to S&E-AERO-AUU separately and are not included in this report.

## CONTENTS

	PAGE
FOREWORD	i
SUMMARY	ii
Section 1 INTRODUCTION	1
Section 2 DAMPER PERFORMANCE REQUIREMENTS	5
2.1 Basic Requirements	5
2.2 Derived Requirements	5
2.3 Other Considerations	11
Section 3 SHAKER DESIGN	13
3.1 Approach	13
3.2 Field Magnet Design	19
3.2.1 Material Selection	19
3.2.2 Analyses	20
3.3 Force Coil Design Analyses	23
3.4 Shaker Construction Details	25
3.5 Summary of Shaker Data	30
3.6 Shaker Assembly Procedures	32
3.6.1 Main Components	32
3.6.2 Assembly Procedure	32
Section 4 POWER AMPLIFIERS	37
4.1 Requirements	37
4.2 UD TA100A Specifications	38
4.3 Power Amplifier Wiring	41
4.4 Current Pumping	42
4.5 Trouble-Shooting Procedure	43
Section 5 DAMPER CONTROLS	47
5.1 Accelerometers	47
5.2 Signal Conditioner - Preamplifier	50
5.3 AC Integrator	52
5.4 Damping Coefficient Controls	52
5.5 Field Supply	55
5.6 System Block Diagram	55
Section 6 VIBRATION TEST SYSTEM	57
6.1 Signal Source	57
6.2 AC-To-DC Converter	58
6.3 Digital Multimeter	61
6.4 Oscilloscope	61
6.5 Electronic Counter - Timer	61
6.6 System Block Diagram	61

## CONTENTS (Continued)

	PAGE
Section 7	OPERATING PROCEDURES 63
7.1	Warm-Up and Offset Adjustments 63
7.2	Set Up For Model and Damper Calibrations 65
Section 8	DAMPER CALIBRATION 66
8.1	Model Configurations 66
8.2	Calibration Methods 67
8.3	Data Reduction Methods 69
8.4	Damper Calibration Results 70
Section 9	WIND TUNNEL TEST PROGRAM 81
9.1	Program Description 81
9.2	AAD Calibration 82
9.3	Miscellaneous Notes 83
Section 10	CONCLUSIONS 90
Section 11	RECOMMENDATIONS 92
11.1	Force Generator Design 92
11.2	Control Principle 92
11.3	Control System Hardware 93
11.4	Full-Power Checkout 94
11.5	Model and Damper Calibrations 94
REFERENCES	97
APPENDIX A	98

## LIST OF ILLUSTRATIONS

FIGURE		PAGE
1	Overall AAD System Block Diagram	3
2	Shaker Design Approaches to Obtain Constant Current-to-Force Conversion	14
3	AAD Shaker Approach	16
4	Schematics of AAD Shaker	18
5	Magnetization Curve for No. 5 SS Relay Steel	21
6	Force Coil Configuration	24
7	Determination of Optimum Field Current	27
8	Field Coil Assembly (Upper Figure)	29
9	Force Coil Assemblies - Top and Bottom Views	31
10	Damper Support Assembly with Force Coils Attached (Bottom Figure)	31
11	Damper Support Assembly	33
12	Damper Support Assembly (Side View)	34
13	Damper Assembly Without Field Coils	34
14	Force Generator Assembly on Assembly Stand	36
15	Power Amplifier	39
16	208v, 3-Phase Power Wiring Diagram	42
17	Current Pump Schematics	44
18	Damper Controls System Block Diagram (One of two Channels)	48
19	Damper Control Panel	49
20	Measured Integrator Frequency Response Curve	53
21	Integrator-Damping Coefficient Control (DCC) Stages	54
22	Damper Mode System Block Diagram	56
23	AC-to-DC Converter with Filter Input Stage	59
24	Measured Frequency Response Curve for Filter-Converter	60

## LIST OF ILLUSTRATIONS CONTINUED

FIGURE		PAGE
25	Vibration Test Mode System Block Diagram	62
26	DCC Dial Calibration for Model Configuration 1	71
27	DCC Dial Calibration for Model Configuration 2	72
28	DCC Dial Calibration for Model Configuration 3	73
29	DCC Dial Calibration for Model Configuration 4	74
30	DCC Dial Calibration for Model Configuration 5	75
31	DCC Dial Calibration for Model Configuration 6	76
32	DCC Dial Calibration for Model Configuration 7	77
33	DCC Dial Calibration for Model Configuration 8	78
34	Analog Damping Measuring Approach	96

## Section 1

### INTRODUCTION

Aeroelastically scaled models have been used in the past in wind tunnel experiments to determine the expected ground wind loads (GWL) for launch vehicles in the on-pad (prelaunch) configuration. One of the critical dynamic characteristics of an aeroelastic model is damping. To obtain high quality test results, model damping must be adjustable and accurately known for each model test configuration. When the wind tunnel test is conducted in a pure freon atmosphere, as in all GWL tests for Saturn launch vehicles, an additional requirement is that damping should be adjustable by remote control so that frequent tunnel entry shall not be required and wind tunnel occupancy time can be minimized.

An electromagnetic damper system using velocity feedback and active force generation has been successfully employed in the past in 3% Saturn V/Apollo and Saturn V/Dry Workshop tests.

According to Skylab Program plans, the Saturn IB vehicle (SA206) will be launched from on top of a special tower structure from Launch Complex 39. Consequently a wind tunnel test series of a 5.5% aeroelastic model of SA206/LC-39 was required. The geometrical and dynamical properties of this model were significantly different from the 3% Saturn V models; and it was not practical to modify the old damper system for the new application. A new system using basically the same operating principles but with a different geometry and extended capabilities was, therefore, required.

The basic principle of the active damper is fairly simple: the model response velocity vector is measured by two mutually perpendicular sensors. The outputs of these transducers drive two electromagnetic force generators which are oriented in the same directions as the corresponding sensors. The resultant force vector will coincide with the instantaneous velocity of the model, the magnitude of this force is proportional to the velocity, and the phase angle between the applied force and the velocity will be  $180^\circ$ . The result is the addition of linear viscous damping to the model. The damping coefficient is adjusted by adjusting the velocity signal-to-force gain. The two-channel damper system is outlined in block diagram form in Figure 1.

The electromagnetic damper system contains two major sub-systems: (1) a pair of electromagnetic force generators and (2) an instrumentation and electrical power sub-system that controls the shakers. The scope of the present work included the development of both sub-systems.

A new electromagnetic force generator design was developed specifically to achieve the goals. Two such force generators (shakers) were required in the damper system to provide equal damping in all azimuths. A two-channel damper control and calibration sub-system was also developed for self-contained operation and checkout of the entire Advanced Active Damper (AAD) system.

Initial system setup, functional checkout and calibration in conjunction with the SA206 model took place during the period



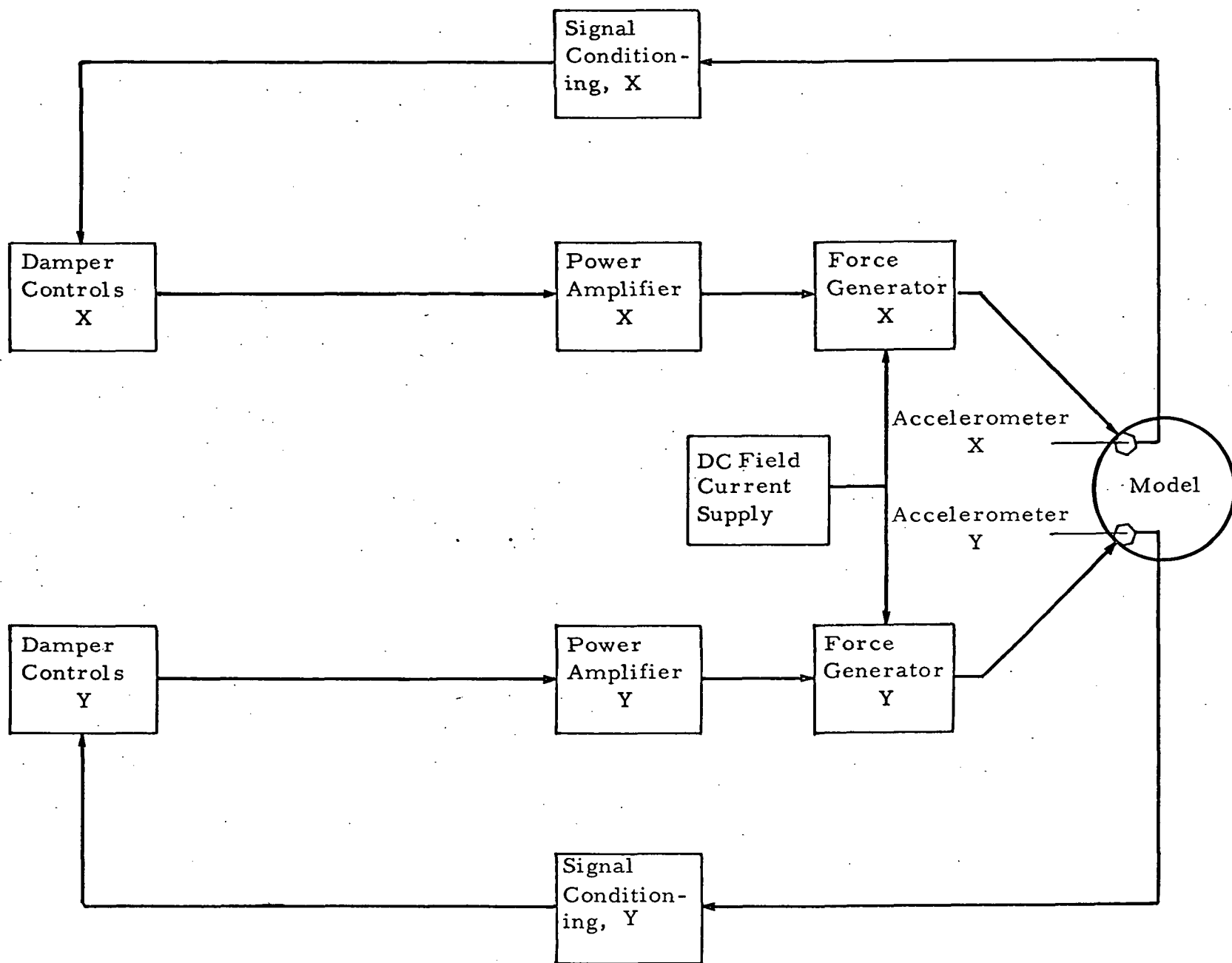


Fig. 1 Overall AAD System Block Diagram

April - June, 1971 in Building 4619, Marshall Space Flight Center, Alabama. The following measurements were conducted for each of eight model configuration:

- (1) First bending mode natural frequencies.
- (2) Mode shapes
- (3) Generalized mass values
- (4) Damping versus control settings

Tests (1) and (4) were made in two mutually perpendicular planes\* containing the two forces generated by the shakers.

Exceptionally good data were obtained for this test series. All results except for AAD calibrations are, however, reported elsewhere,\*\* and are not described in this document.

The wind tunnel test program began on 14 October 1971 and ended one month later. Tests were conducted at NASA/Langley Research Center's 16-foot Transonic Dynamics Tunnel. Five of the eight calibrated model configurations were tested. The AAD system was used for final calibration of the dynamic properties of the model configurations in the wind tunnel test setup as well as for providing damping during wind tunnel tests.

Detailed descriptions of all above-outlined engineering tasks are documented in the following Sections of this final report.

---

\* These planes are referenced to as the X- and Y- planes in this report. The X- plane contains the vertical axes of the vehicle and LUT models.

\*\* Internal Document, MSFC Unsteady Gas Dynamics Branch.

## Section 2

## DAMPER PERFORMANCE REQUIREMENTS

2.1 Basic Requirements

Basic performance requirements of the AAD system stem directly from the criteria that the overall dynamic capability of the model as a load measuring instrument in wind tunnel tests will not be reduced on account of the damper. Specifically,

(1) The AAD shakers must not physically interfere with the model, nor should they dynamically couple to model responses except as a pure damper in bending modes. The shakers must have interference-free stroke capabilities greater than or equal to that of the model in all directions at the station where the damper is attached. The maximum model stroke capability at the damper station (station 91.6) is obtained from the allowable total base bending moment (static plus dynamic), the modal bending moment per unit tip deflection and the mode shape.

(2) The AAD must provide a sufficient damping force to balance an aerodynamic excitation which is theoretically sufficient to induce model responses up to the allowable strength under all wind tunnel conditions.

(3) The AAD must provide adjustable damping from 0.5% to 4.0% of critical modal damping in the first bending mode of the model in all simulated fuel configurations.

2.2 Derived Requirements

The GWL model is an old 5.5% aeroelastic model of Saturn IB/Apollo, modified to satisfy scaling requirements of the SA206/LC-39 configuration. The exact dynamic strength of the modified model

was not firmly determined at the time the AAD design was to be completed. The dynamic strength of the old model had to be used instead. On this basis, allowable bending moments of  $194 \times 10^3$  and  $332.5 \times 10^3$  in-lbs at Model Station 11.2 were used for the Empty and the Fully Fueled configurations, respectively. The allowable base bending moment for the Intermediate configuration was in between these values and did not affect the AAD design.

Calculated full-scale dynamic characteristics of the Saturn IB/Skylab were obtained from Reference 1, and are listed in Table I.

Aeroelastic scale factors were obtained from Reference 2, and are listed below:

Frequency Scale Factor: 48.4

Generalized Mass:  $6.24 \times 10^{-4}$

Slope/(Inch of Tip Deflection): 18.2

Modal Bending Moment: 0.0803

Ideal model characteristics listed in Table II were obtained from predicted full-scale values of Table I, using the above scale factors. Since the mid-plane of the AAD will be located at Model Station 91.6, all model characteristics in Table II are referenced to that station, the damper station.

It is seen from Table II that the stroke requirement is  $\pm 0.85$  inches without mechanical interference as specified by the Fully-Fueled configuration.

Vehicle On Pedestal Tower  
No Structural Connection to LUT  
First Bending Mode Properties Only

Configuration	First Mode Natural Freq Hz	Generalized Mass (1) #-sec <sup>2</sup> /in	Modal Bending Moment (2) in-#/in@tip	Mode Shape Ø(1650)	Generalized Mass (3) #-sec <sup>2</sup> /in	Modal Slope Ø'(1650) (in/in)/in@tip	Case No. (Ref. 1)
Empty	0.5005	63.21	1.83x10 <sup>6</sup>	0.44	326.2	3.68x10 <sup>-4</sup>	1
Intermediate	0.4504	86.70	2.01x10 <sup>6</sup>	0.46	410.0	3.14x10 <sup>-4</sup>	3
Fully Fueled	0.3055	262.22	2.45x10 <sup>6</sup>	0.55	867.0	3.63x10 <sup>-4</sup>	6

Notes: (1) Referenced to vehicle tip.  
(2) @ Station 200.  
(3) Referenced to Station 1650.(Model Station 91.6)

Table I PREDICTED FULL-SCALE DYNAMIC PROPERTIES OF SATURN IB/LC-39 Configurations

Simulated Configuration	First Mode Natural Frequency Hz	Generalized Mass (1) #-sec <sup>2</sup> /in	Mode Shape $\Phi$ (91.6)	Modal Slope $\Phi'$ (91.6) (in/in)/in @ tip	Modal Bending Moment (2) in-#/in @ tip	Allowable Deflection @ Sta 91.6 (3) in.	Maximum Slope at Sta 91.6 (4)	Critical Damping Coef. (5) #/(in/sec)
Empty	24.2	0.203	0.44	$6.70 \times 10^{-3}$	146.8	0.58	$8.83 \times 10^{-3}$	61.8
Intermediate	21.8	0.256	0.46	$6.65 \times 10^{-3}$	161.3			70.1
Fully Fueled	14.8	0.540	0.55	$6.59 \times 10^{-3}$	216.0 (6)	0.85	$10.2 \times 10^{-3}$	100.5

Notes: (1) Normalized to Station 91.6

(2) At Station 11.2

(3) @ Allowable Bending Moment

(4) @ Allowable Bending Moment

(5) Reference to Station 91.6

(6) Measured Modal Bending Moment of Modified Model

Table II IDEAL MODEL CHARACTERISTICS (First Bending Mode Only)

The equation of motion governing the dynamic responses of the model in the first mode under wind tunnel test conditions is

$$m \left[ \ddot{q}(t) + 2\zeta\omega_1\dot{q}(t) + \omega_1^2 q(t) \right] = Q(t)$$

where  $q(t)$  is the generalized coordinate representing the model response at the damper station,  $m$  the generalized mass,  $\zeta$  the generalized damping factor,  $\omega_1$  the first mode natural frequency in radians per second, and  $Q$  the generalized force in the first mode due to the unsteady aerodynamic force, referenced to the damper station.

The damping force is the sum of two components: inherent model structural damping and damping added by the AAD. The required force capability of the shaker was established in the following manner for design purposes:

(1) The maximum response of the model will occur at minimum total damping of the model used in the test series, i. e., at 0.5% of critical damping.

(2) The magnitude of the maximum response will be less than or equal to  $\pm 0.85$  inches at the damper station.

(3) The damping force under this condition is  $2\zeta\omega_1\dot{q}$ .

The peak damping force is

$$2\zeta m\omega_1^2 q_0 = 2 \times 0.005 \times 0.85 m\omega_1^2$$

where  $q_0$  is the amplitude of  $q(t)$ . For the Empty configuration, the damping force amplitude is 24.3 lbs (0 - peak); for the Fully Fueled configuration this is 40.6 lbs. For the Intermediate configuration, the damping force could not be computed during AAD design because of lack of data, but was estimated to be in the neighborhood of 30 lbs. The critical requirements is the 40.6 lbs for the

Fully Fueled configuration.

(4a) If the aerodynamic excitation is sinusoidal and if its magnitude is independent of the magnitude of the response, then  $q_0$  is inversely proportional to the damping,  $\zeta$  :

$$q_0 = A/\zeta$$

the value of A is given by the product of the minimum test damping ( $\zeta = 0.005$ ) and the maximum response (0.850")

Thus

$$q_0 = (0.005 \times 0.85) / \zeta = 0.00425/\zeta$$

(4b) If the aerodynamic excitation is a wideband random process, and if its magnitude is also independent of the motion of the model, then the rms response,  $\bar{q}$ , is inversely proportional to the square root of damping, i. e.

$$q_0 = B/\sqrt{\zeta}$$

The value of B is determined from the condition that when

$$\zeta = 0.005$$

$$\bar{q} = 0.85/4^* = 0.213$$

Thus,

$$B = 0.015$$

The rms response at maximum damping ( $\zeta = 0.04$ ) is 0.075".

(5a) If  $Q(t)$  is motion independent, the required total damping force is constant for each model configuration, regardless of the damping. Therefore, for the Fully-Fueled case, the total required damping force amplitude is always 40.6 lbs. A fraction of this damping force is supplied by the inherent model damping, and the remainder by the AAD. The ratio between them is given

---

\* Assuming the peak-to-rms ratio is 4 for the response.



by  $f_a/f = (\zeta - 0.005) / \zeta$

where  $f_a$  is the force requirement for the AAD, and  $f$  is the total damping force. Thus, we have  $f = 24.3, 30, \text{ or } 40.6 \text{ lbs.}$  for Empty, Intermediate and Fully Fueled configurations, respectively. For the most severe case,  $f = 40.6 \text{ lbs.}$  and

$$f_a = \frac{0.035}{0.040} \times 40.6 = 35.5 \text{ lbs. (0 - pk)}$$

(5b) For the Fully-Fueled configuration, the total rms damping force at  $\zeta = 4\%$  is  $28 \text{ lbs} (= \zeta c_{cr} \omega_1 \bar{q}_0)$ .

The required contribution from the damper is

$$\frac{0.04 - 0.005}{0.04} \times 28 = 24.5 \text{ lbs}$$

This rms force requirement is, therefore, almost the same as that for the sinusoidal case of  $25.1 \text{ lbs} (= 35.5 \text{ lbs} / \sqrt{2})$

### 2.3 Other Considerations

The following requirements must also be satisfied by the AAD in a practical application:

(1) Symmetry - The AAD must provide adjustable damping in each of two orthogonal planes in order to provide equal damping in all directions.

(2) Coupling - The AAD must not couple to the dynamics of the model (except for damping) so that the model may be designed and checked out independently of the damper.

(3) Motion Independence - The damping provided by the AAD must be independent of the response of the model in all directions.

## Section 3

## SHAKER DESIGN

3.1 Approach

In order to maintain the same damping in the model for all allowable model response amplitudes (at a given control system gain), the force generated by the shaker per unit armature current must be independent of the instantaneous relative position of the armature with respect to the field magnet. The two conventional approaches to achieve this displacement insensitivity are shown in Figure 2. In Approach A, the length of the armature coil is greater than dimension  $d$  of the space between the pole pieces of the field magnet by at least the double-amplitude stroke requirement of the shaker so that a constant number of turns of the coil is always in the magnetic field. All commercial shakers utilize this approach because it requires a smaller magnetic field and, hence, a smaller magnet and overall size. To obtain long strokes, the coil must be lengthened, which would increase the coil impedance and the drive voltage requirement. Also, a constant current -vs- force relationship hinges on the uniformity of the (long) coil winding which is not easily achieved. In Approach B of Figure 2, dimension  $d$  of the magnetic field is longer than the coil length so that, again, the same number of turns of the coil (in this case, the entire coil) are within the magnetic field for all allowable relative positions of the armature and the field magnet. The obvious disadvantage in this case is the large magnet size required to accomplish the design. However, there are three advantages which tend to offset this disadvantage: (1) The coil is much shorter so that the coil impedance (resistance and inductance) is reduced. Matching it to a solid-state power amplifier is

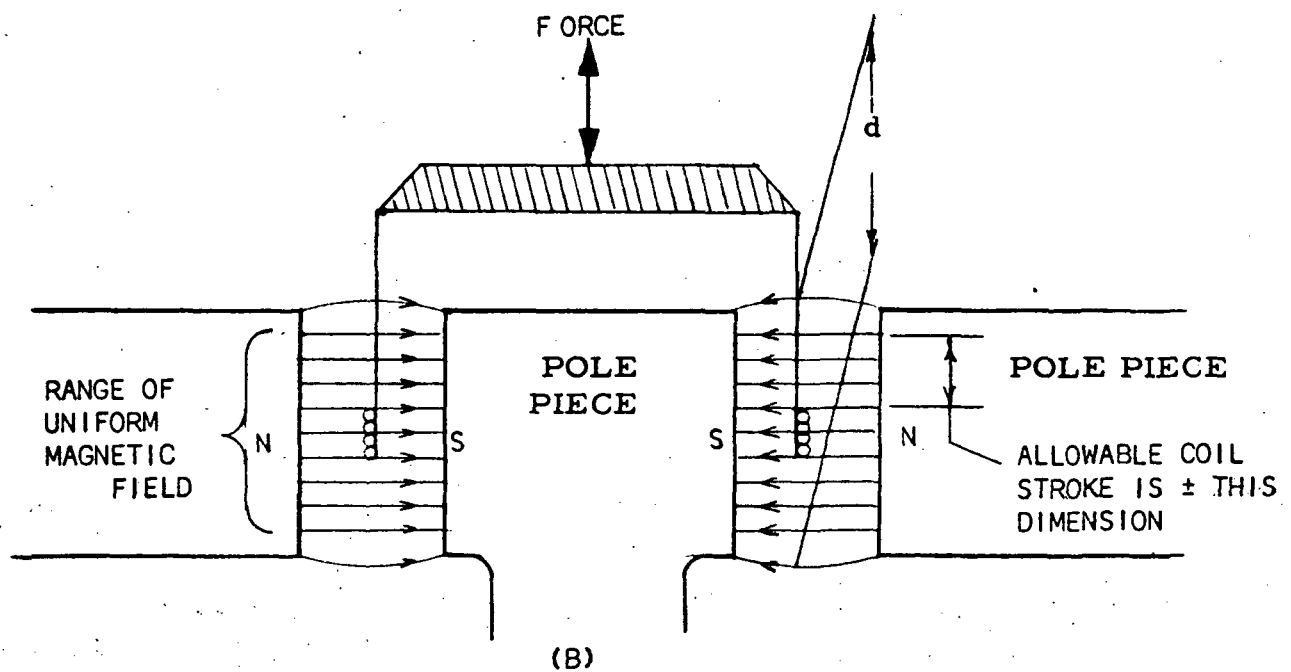
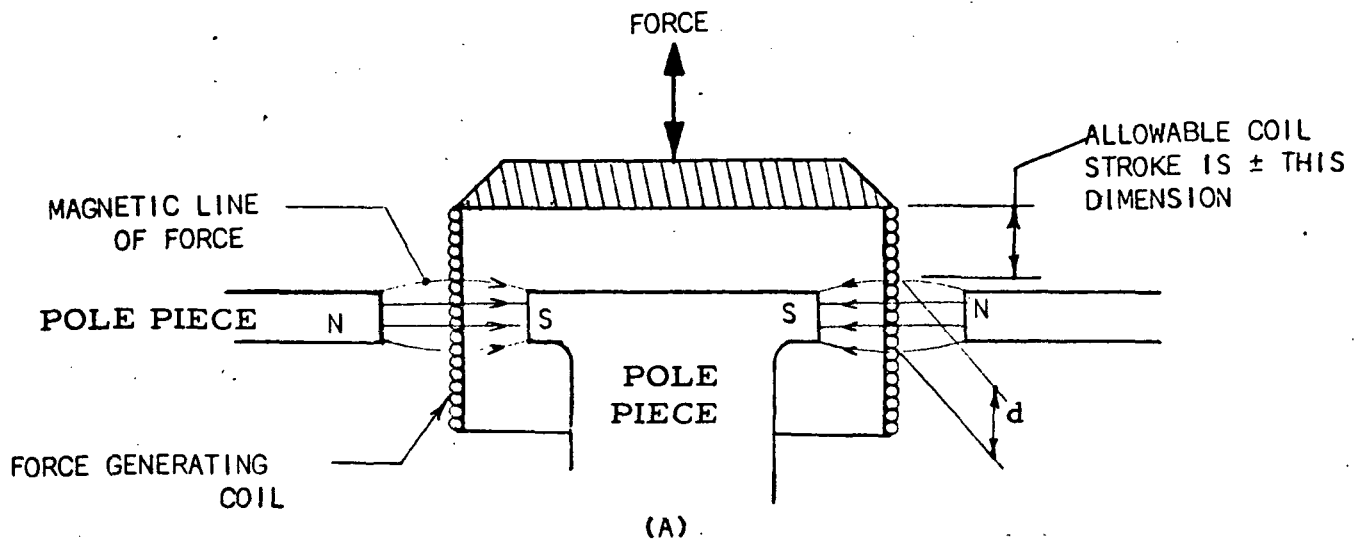


Fig 2 Shaker Design Approaches to Obtain Constant Current-to-Force Conversion

a lot easier, (2) The linearity of the force-current relationship is independent of the uniformity of the coil winding. For a special-purpose, one of-a-kind design, this advantage can be significant, and (3) The coil design can be made much more efficient if longer stroke is required. A combination of Approach A and Approach B was used in the AAD design.

Since the two-axis force generator system is to be designed for large stroke capabilities in two directions, cross-coupling could be a serious problem. The selected design approach completely eliminates this and many associated problems by using flat magnetic field gaps and flat coils, as shown in the schematic drawing of Figure 3. The coil carrier can be rigidly attached to the model without the use of flexures or linkages so that undesirable mechanical damping and/or stiffening is completely avoided.

Advantages offered by permanent magnets are realizable in volume-production of shakers and speakers as special manufacturing processes and equipment may be used. With a special-purpose force generator, an electromagnet is preferred because (1) easy-to-machine, soft magnetic alloys are employed instead of either Alnico alloys or ceramics, for which little or no machining is possible by conventional means, (2) the magnetic circuit design is more reliable (as compared to circuit design for a permanent magnet where considerable art is required in predicting the magnetization of the permanent magnet), and (3) once magnetized, a permanent-magnet shaker cannot be taken apart without causing irrecoverable demagnetization (to a low field strength).

- A. Upper Core
- B. Lower Field Pc.
- C. Magnetic Gap
- D. Flat Force Coil
- E. Force Coil Carrier

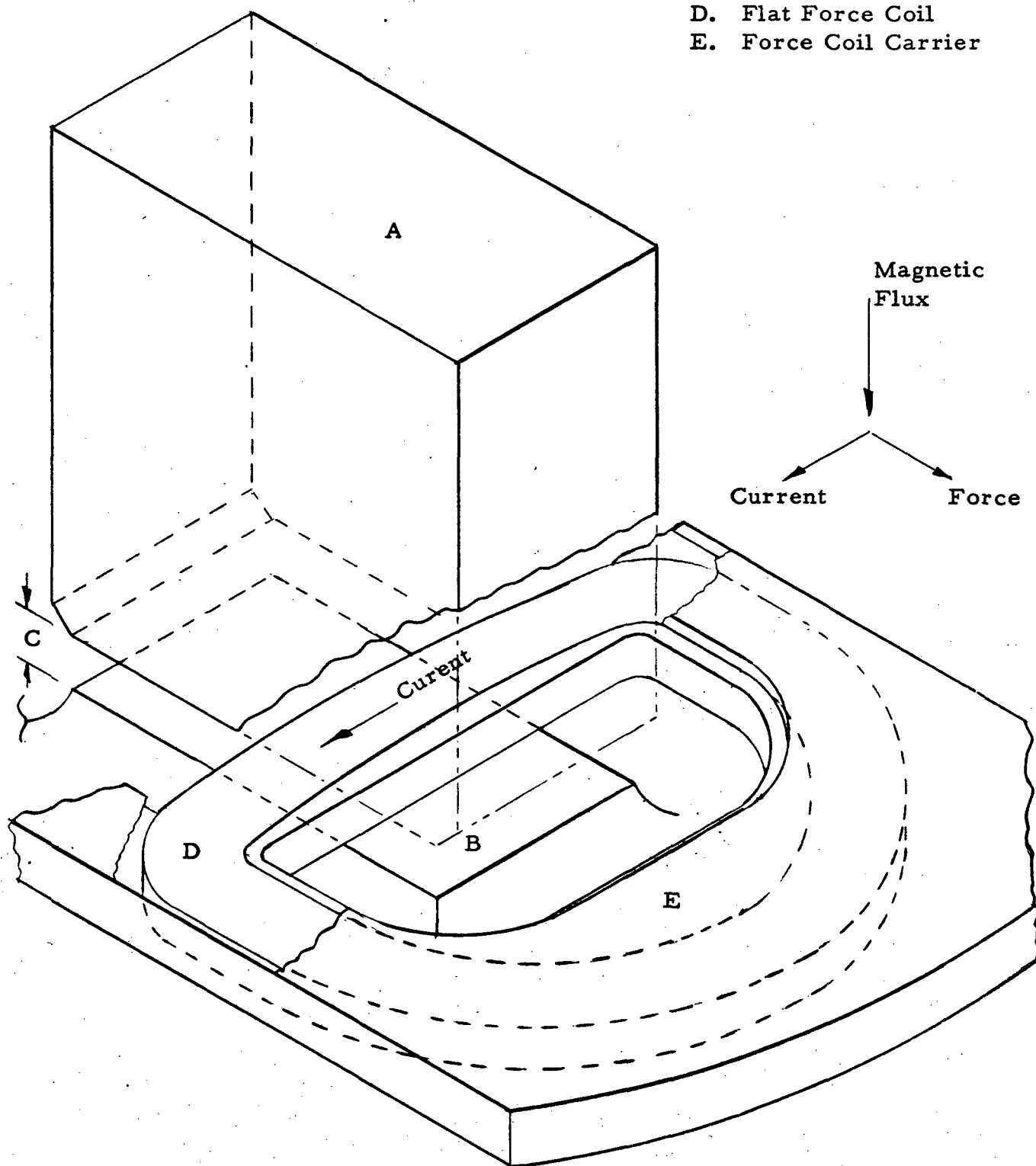


Figure 3 AAD SHAKER APPROACH

The last restriction was considered to be too severe for the present application.

The final over-all shaker configuration design of the AAD was achieved after a lengthy design process during which power dissipation, electrical compatibility with available field power supply and power amplifiers, weight, armature impedance, manufacturability, durability, ease of maintenance and trouble-shooting, reliability, ease of installation, and many other factors were weighed against specified and implied requirements and against one another. A simplified schematic drawing of the AAD shakers is shown in Figure 4. A detailed assembly drawing of the shakers is included in Appendix A.

Referring to Figure 4, the two force coil assemblies are attached to an aluminum ring structure which is in turn rigidly mounted on the model. The two electromagnets are mechanically connected to each other via the four short spacer posts, the total weight is supported vertically by a specially designed bearing assembly which in turn, rests on the 1/4" aluminum plate of the Damper Support Assembly.

The electromagnet assembly weighs approximately 85 lbs. The horizontal suspension system consists of 12 springs which have a combined stiffness of 9.6 lbs./in. in all horizontal directions.

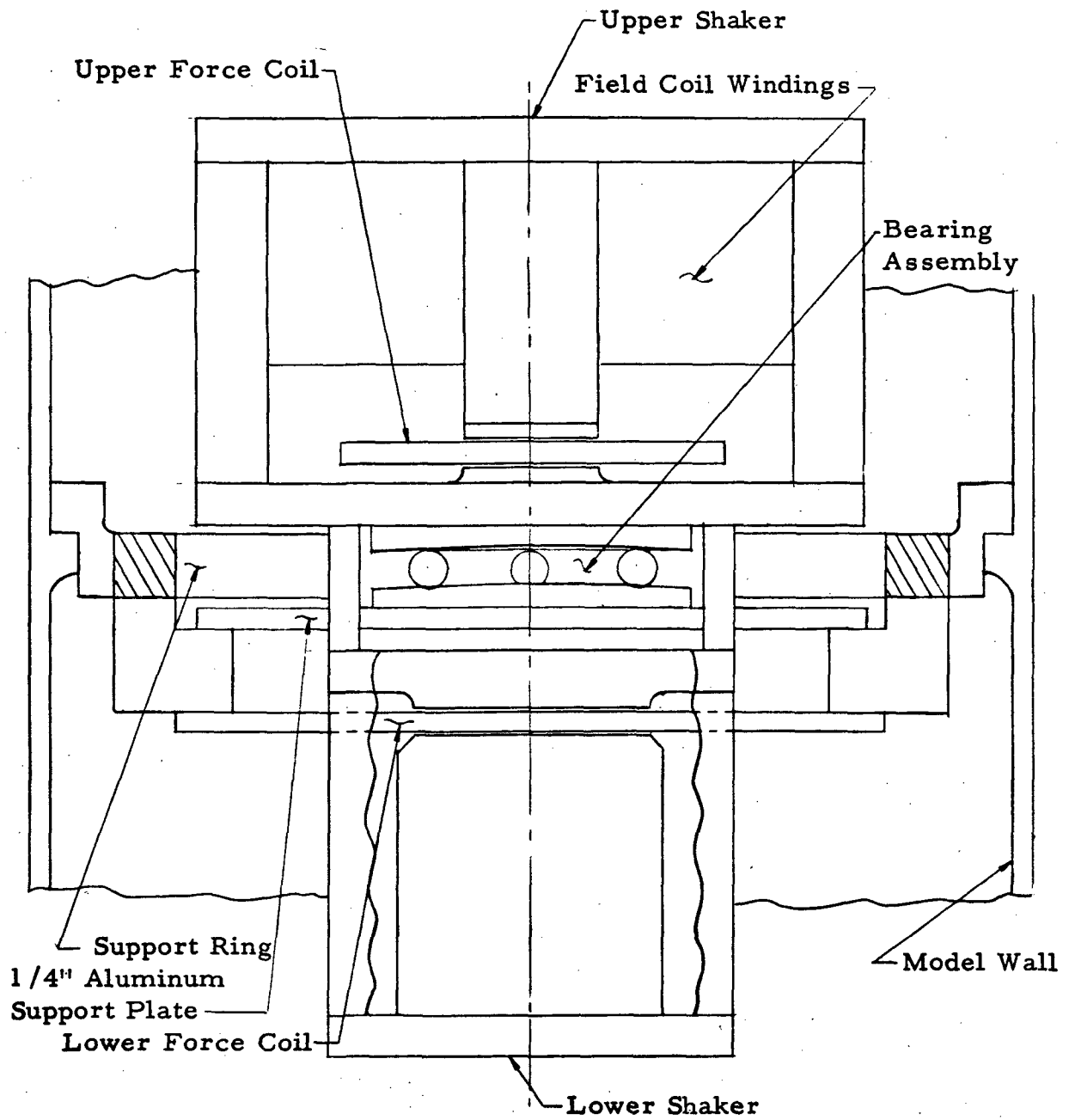


Fig 4 Schematics of AAD Shakers



The natural frequency of the electromagnets in any horizontal direction is

$$\text{Frequency} = (9.6 \times 386.4/85)^{1/2}/2\pi = 1.02 \text{ Hz}$$

Since the lowest model natural frequency is 14.8 Hz, the motion of the model is reduced by a factor of 200 when it is transmitted to the electromagnets.

The entire two-axis shaker assembly is enveloped within a circular cylindrical volume of approximately 9.75" in diameter and 11.5" in height. The moving element of the two shakers and the interface structure between the model and the dampers weighs approximately 9 lbs.\*

The stroke capability of the design is 0.85 inches in all directions.

### 3.2 Field Magnet Design

#### 3.2.1 Material Selection

The electromagnet core material was selected on the basis of the following considerations: (1) The core will be of significant dimensions so that thin electrical steels (mostly rolled silicon steels used for transformer laminations) are ruled out. (2) The application is for d. c. operations. Core loss which occurs at high frequencies will be of no concern, a laminated core construction is inappropriate anyhow. (3) The material must have a magnetization curve which combines high saturation flux density and low coercive force. (4) The material must be readily available and easily machined by conventional methods (drilling, turning, and milling).

---

\*The weight of this moving element can be reduced with lightening holes, cutouts, etc. However, since this wieght can be easily compensated for in the SA 206 application, no such attempt was necessary.

The selection is consequently narrowed down to one of the commercial "relay steels" (essentially silicon-iron alloys) The AAD electromagnets were actually made of Allegheny Ludlum Steel Corporations' Relay 5 Screw Stock. The magnetization curve for this material in properly annealed condition is shown in Figure 5 which was obtained from Reference 3. The optimum operating point for this material for the present application is near the "knee" of the magnetization curve where a flux density of approximately 14,000 Gauss is possible with a magnetizing force of less than 3 Oersteds.

### 3.2.2 Analyses

After several design iterations a magnetic gap dimension of 0.336" was found to be near optimum. In the air gap, the permeability is 1.0 so that to maintain a flux density of 14,000 gauss across it would require a field strength of 14,000 Oersteds and a magnetomotive force of

$$\begin{aligned} 14,000 \times 0.336 &= 4,704 \text{ Oersted-in.} \\ &= 9,500 \text{ ampere-turns} \end{aligned}$$

The mean magnetic length through the electromagnet core material is approximately 15", so that an additional

$$3 \times 15 \times 2.02 < 100 \text{ ampere-turns}$$

will be required to establish the desired 14,000 gauss in the air gap. The total magnetomotive force required is, therefore, less than 9,600 ampere-turns. In the design, a No. 16 (AWG) magnet wire with a heavy insulation film was selected. At a "current density" of 540 circular mils per ampere (2360 amperes per square

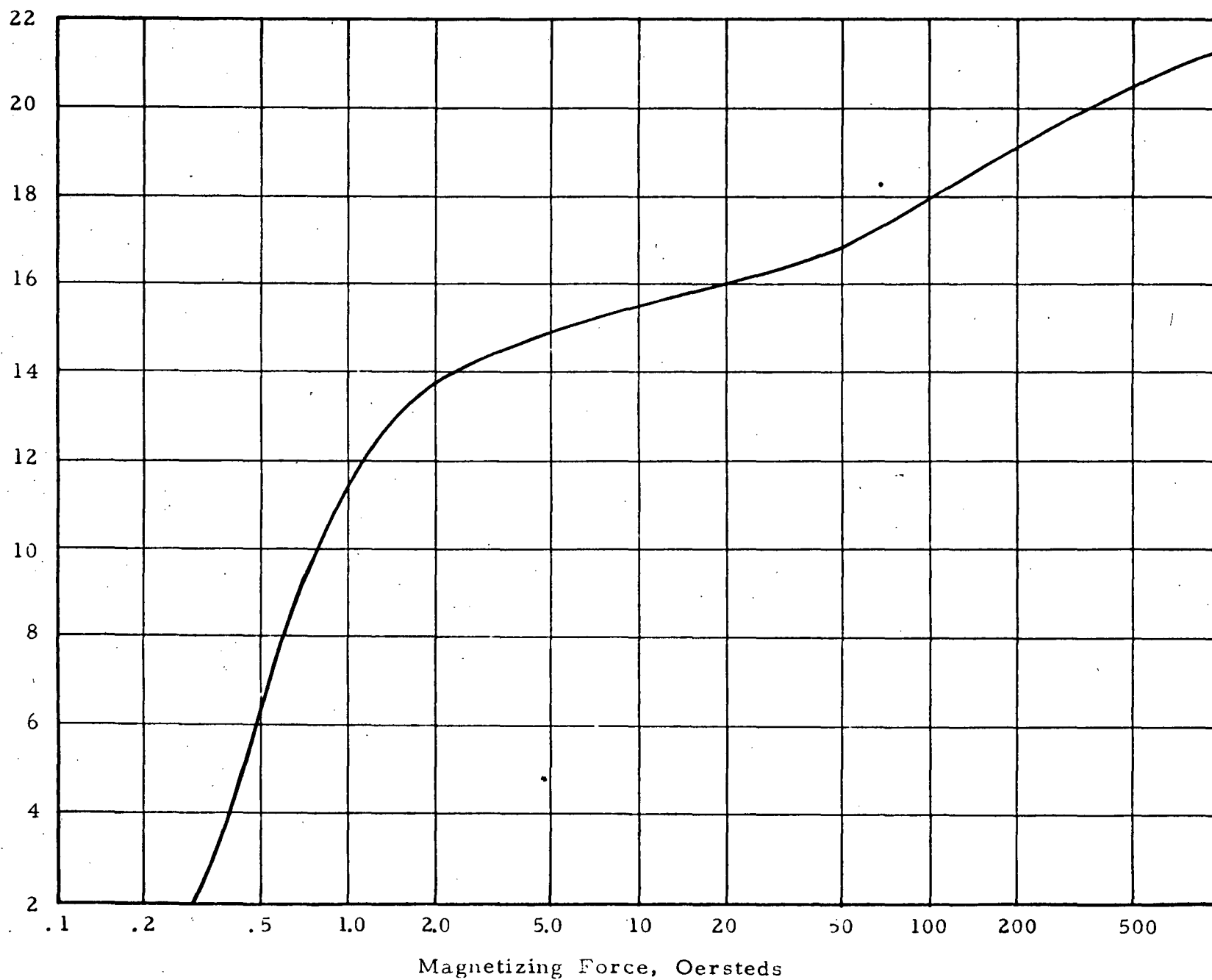


Fig. 5 Magnetization Curve For No. 5 SS Relay Steel

inch), the continuous dc current is 4.8 amperes. The required number of turns of the field coil is, therefore,

$$9,600/4.8 = 2,000$$

The average length of each turn of the coil is approximately 14 inches, so that the total length of the field coil wire is

$$\frac{14}{12} \times 2,000 = 2,333 \text{ ft.}$$

At room temperature, the resistance per one thousand feet of No. 16 copper wire is 4.02 ohms. The calculated total field coil resistance at room temperature is

$$4.02 \times 2.333 = 9.38 \text{ ohms}$$

The minimum rate of heat generation of the field coil is

$$I^2 R = (4.8)^2 \times 9.38 = 216 \text{ watts}$$

The insulation on the magnet wire can withstand 356° F. At that temperature, the resistance of the wire would have increased by 63% (from room temperature resistance) to 15.3 ohms, and the heat generation rate would be 352 watts. In this application, air cooling will be employed to hold the thermal equilibrium temperature to 255° F or less, the coil resistance will be 13.2 ohms or less and the voltage required to drive the 4.8 amperes of current through each field coil will be less than 63.2 volts. At thermal equilibrium at 255° F, the heat generation rate is 303 watts.

A schematic drawing of a field magnet is included in Appendix A of this report.

### 3.3 Force Coil Design Analyses

The design formula for the force coil is

$$F = 0.571 \times 10^{-6} BNIL$$

where F is the force (in lbs) exerted on a coil of N turns carrying a current of I amperes in a magnetic field of B Gausses. The length of each turn of the coil in the magnetic field is L inches.

The final design of the force coil is shown in Figure 6. With

$$B = 14,000 \text{ gaussses}$$

$$L = 1.547 \text{ inches}$$

$$N = 84$$

$$F = 35.5 \text{ lbs (0 - pk)}$$

the required peak current is 34.2 amps. The design current-to-force conversion factor is 1.04 lbs/amp.

The force coil is made of a copper strip 0.01" thick by 0.25" wide. Insulation is provided by a 0.0025" Mylar tape inserted between successive layers of the copper strip. A 0.001" gap between layers of the coil is estimated for the construction of the coil. This copper strip has a cross-sectional area of 0.0025 square inches, and its calculated resistance is 3.25 ohms per 1,000 ft. at room temperature. The mean-length-per-turn of the force coil is one foot, so the total resistance of the force coil at room temperature is

$$3.25 \times 84 \times 10^{-3} = 0.273 \text{ ohms}$$

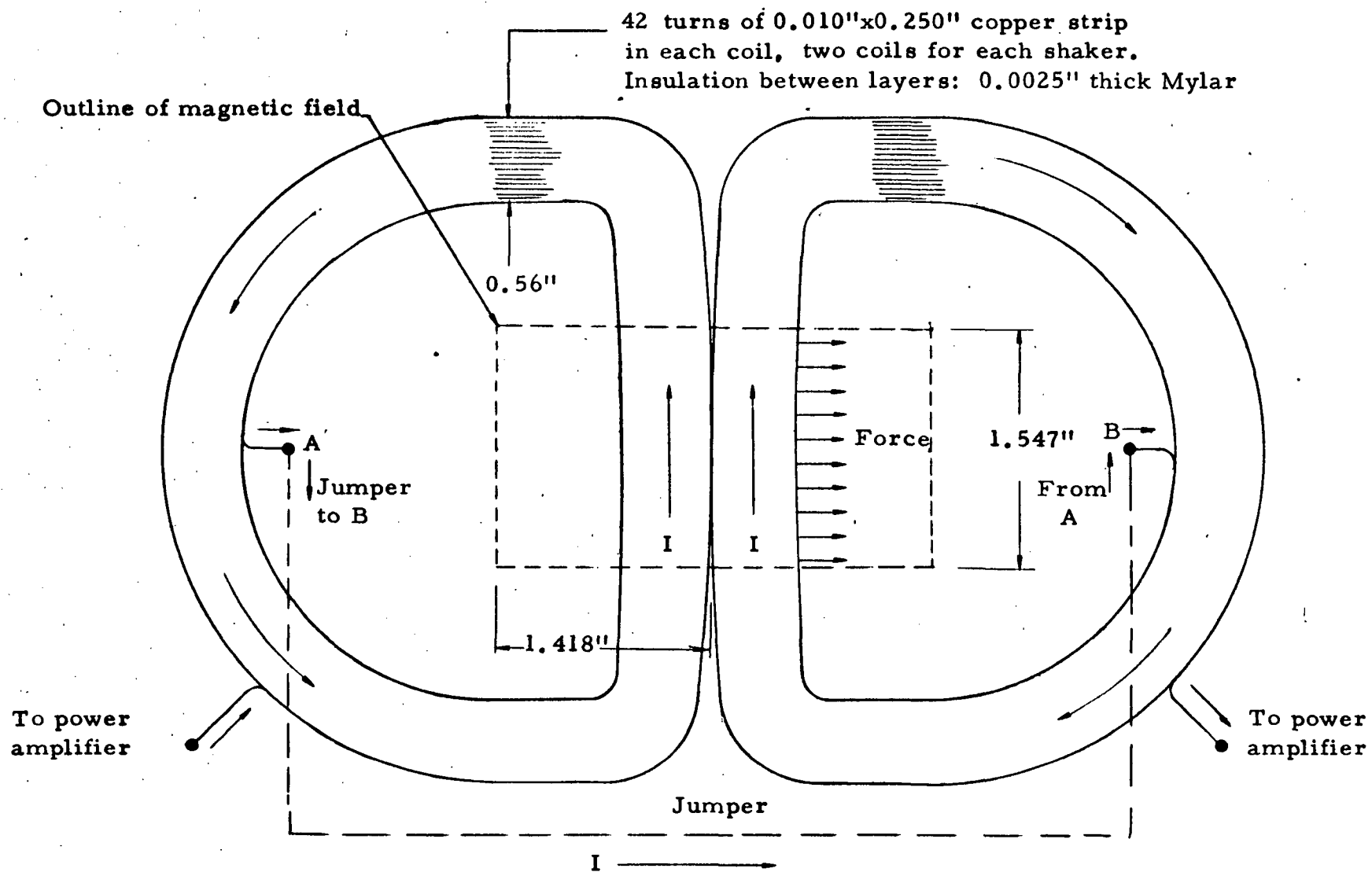


Fig. 6 FORCE COIL CONFIGURATION

Assuming a sinusoidal force, the power dissipation at the maximum force level is

$$0.273 \times (34.2 \times 0.707)^2 = 160 \text{ watts}$$

Assuming thermal equilibrium can be established at 255°F at maximum power level with air cooling, the resistance of the force coil will be 0.384 ohms, and the power dissipation is 225 watts. On the other hand, if the aerodynamic excitation is random, and if the peak-to-rms ratio of the model response is 4, the power dissipation is only 28.1 watts.

The peak voltage required to drive 34.2 amps of peak current through the force coil is

$$34.2 \times 0.384 = 13.1 \text{ volts}$$

The back emf imposed on the coil due to its velocity in the magnetic field will always be in phase with the applied voltage in this particular mode of operation (as dampers) of the shakers. The actual voltage requirement is therefore less than 13.5 volts.

### 3.4 Shaker Construction Details

#### 3.4.1 Field Magnets

The core material for the electromagnet is Allegheny Ludlum Corporation's Relay 5 SS material, annealed after rough-machining in a dry hydrogen atmosphere at 1850°F for three hours, and followed by very slow cooling. After finish-machining, all parts of the magnets were cadmium-plated (less than 0.0005" thick) for rust prevention.

Each field magnet consists of 2,000 turns of No. 16 magnet wire (Belden, Heavy Polythermaleze), vacuum impregnated with a varnish material (Isonel 31, 8 hours at 300°F). Each magnet weighs approximately 42 lbs.

At room temperature, the resistance of each field coil is approximately 11 ohms (measured). The projected coil resistance @ 255°F is 15.5 ohms, and the heat generation rate at 3.0 amps is 140 watts for each shaker.

The optimum operating current of the field magnets was found to be 3.0 amperes by a test conducted during calibration. See Figure 7. The resulting magnetic flux density in the air gap is approximately 8,850 Gausses. The armature current-to-force conversion factor should, therefore, be reduced from the original design value by the factor (8,850/14,000) to 0.642 lbs/amp.\*

The initial (immediately after the magnets are energized) heating power is 99 watts for each magnet or 198 watts, total. The total voltage drop across the two series-connected coils is 66 volts (measured) at initial power turn-on.

During a typical, 3-hour calibration test without forced air cooling in the model which is in a room temperature environment, and with roughly a 70% duty cycle, the voltage at 3.0 amperes would increase by some 15%, to approximately 75 volts (measured). A temperature rise to 135°F is indicated. The magnet wire insulation

---

\* Later calibration tests showed that the conversion factor of the shaker was actually better: 0.75 lbs/amp. (See Page 80.)



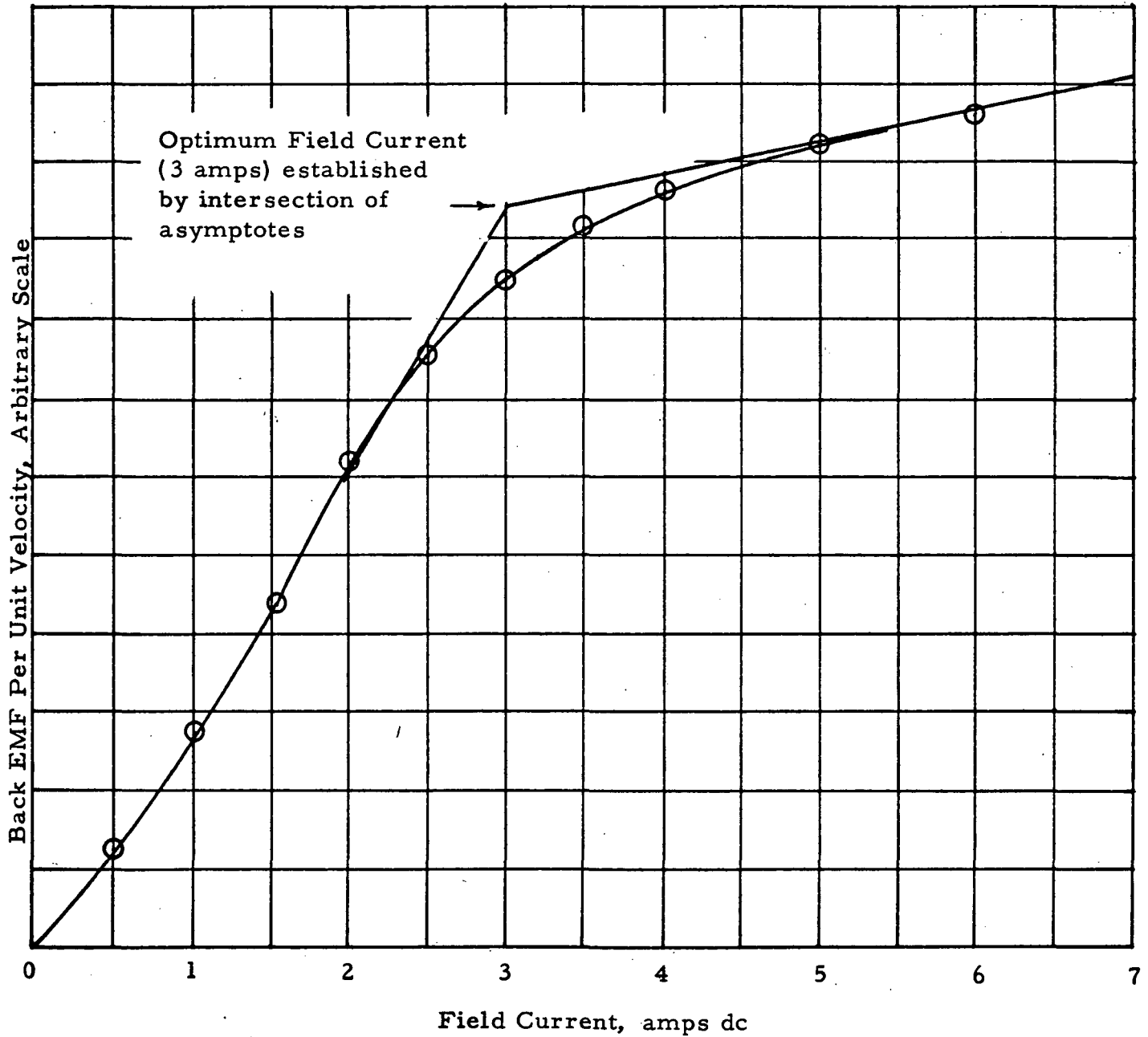


Figure 7 Determination of Optimum Field Current

is capable of withstanding  $392^{\circ}\text{F}$  continuously. Figure 8 is photographs of a field magnet.

### 3.4.2 Force Coils

Each shaker armature contains two D-shaped coils imbedded in an aluminum carrier plate. A drawing of the armature assembly is included in Appendix A. The armature has 84 turns of an insulated copper strip which has a rectangular cross-sectional area of  $0.01'' \times 0.25''$ . Insulation is provided by a Kapon<sup>(1)</sup> tape of  $0.0025''$  thickness. The coil was wound on a mold into the required shape, bonded with a high temperature epoxy<sup>(2)</sup>, and was cured at  $300^{\circ}\text{F}$ . The two D-shaped coils were inserted in the aluminum carrier, soldered to the insulated terminals and permanently bonded with Emerson-Cummings' 2651 MM, a high-temperature plastic. Curing was carried out under a heat lamp at approximately  $250^{\circ}\text{F}$  for 20 minutes. After curing, each coil was painted with a thin layer of Glyptal<sup>(3)</sup>. The two D-shaped coils are connected in series by an external jumper made of 6 inches of No. 14 square magnet wire.

The room-temperature resistance of the assembled force coils are 0.327 ohms and 0.342 ohms, and are higher than the expected 0.273 ohms. The inductance of each armature coil was measured and was approximately  $316 \times 10^{-6}$  Henries. The terminal-to-terminal capacitance was found to be 700 pf.

---

(1) Manufactured by the Minnesota Mining & Manufacturing Co.

(2) Manufactured by Hysol Corporation.

(3) A high temperature insulating paint manufactured by General Electric.

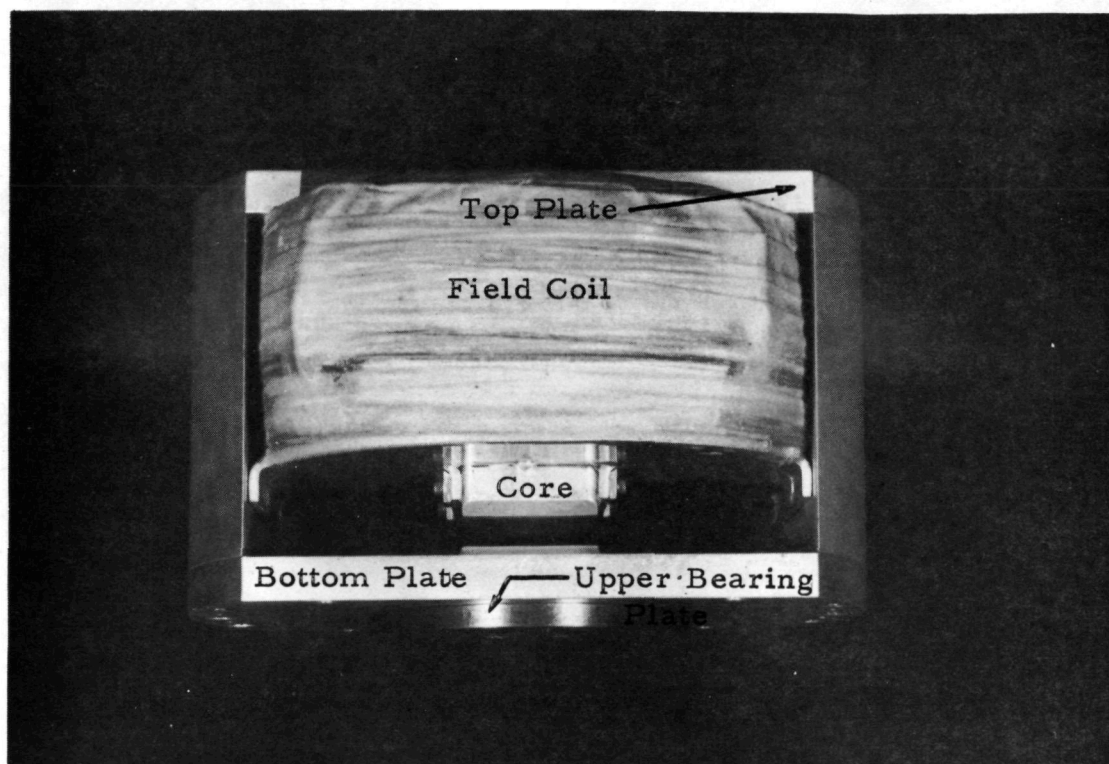


Figure 8 - Field Coil Assembly (Upper Shaker)

Figure 9 is a photograph of force coil assemblies. Figure 10 is a photograph showing the assembled moving element of the AAD shakers.

### 3.5 Summary of Shaker Data

The following is a tabulation of pertinent performance, physical, mechanical and electrical data on the electromagnetic shakers of the AAD System in the "as made" configuration.

Current-To-Face Conversion Factor	0.75 lbs/amp
Back emf per Unit Velocity	0.085 volts/(in/sec)
Stroke Capability (all directions)	$\pm 0.85$ in.
Maximum Force	35.5 lbs (0-pk)
Field Magnet Current	3.0 amps d.c.
Field Coil Resistance at R.T.	11.0 ohms (Each Shaker)
Field Coil Resistance at 225 <sup>o</sup> F	15.5 ohms (Each Shaker)
Maximum Field Coil Supply Voltage Required	93 volts(2 Shakers in Series)
Force Coil Resistances @ R.T.	0.327, 0.342 ohms
Force Coil Resistances @ 255 <sup>o</sup> F	0.462, 0.482 ohms
Max. voltage requirement (at Rated Force)	16.15, 16.85 volts (0-pk)
Force Coil Inductance	$316 \times 10^{-6}$ Henries (each shaker)
Force Coil Capacitance (terminal to terminal)	700 pf
Moving Element Weight (Armatures & Support)	9.0 lbs.
Stationary Element Weight (Field Magnets and Spacers)	85 lbs.
Envelope Dimensions	9.75 in. (D) x 11.5 in.(H)



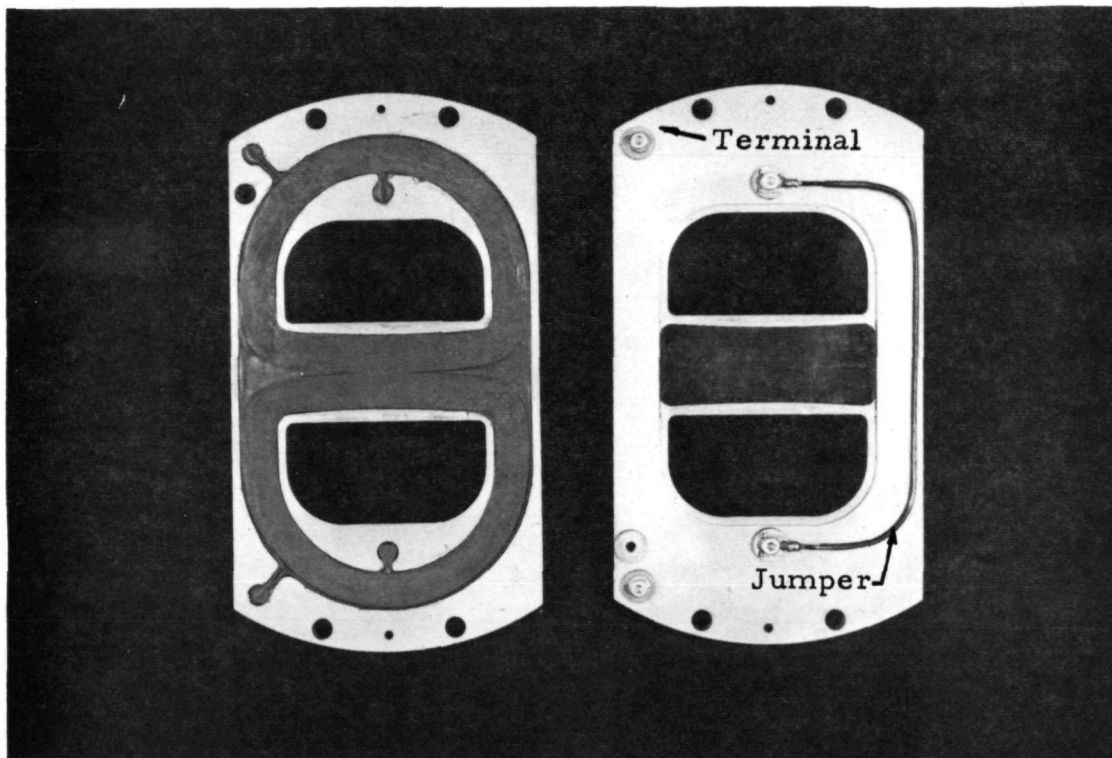


Figure 9 Force Coil Assemblies - Top and Bottom Views

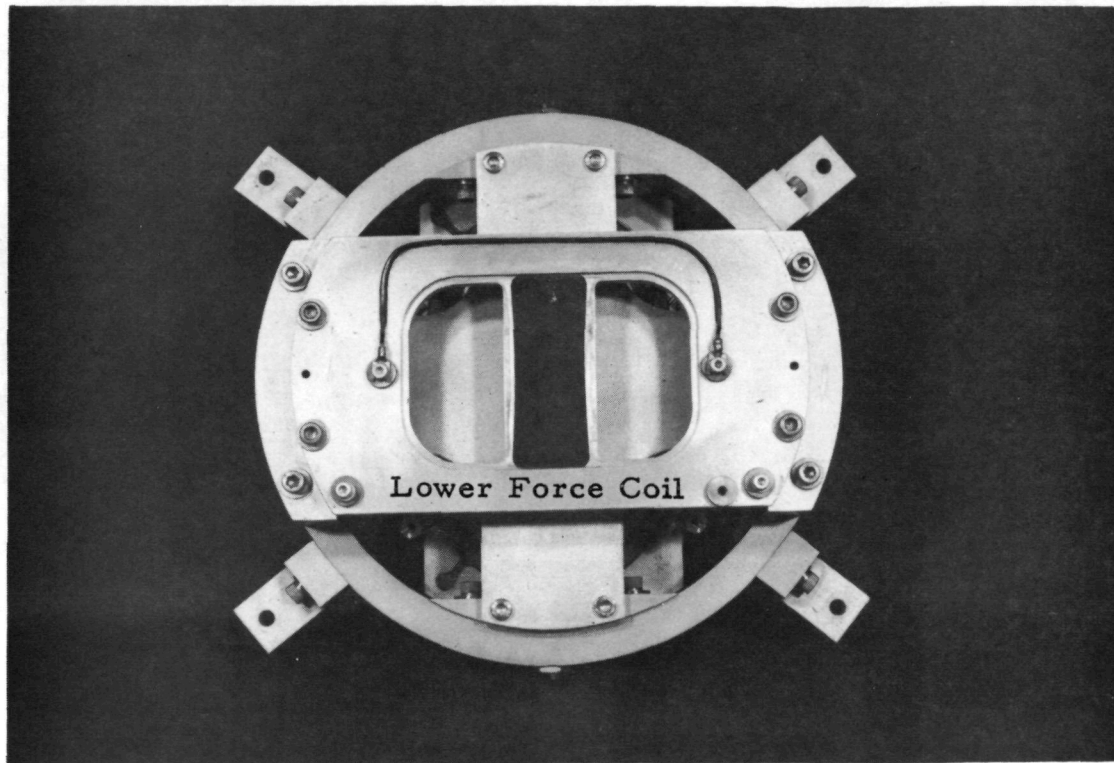


Figure 10 Damper Support Assembly With Force Coils Attached (bottom view)

### 3.6 Shaker Assembly Procedures

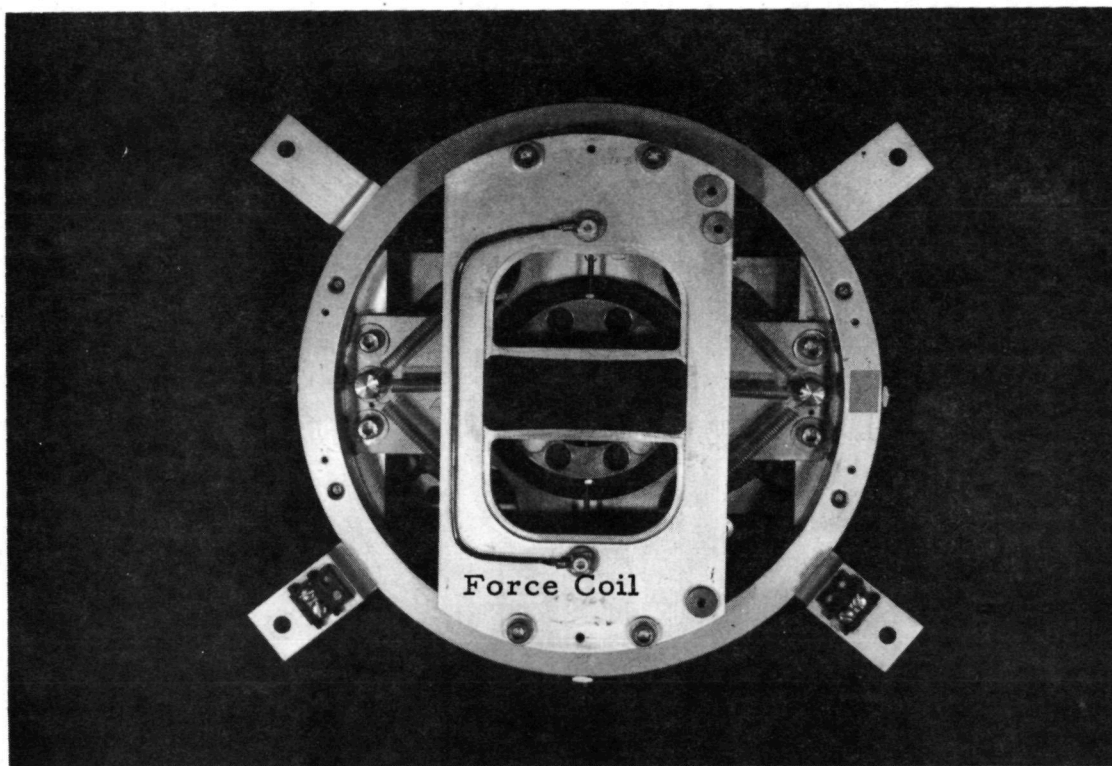
#### 3.6.1 Main Components

	<u>Drawing Number</u>
(1) Damper Support Assembly	20009 (Figs. 11, 12)
(2) Bottom Plate and Side Pieces, Upper Shaker	20013 - 1
(3) Upper Plate and Side Pieces, Lower Shaker	20013 - 2
(4) Force Coil Assembly - Upper Shaker or Lower Shaker	20018 20018
(5) Top Plate and Field Coil - Upper Shaker	20021
(6) Bottom Plate and Field Coil - Lower Shaker	20021
(7) Assembly Stand	(No Drawing)

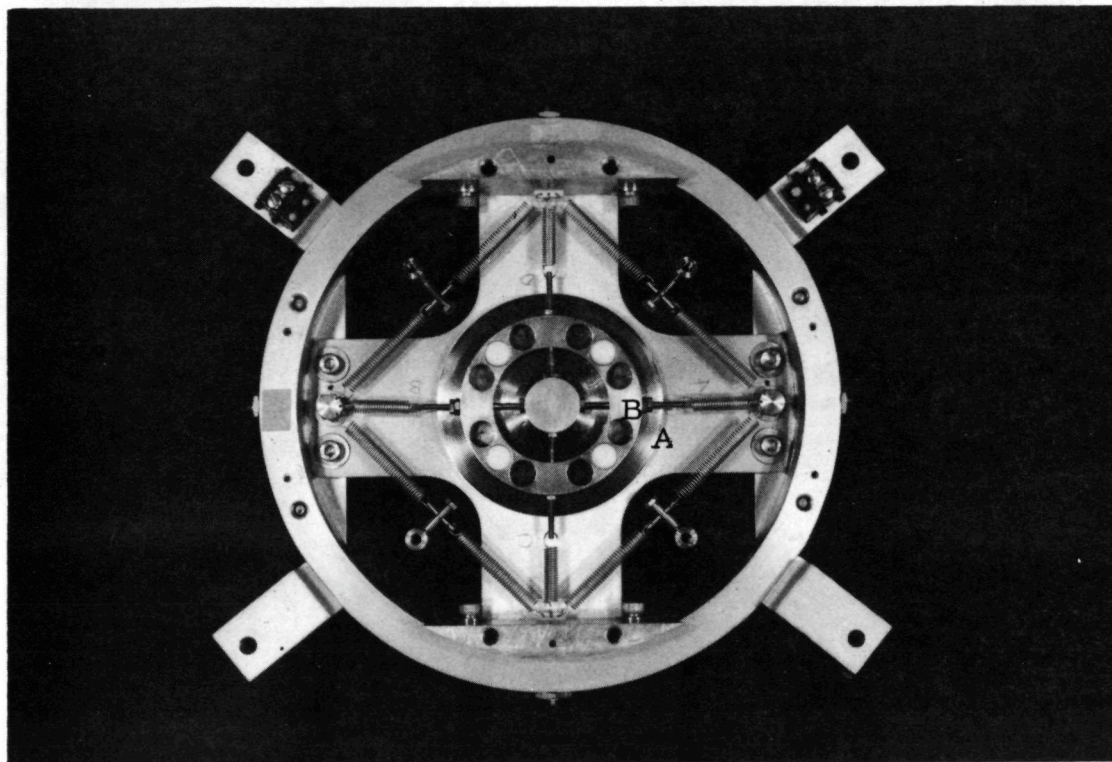
#### 3.6.2 Assembly Procedure

- (1) Place assembly stand on work surface.
- (2) Place damper support assembly on assembly stand with bearing retainer up. Fasten to stand with 4 10-32 machine screws.
- (3) Support lower shaker (top plate and side piece assembly) up against underside of damper support assembly. Note orientation marks No. 1 and 2. Insert shaker spacer posts into counter-bored holes, and fasten with 10-32 x 3/4 socket head cap screws. When tightening screws align the spring holder bar with the scribed marks on the top of the lower shaker.
- (4) Place ball bearings in bearing retainer.





Top View, With Force Coils Attached

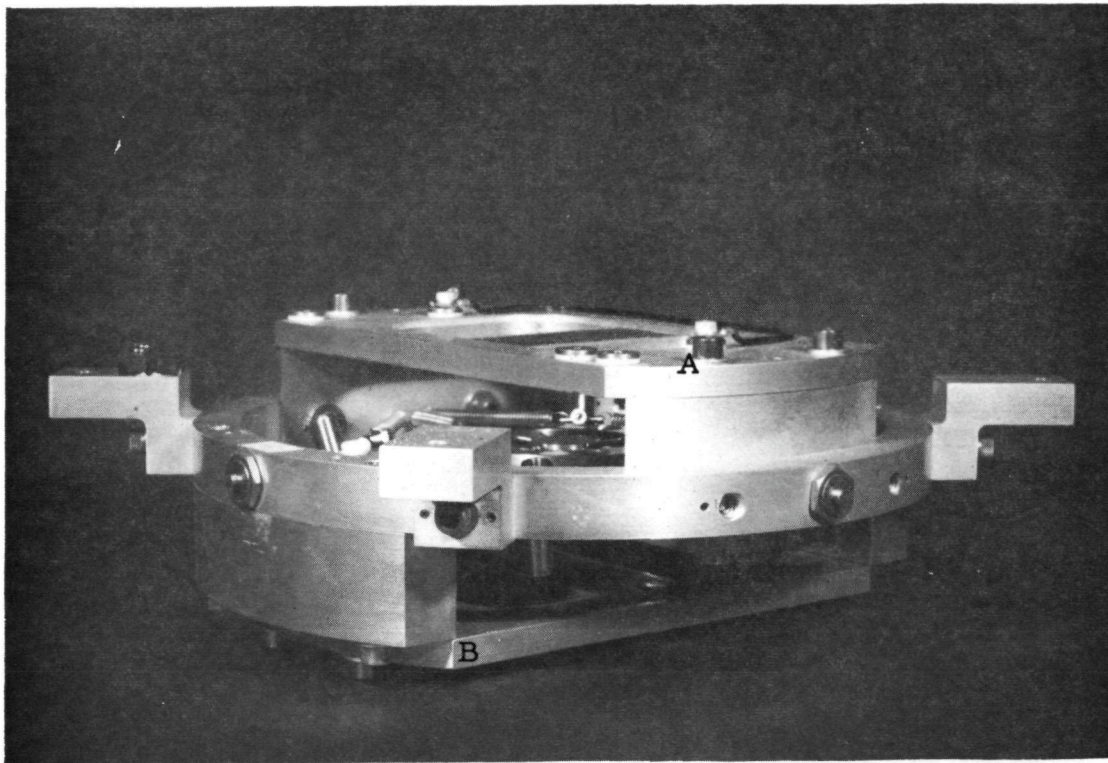


A: Lower Bearing Race

B: Bearing Retainer

Top View, Without Force Coils

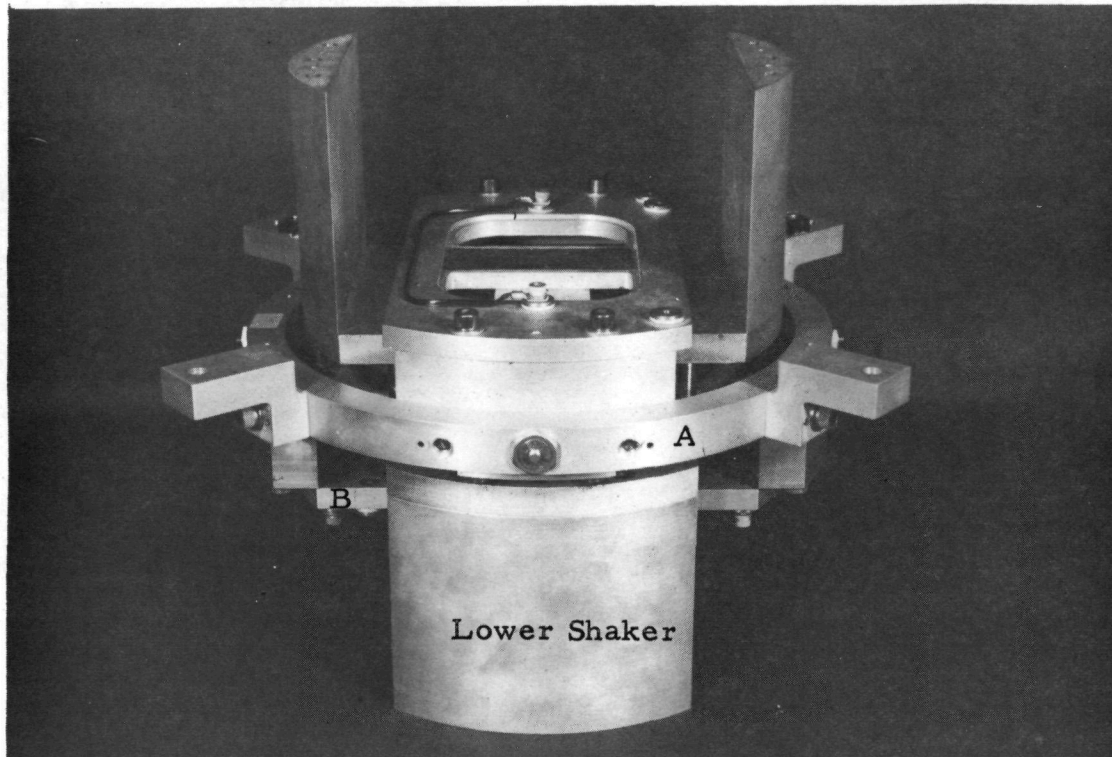




A; Upper Force Coil Assembly

B: Lower Force Coil Assembly

Figure 12 Damper Support Assembly (side view)



A: Damper Support Ring

B: Lower Force Coil

Figure 13 Damper Assembly Without Field Coils



(5) Place bottom plate and side piece assembly of upper shaker on top of spacer posts noting alignment marks Nos. 3 and 4. Bolt with 10-32 x 1/2" socket head cap screws.

(6) Place the upper force coil assembly (with wires up) on the damper support assembly (note alignment letter "A"). Use an .020 thick shim washer between the parts (4 places). Line up with 2 1/8 x 3/4 roll pins and bolt with 1/4-20 x 3/4 socket head cap screws and 1/4" light washers. Figure 12.

(7) Hold the lower force coil up in place against the damper support assembly (note alignment letter "B", and wires down). Use an .017 thick shim washer between the parts ( 4 places). Line up with 2 1/8 x 3/4 roll pins and bolt with 1/4-20 x 3/4 socket head cap screws and 1/4" light washers. Figure 13 shows the partial assembly up to this point. (Assembly Stand not shown)

(8) Place top plate and coil for upper shaker in place (note alignment letter "C"). Line up with roll pins and install 1/4-20 x 3/4 socket head cap screws.

(9) Place bottom plate and coil for lower shaker in place (note alignment letter "D"). Line up with roll pins and install 1/4-20 x 3/4 socket head cap screws. Figure 14 shows the assembled AAD shaker sub-system.

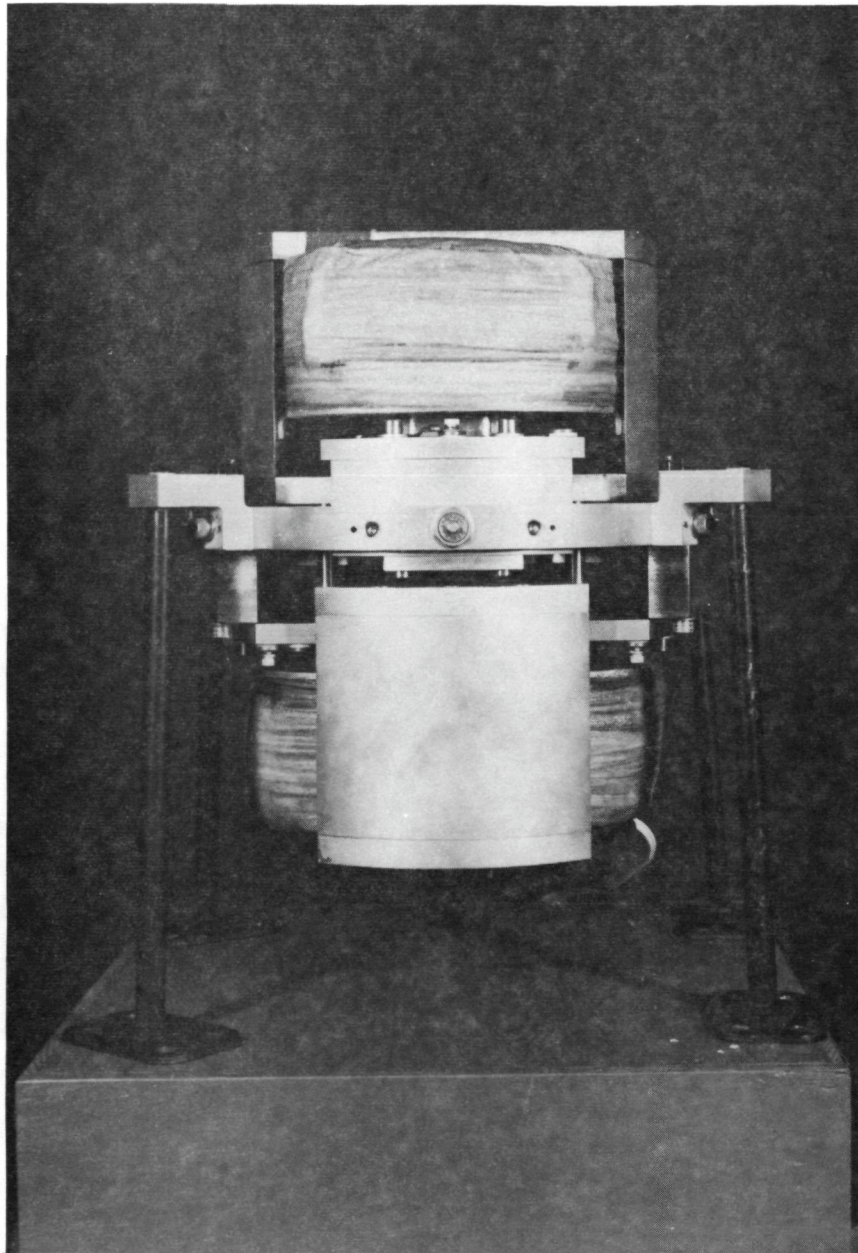


Figure 14    Force Generator Assembly  
On Assembly Stand

## Section 4

## POWER AMPLIFIERS

4.1 Requirements

The AAD shakers are to be driven by power amplifiers which, on account of low frequency stability considerations, must be direct-coupled. The actual power amplifier selection process was closely related to many other tasks of the overall development program, and in particular, was directly involved with the shaker design process. After the shaker design was firmly established, however, the performance requirements could be clearly stated as follows:

- |     |                                    |  |
|-----|------------------------------------|--|
| (1) | Minimum Output Current             | $\geq 35$ amps (0-pk)<br>24.7 amps (rms)     |
| (2) | Minimum Output Voltage Swing       | $\geq 13.5$ volts (0-pk)<br>9.55 volts (rms) |
| (3) | Minimum Load (Resistive Component) | $\leq 0.3$ ohms                              |
| (4) | Bandwidth ( $\pm 0.5$ dB)          | $\geq 0 - 200$ Hz                            |

Since the immediate application of the AAD system was to be the Saturn IB/LC-39 GWL tests at LaRC's 16 ft. TDT and since tunnel time at this facility is extremely costly, an additional requirement is that equipment must be as reliable as possible to minimize the probability of breakdown during wind tunnel tests. Furthermore, if a breakdown does occur, the equipment must be easily repairable in the field.



At the time when the power amplifier was to be procured, there were only two makes of direct-coupled power amplifiers with power capabilities in the required range: Unholtz-Dickie Corporation's Model TA100A series and Ling Electronics' Model TP850. UD's TA100A was selected on account of its higher output power capability which was expected to provide additional margins of safety.

#### 4.2 UD TA100A Specifications

The UD TA100A is shown in Figure 15. Published specifications for the unit are:

##### ELECTRICAL

Output:	Voltage - 45 v rms, 63.6 v 0-pk. Current - 35 amps, rms, 49.5 amps 0-pk.
Power Output:	1500 VA
Allowable Load:	Any power factor from 0.4 leading to 0.3 lagging with 0.2 ohm resistive component or greater. Full current delivered to any load of 0.2 ohms to 1.3 ohms. Load must be floating or balanced with respect to ground.
Output Stage Dissipation:	Transistor rated dissipation 4 KW. Sink rated dissipation 3 KW.
Input:	Differential input available. Full output obtained with 3.5 V rms single ended input. Input attenuator supplied for use with conventional servos (10V output).
Input Impedance:	10 kohms
Frequency Response:	$\pm 0.5$ dB d-c to 10 kHz

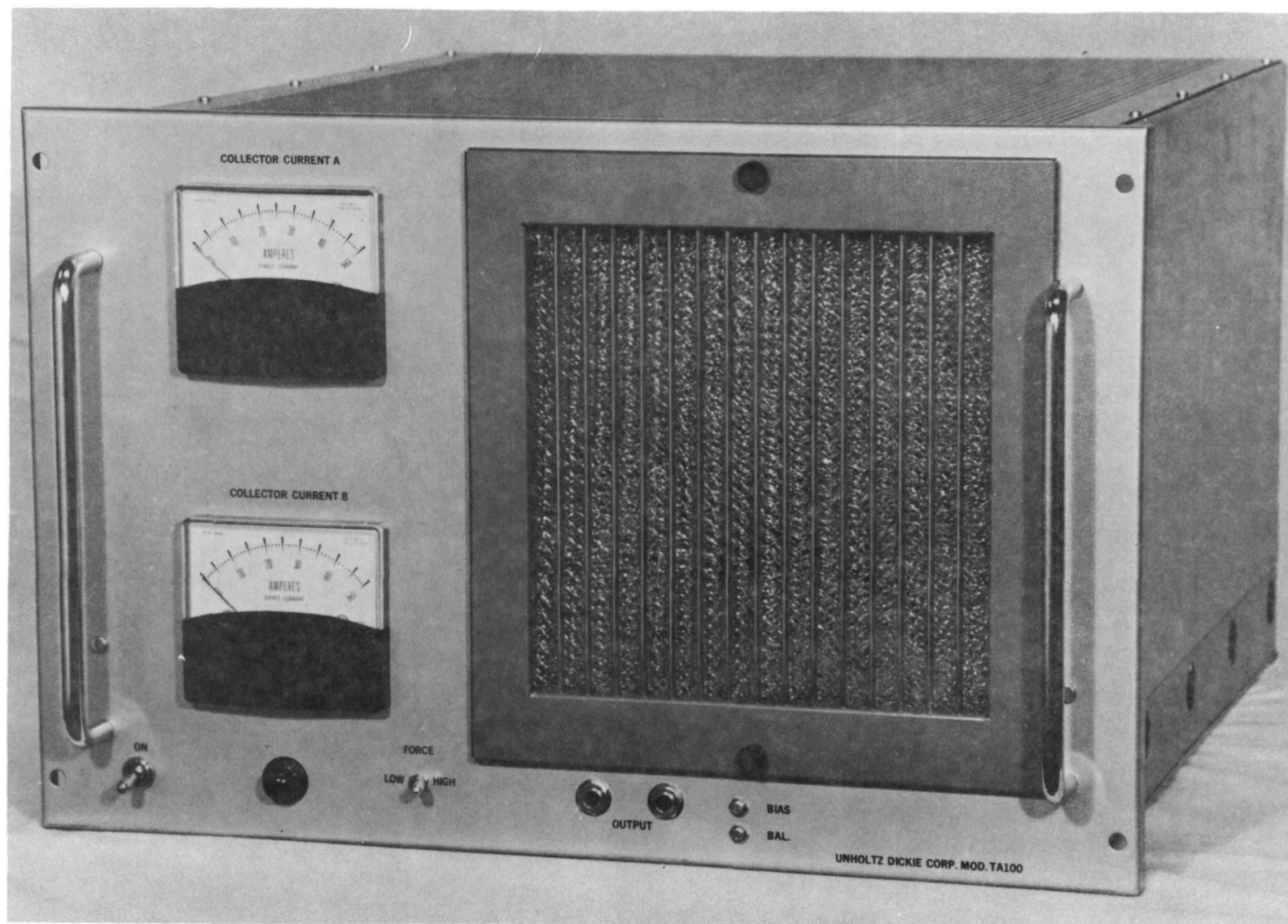


Figure 15 Power Amplifier



ELECTRICAL (Continued)

Max. Power vs Frequency:	Rated output from 5 Hz to 3000 Hz; decreasing to 45% of rated current and voltage at 0.5 Hz; and 35% of rated current and voltage at DC
Distortion:	Less than 1% for matched resistive load from d-c to 3 kHz
Circuitry:	All solid state circuit uses silicon transistors and rectifiers exclusively
Protective Devices:	(a) Instantaneous electronic current limiting (b) Maximum current shutdown rated at 115% (c) Thermal monitors on heat sinks for overtemperature shutdown
Metering:	Output stage current meter monitors each half of push-pull output
Front Panel Controls:	Bias adjustment Potentiometer. Zero Set Potentiometer. (This control allows adjustment of the d-c output from +10 to -10 V for zero input) On-Off Switch and Pilot Light. Output Voltage Monitor Jacks.

PHYSICAL

Size:	19" Rack mounting with 12-1/4 panel height, 19-1/2 depth plus 2-1/2" for cable connections at rear
Cooling:	Forced air cooled with integral blower and filter. Air inlet on front panel. Reusable filter removable from front
Input Power:	3 phase, 60 Hz, taps at 200 to 480 V, 2.3 KW. 115 V, single phase, 1 amp control circuit

PHYSICAL (Continued)

Connections:  
(Rear of Chassis)

## Inputs:

Signal	- 2 each BNC
Power	- AN3102A-18-4P
Control	- WK-4-32S

## Outputs:

NK-P4-32S

Weight: 125 pounds

4.3 Power Amplifier Wiring

The TA100A and its load are protected against overcurrent, over voltage, excessive bias and d.c. drift, and over temperature via quick-acting fuses and via electronic sensing and automatic power shutdown. This is accomplished by five relays located within the power amplifier chassis. When an anomalous operating condition occurs, one of the relays will open, breaking an additional relay circuit which holds the magnetic contactor through which the basic 3-phase power to the unit is applied. Wiring for the 3-phase power is shown in Figure 16.

4.4 Current Pumping

The resistance of the AAD shaker force coil can increase by as much as 41% as the operating temperature of the coil increases from 70°F to 255°F. For a given voltage (ac or dc) the resulting current and output force will vary by the same percentages. Therefore, the power amplifier operating as a voltage device cannot be expected to provide consistent damping.

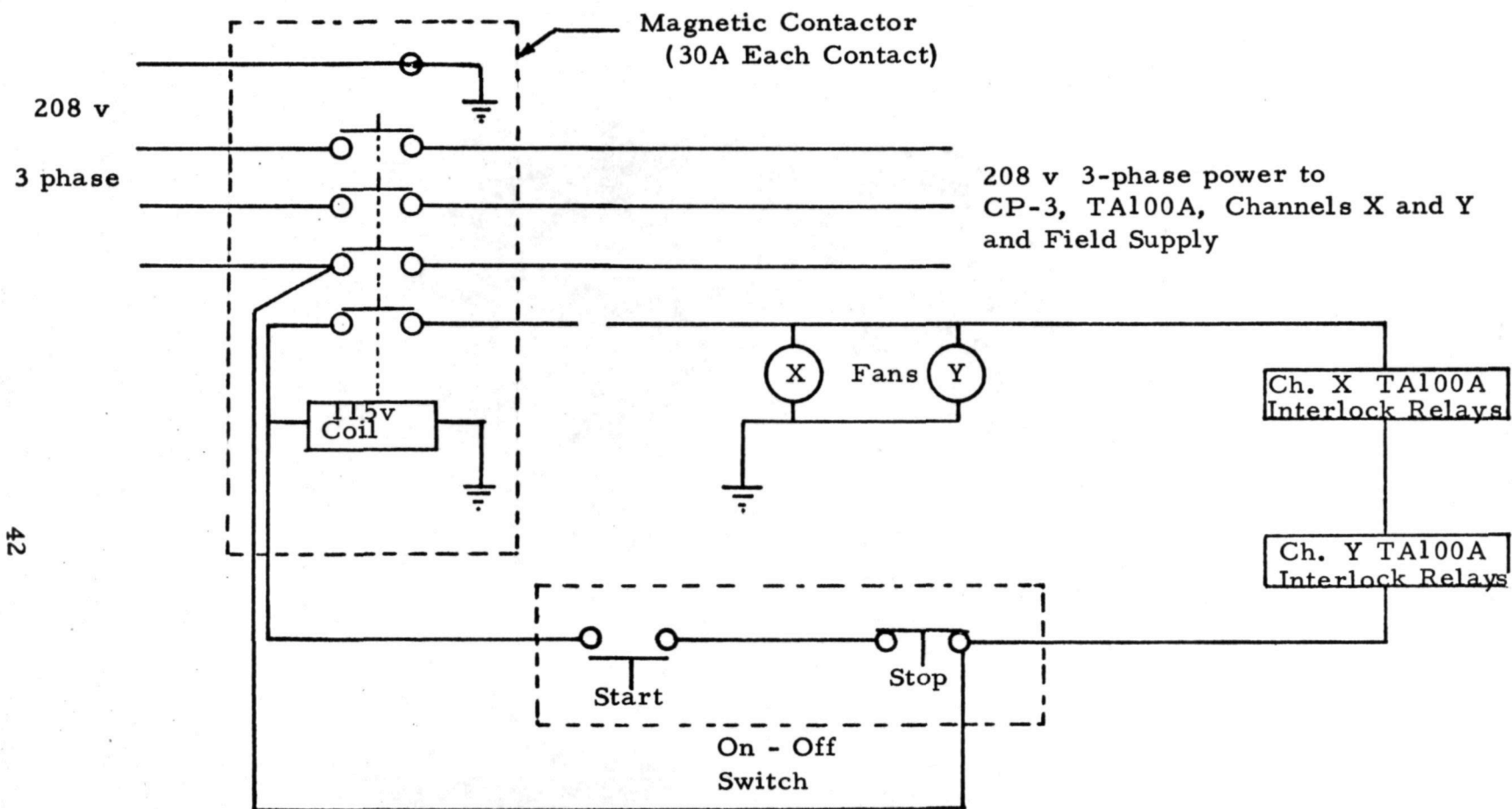


Figure 16 208 v, 3-Phase Power Wiring Diagram

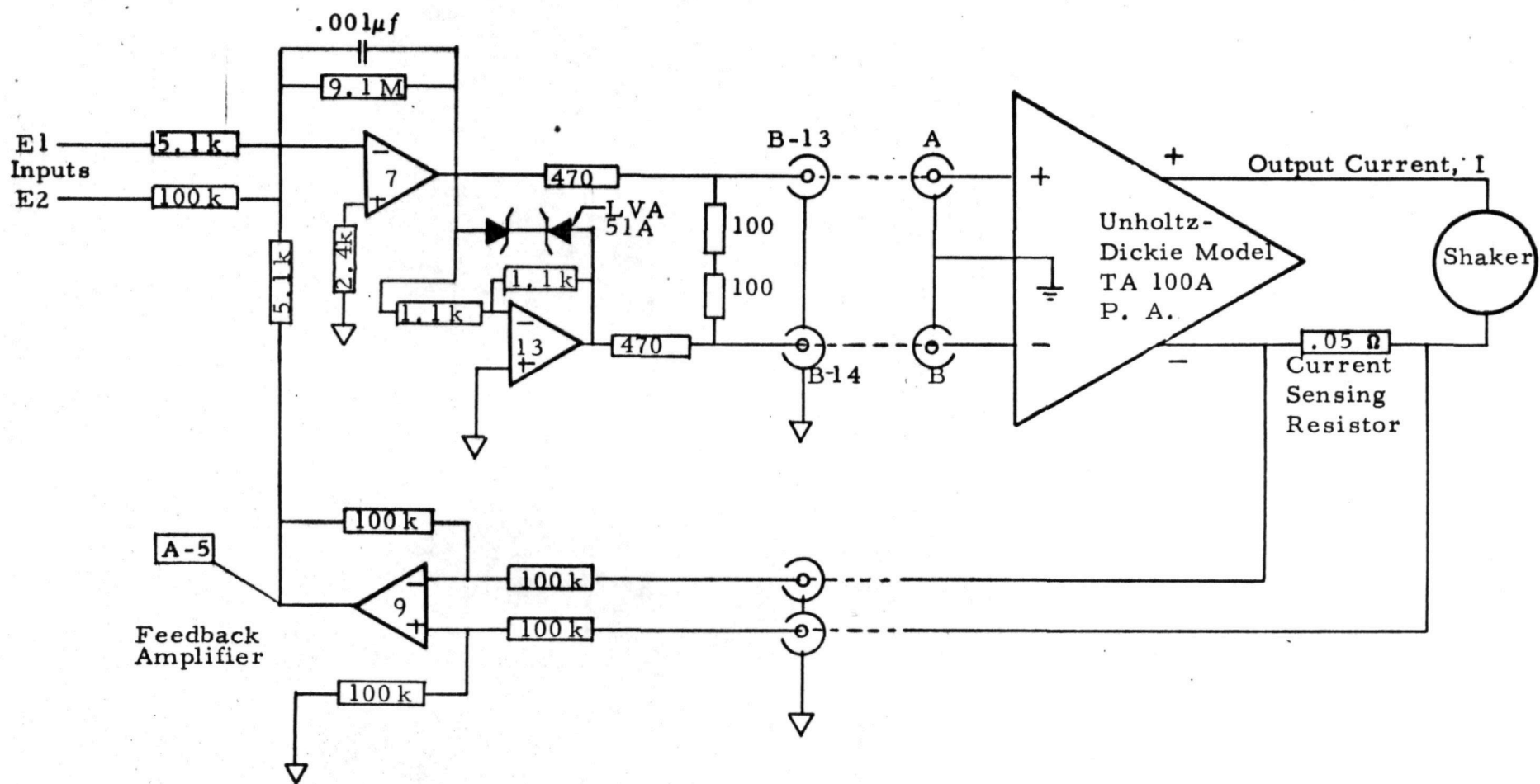


However, the power amplifier can be converted to a current control device by current feedback, i. e., by sensing the actual output current and using negative feedback techniques. The resulting "current pump" will deliver a specified amount of dynamic current according to an input voltage command signal regardless of the load impedance and the back emf. The "current pump" design is shown in Figure 17 and produces a 20-amp output current for each volt of input voltage.

#### 4.5 Trouble-Shooting Procedure

As stated previously, the TA100A will automatically shut down when safe operating conditions are exceeded. When such an event occurs, the following trouble shooting procedure should be followed to locate and correct the problem:

- (1) Turn off 208 3-phase power, wait for at least 10 minutes.
- (2) Turn both Balance and Bias Controls (front-panel controls) fully CCW.
- (3) Turn Balance Control 12-1/2 turns CW.
- (4) Turn Bias Control 18 turns CW.
- (5) Pull out pre-amplifier card (PC-1, UDC Dwg. D7467) which is located on underside of chassis.
- (6) Pull out both 1-amp fuses to driver stage (between Rel01 and 100 ohm base resistors to Transistors Q17 and Q18).
- (7) Pull out all six KAW 10 output fuses from power stage.
- (8) Pull out +46-volt Power Supply card (PC-2).
- (9) Check all semiconductors and passive elements on PC-2. Replace all damaged components.



(10) Check, and replace if necessary pass transistors Q54 and Q56 and all transistors in the driver and output stages (electrode to electrode resistances, forward and backward).

(11) Check all passive loads of the  $\pm 46$ -volt power supply for shorted loads.

(12) Check all coils and contacts of Relays 101, 102, 103, 104, and 105.

(13) Replace PC-2.

(14) Turn on 208 3-phase power

(15) Measure outputs of  $\pm 46$ -volt supply. They should be within  $\pm 1$  v of the  $\pm 46$ -volts.

(16) Turn off 208 3 phase power.

(17) Check all semiconductors and passive elements on PC-1. Replace all damaged components.

(18) Insert PC-1.

(19) Apply 208 3-phase power.

(20) Measure output voltages of pre-amp. Should be less than 20 v with respect to ground.

(21) Adjust Balance Control to bring positive and negative outputs to equal values with respect to ground (e.g., +5 v at each terminal).

(22) Adjust Bias Control to bring pre-amp outputs to +2 v and with respect to ground.

(23) Turn off all ac power.

(24) Insert 1A fuses.

(25) Apply 208 3-phase ac power.

(26) Measure pre-amp output voltages.

(27) Turn off all ac power and wait at least 10 minutes  
(to discharge  $\pm$  75-volt power supply filter capacitors).

(28) Insert KAW 10 fuses.

CAUTION: DO NOT ATTEMPT TO TURN ON THE POWER  
AMPLIFIER AFTER SHUTDOWN WITHOUT GOING THRU THE  
ABOVE PROCEDURES AS ADDITIONAL DAMAGES WILL BE  
CAUSED.

CAUTION:  $\pm$  75-VOLT POWER SUPPLY FILTER CAPACI-  
TORS HAVE LONG DISCHARGE TIMES. DO NOT CAUSE  
DISCHARGE THRU OUTPUT TRANSISTORS - EVEN WHEN  
AC POWER HAS BEEN TURNED OFF.



## Section 5

### DAMPER CONTROLS

Components in the Damper Controls sub-system perform the following functions in the Damper Mode of operation: (a) sensing model accelerations, (b) signal conditioning, (c) converting (integrating) acceleration signals into velocity signals, (d) providing gain (damping) variation, (e) power amplification to drive the shakers, and (f) providing monitoring signals (response and damper force output data). Figure 18 is a simplified block diagram showing major components of the sub-system. The power amplifiers have already been described in detail. All other components are described below. Control electronics for (c), (d), and (f), as well as for performing several other functions are located on a single chassis. Its front panel is the Damper Control Panel or the DCP, see Figure 19.

#### 5.1 Accelerometers

Two accelerometers of different types are provided for each damper channel. Both types are products of MB Electronics (Models 303 and 354). The Model 303 is a standard piezoelectric sensor with a nominal sensitivity between 10 - 20 pcg/g, and is compatible with most charge amplifiers. The Model 354 has built-in electronics and must be used with one of MB's signal conditioner-preamplifiers. The advantage of the integral sensor-electronics is that the motion of the cable between the sensor and the preamplifier does not affect the output of the sensor. This result is achieved by lowering the output impedance of the sensor with built-in electronics.

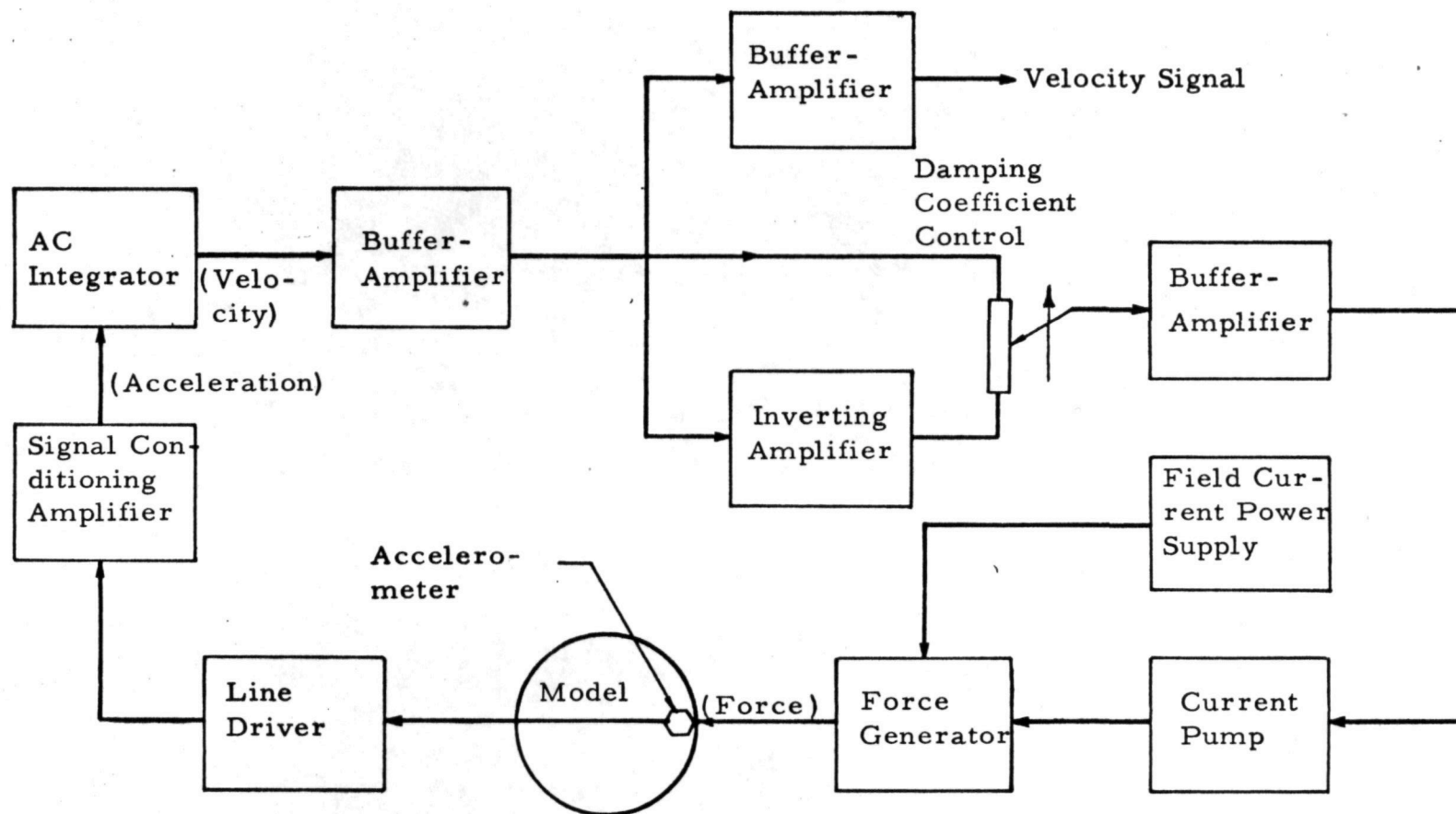


Fig 18 Damper Controls System Block Diagram (One of two channels).

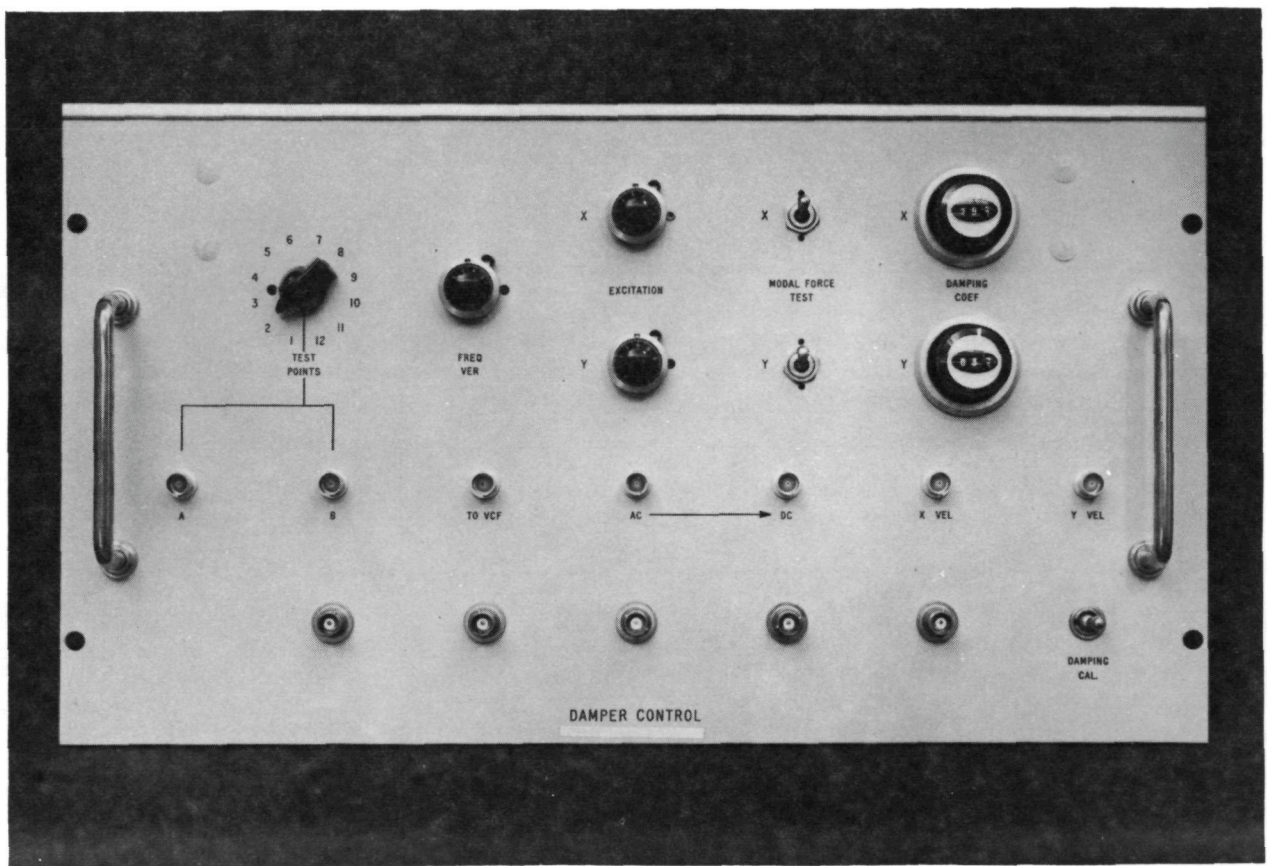


Figure 19 Damper Control Panel



The major disadvantage of this approach is the lowered tolerable operating temperature: 150°F maximum. The Model 303 withstands a maximum ambient temperature of 500°F. Most damper calibration tests were conducted with the Model 303.

## 5.2 Signal Conditioner - Preamplifier

MB Electronics' Zero Drive electronics are used for the accelerometers. The preamplifier is the Model N400. For the Model 303 accelerometer, a separate, impedance-lowering Line Driver is required. The output of the Line Driver is a current which is proportional to the acceleration being measured. The overall output is independent of the impedance of the cable (and its dynamic variations) between the Line Driver and the N400. However, the cable between the Model 303 and the Line Driver is still vulnerable, and distortions and errors due to "cable whipping" are still possible. The Line Driver is included in the Model 354 so it is used directly with the N400.

Four channels of N400 are provided in the Damper Controls sub-system. Each unit provides ranging, sensitivity normalization, and selective bandpass filtering. Three parallel outputs are provided by each amplifier in addition to a front-panel meter indication of the peak or rms acceleration.

Specific transducer-amplifier pairings used in the calibration tests are listed in Table III.



Table III Accelerometer-Amplifier Sensitivities for AAD Calibration

Model Config	Accelerometer			N400 Amplifier			Overall Sensitivity
	Type	S/N	Sensitivity	Range	Sensitivity	Filter	
1, 2, 4, 5, 7, 8 X	303	149266	11.8 pcb/g	10g f. s.	11.8 pcb. g	H. P. 5Hz	10g/volt
1, 2, 4, 5, 7, 8 Y	303	162952	16.0 pcb/g	10g f. s.	16.0 pcb/g	H. P. 5Hz	10g/volt
6 X	303	149266	11.8 pcb/g	3g f. s.	23.6 pcb/g	H. P. 5Hz	6g/volt
6 Y	303	162952	16.0 pcb/g	3g f. s.	32.0 pcb/g	H. P. 5Hz	6g/volt
3 X	354	140	24 mv/g	10g f. s.	24 mv/g	H. P. 5Hz	10g/volt
3 Y	354	138	21.8 mv/g	10g f. s.	21.8 mv/g	H. P. 5Hz	10g/volt

### 5.3 AC Integrator

Two channels of electronics for integration of the N400 output form the input stage of the Damper Controls proper. Each integrator consists of a dc blocking input, a passive R-C integrator and a high impedance buffer amplifier. Measured frequency response of the integrator is shown in Figure 20. It is seen that for frequencies above 5 Hz true integration is achieved.

The integrator output is a voltage signal proportional to the instantaneous velocity of the model at the Damper Station.

### 5.4 Damping Coefficient Controls

The polarity and overall amplification of the velocity signal from each integrator is controlled by a 10-turn potentiometer which is located on the upper right-hand corner of the DCP and is identified by the label "Damping COEF" (X or Y). This control will be referred to as the Damping Coefficient Control, or simply DCC.

The control circuitry is shown in Figure 21. The inverting amplifier stage preceding the DCC has a gain of -1.98 so that a null voltage output is obtainable. The DCC dial is graduated from 0.000 (fully CCW) to 1000.0 (fully CW). The two actual null positions are 349.9 for the X-channel and 339.1 for the Y-channel. Dial settings greater than null results in positive damping, and vice versa. The potentiometer output is further amplified by a buffer-amplifier by a factor of 20.6.

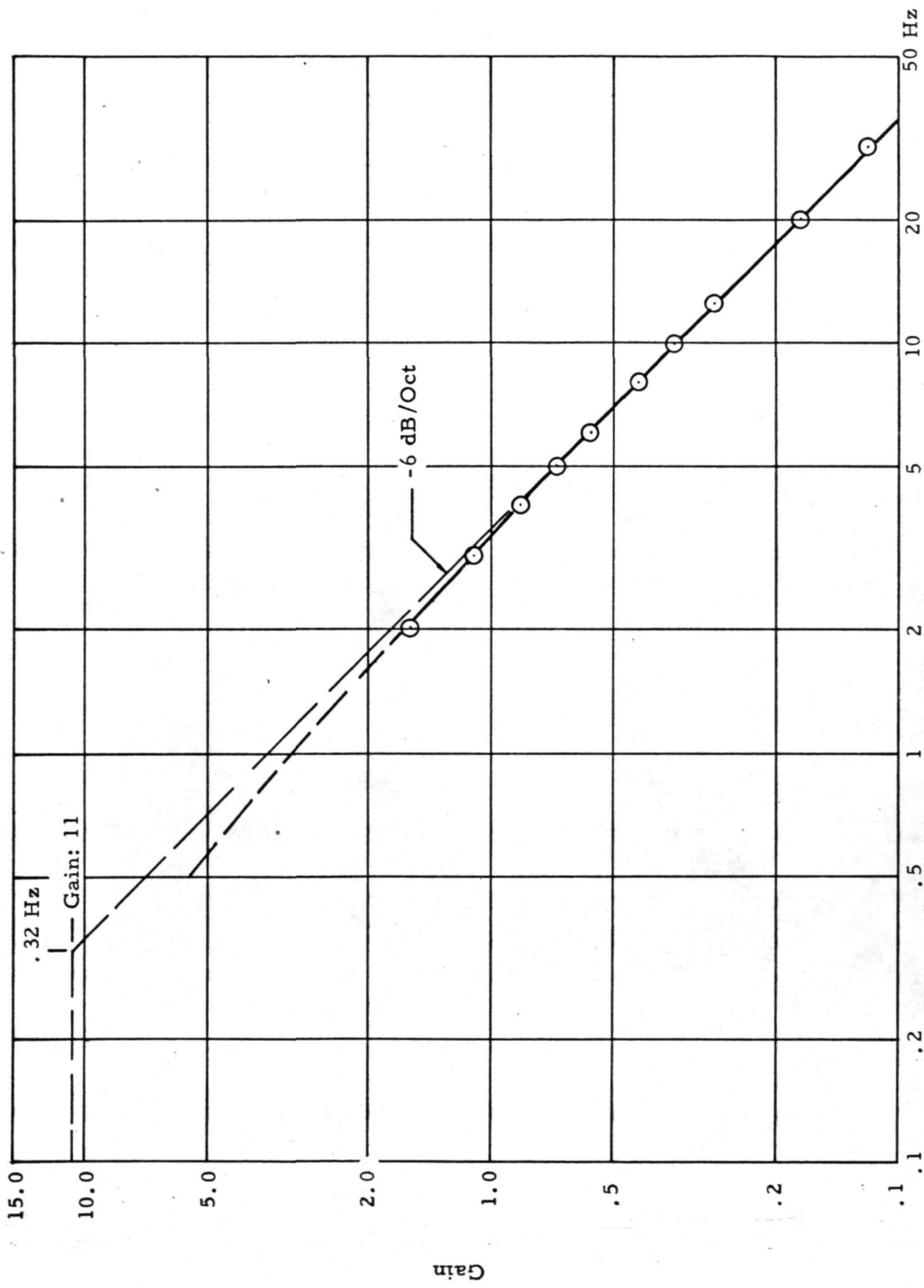


Fig 20 Measured Integrator Frequency Response Curve

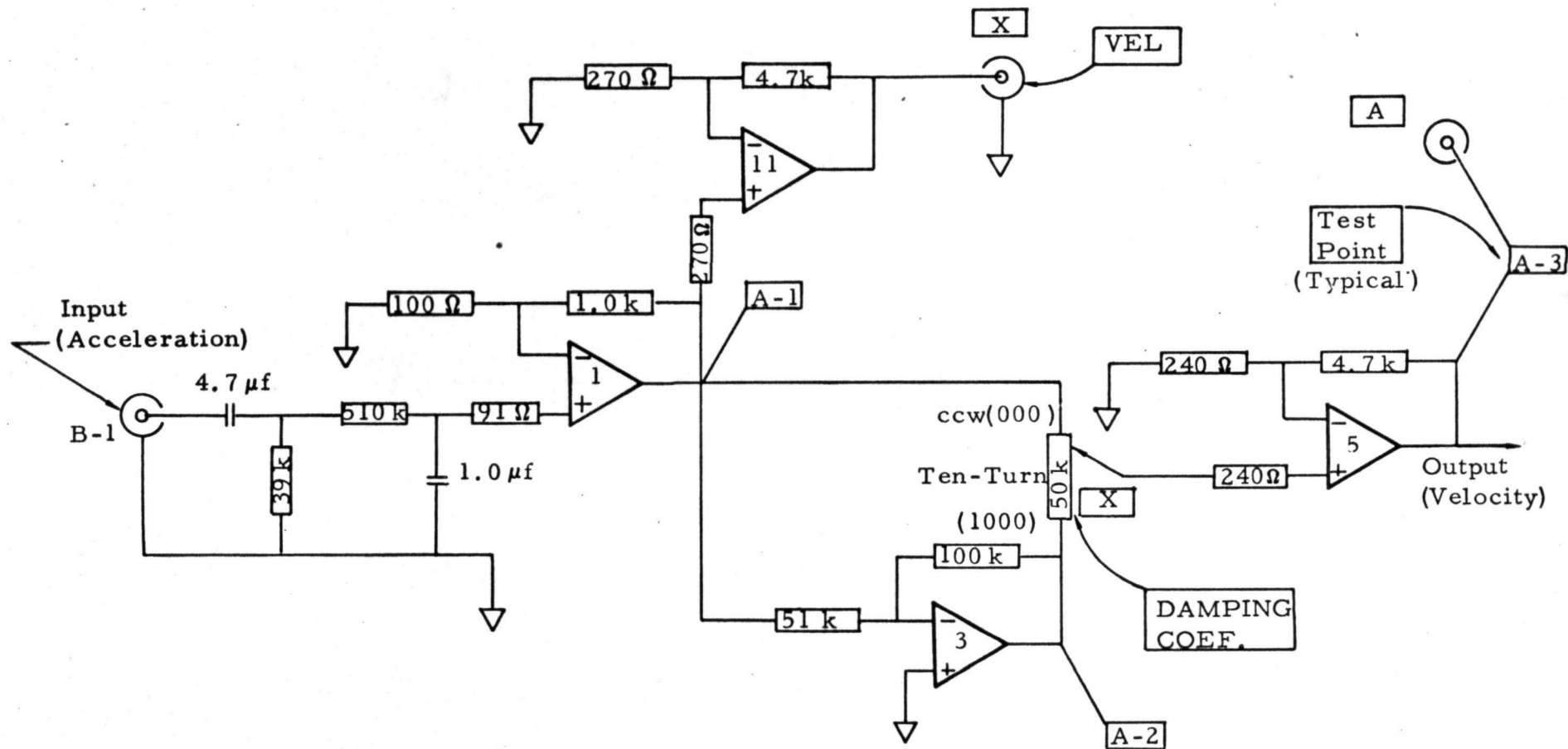


Fig 21 Integrator-Damping Coefficient Control (DCC) Stages

### 5.5 Field Supply

The shaker electromagnets are connected in series and draw a 3.0-ampere current from a regulated dc power supply -- Model 160-15, Electronic Measurements Division, the Rowan Controller Company. The capability of Model 160-15 is 160v dc at 15 amperes. The front panel meters on the unit itself are used to set up the required field current.

### 5.6 System Block Diagram

Figure 22 is a block diagram showing the Damper Mode of operation of the AAD.



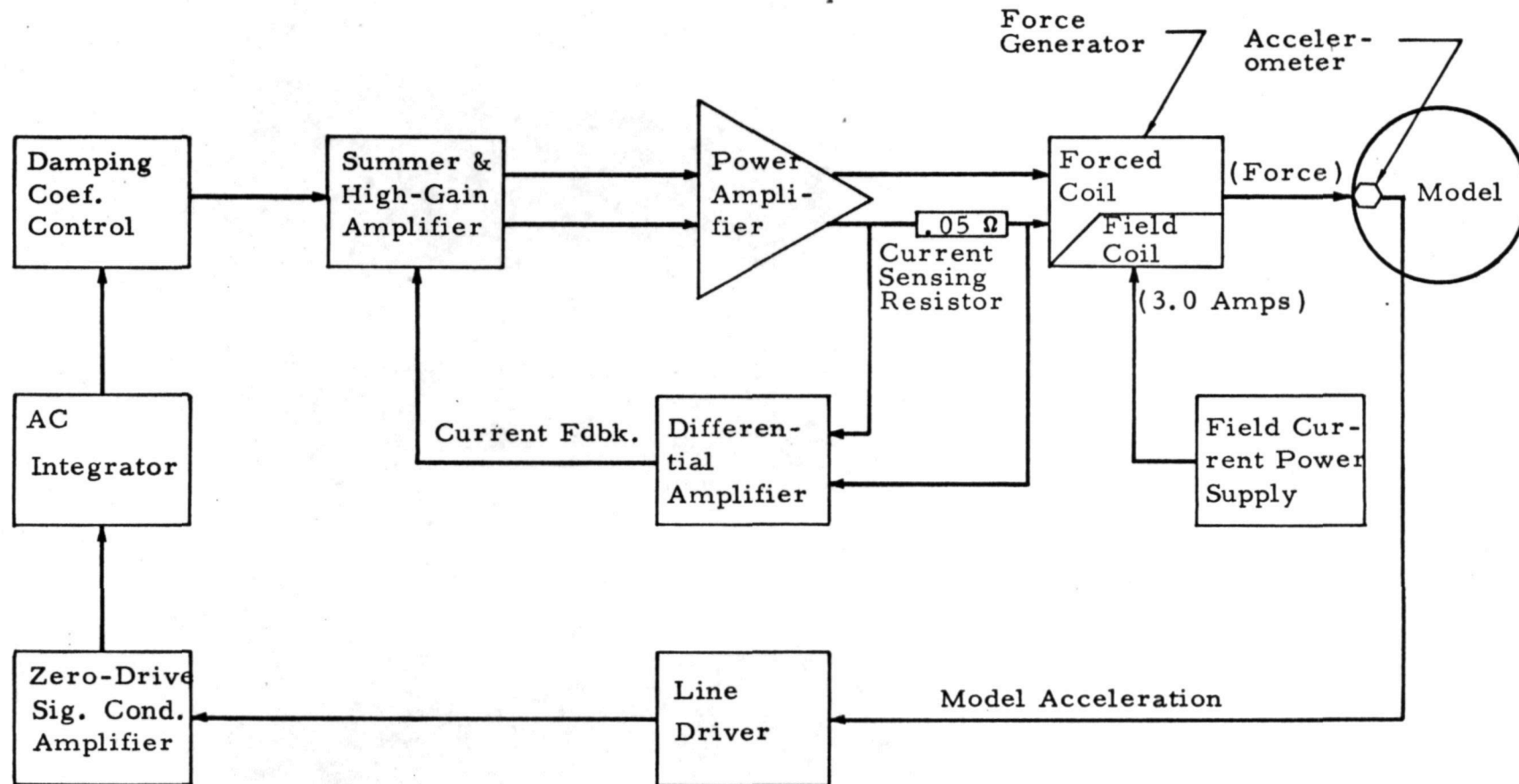


Fig 22 Damper Mode System Block Diagram

## Section 6

## VIBRATION TEST SYSTEM

The AAD system contains most of the essential components for conducting vibration checkout of the model. The following additional equipment was incorporated in the design to accomplish this purpose.

### 6.1 Signal Source

An Exact Model 123 Waveform Generator is used to supply a sinusoidal signal to drive the power amplifier-force generators, and to supply a square wave for triggering and timing purposes. The Model 123 is a Voltage Controlled Function Generator (VCF) which, in addition to self-contained front panel controls, may be controlled by an external dc voltage. The output signal frequency of the Model 123 in the AAD is determined by the combined setting of its panel controls and a second, vernier control voltage derived from a highly regulated power supply via a 10-turn potentiometer located on the DCP which is identified by the label "FREQ VERNIER". The control voltage is obtained from the BNC jack labeled "TO VCF". The resulting frequency resolution under manual control of the potentiometer is virtually infinite.

The short term (10-minute) frequency stability of the Model 123 was measured and the frequency was found to vary less than 0.036% of the set value.

The maximum output voltage of the VCF into a 50 ohm load is 5.0 volts, 0-peak.

In the Vibration Test mode of the AAD system, the sinusoidal output of the VCF is summed with the velocity signal at the input of the current pump for each channel. The resulting signal is ultimately converted into a force on the model containing both excitation and damping components. The excitation amplitude of each channel is set by a 10-turn potentiometer whose control is identified as "EXCITATION" (X or Y) on the DCP. The excitation amplitudes of both channels are also controlled simultaneously by the VCF Output Level Control on its own front panel.

For conducting damping calibration tests, the sinusoidal excitation signal may be cut off by a toggle switch identified by "DAMPING CAL" on the lower right-hand corner of the DCP.

## 6.2 AC-to-DC Converter

A band-limited ac-to-dc converter was incorporated in the system to provide accurate digital readout capability of low frequency ac signal amplitudes during vibration tests and calibration. A Burr-Brown Model 4128 True RMS detector module was used with a bandpass input filter ( -3dB frequencies of 6 Hz and 36 Hz). Figure 23 is a detailed schematic of the filter-converter circuit whose measured frequency response curve is shown in Figure 24.

This input filter may be bypassed to allow true rms measurement of random signals. The sensitivity of the rms converter is set to 0.948 volts rms input per 1 volt dc output. The input to the



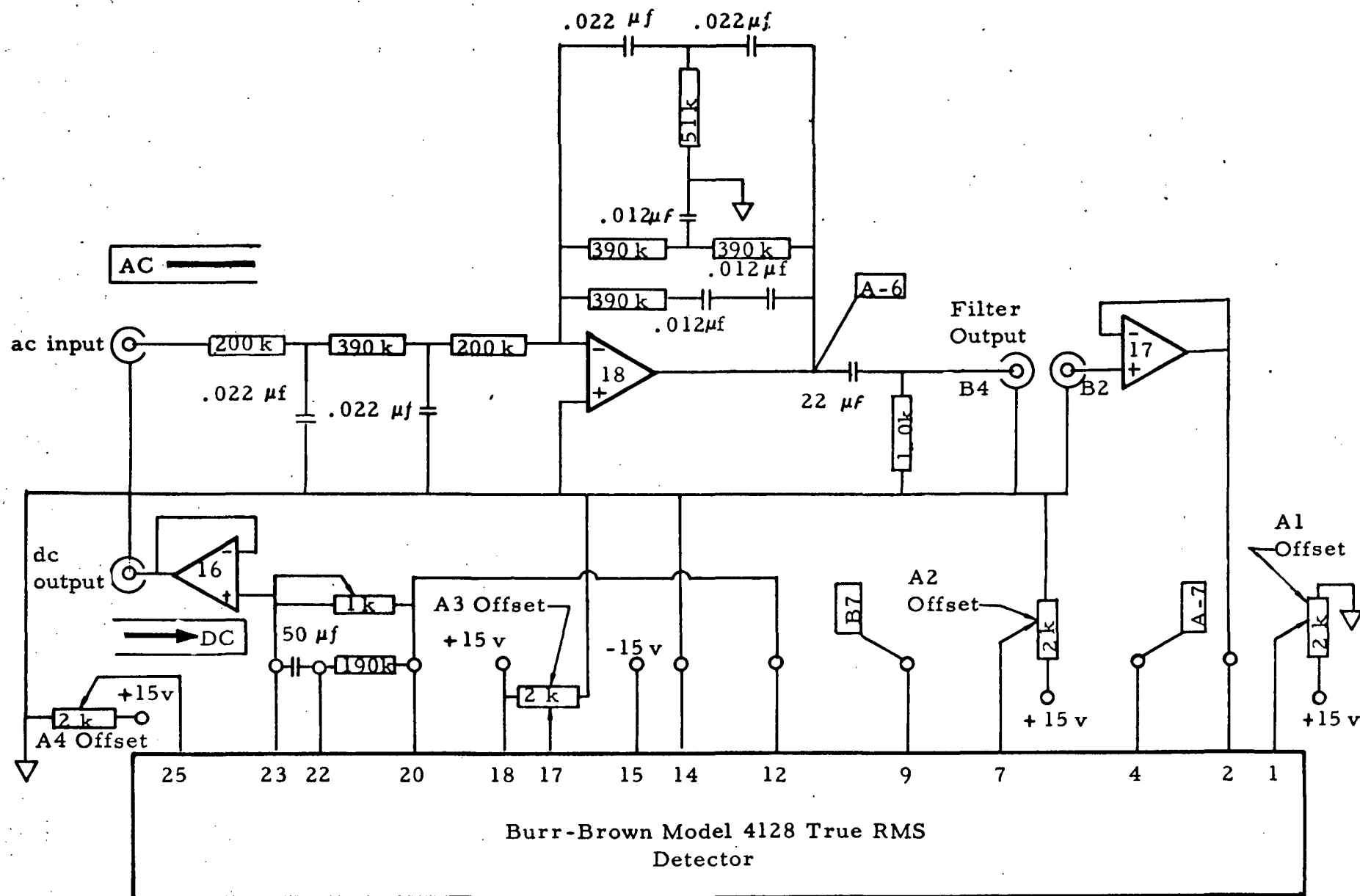


Fig 23 AC-To-DC Converter with Filter Input Stage

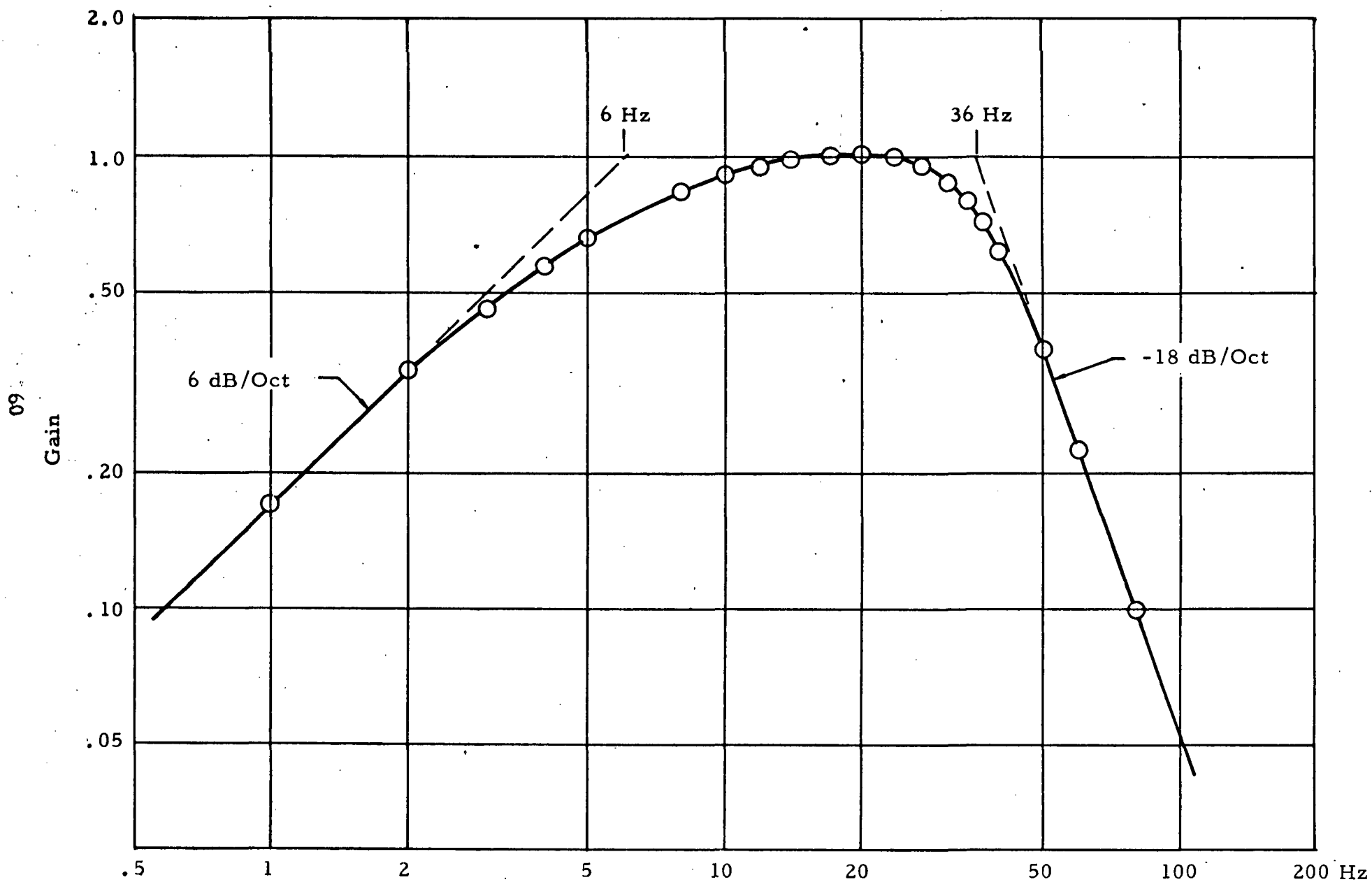


Fig 24 Measured Frequency Response Curve for Filter-Converter

ac-to-dc converter is a BNC jack on the DCP identified by the label "AC →". The dc output is available from another BNC jack identified by the label "→DC".

### 6.3 Digital Multimeter

A 3-1/2 digit multimeter (Eldorado Model 1800) is also included in the Vibration Test sub-system. All vibration tests and damper calibrations were conducted with this DMM as the primary readout device as it can measure dc volts, ac volts (40 Hz to 20 KHz), ac, dc current and resistance. The accuracy of this DMM is 0.1% of full scale and the display rate is 5 readings per second.

### 6.4 Oscilloscope

A two-channel, low frequency CRT oscilloscope (Hewlett-Packard Model 1205B) is included in the system for signal monitoring and for finding and establishing vibration test conditions. The band width of the 1205B is 500 KHz and the maximum sensitivity is 5 mv/cm.

### 6.5 Electronic Counter - Timer

A Monsanto 100B Electronic Counter-Timer with seven digits of display is used for vibration period measurements.

### 6.6 System Block Diagram

Figure 25 is a system block diagram of the Vibration Test Mode.

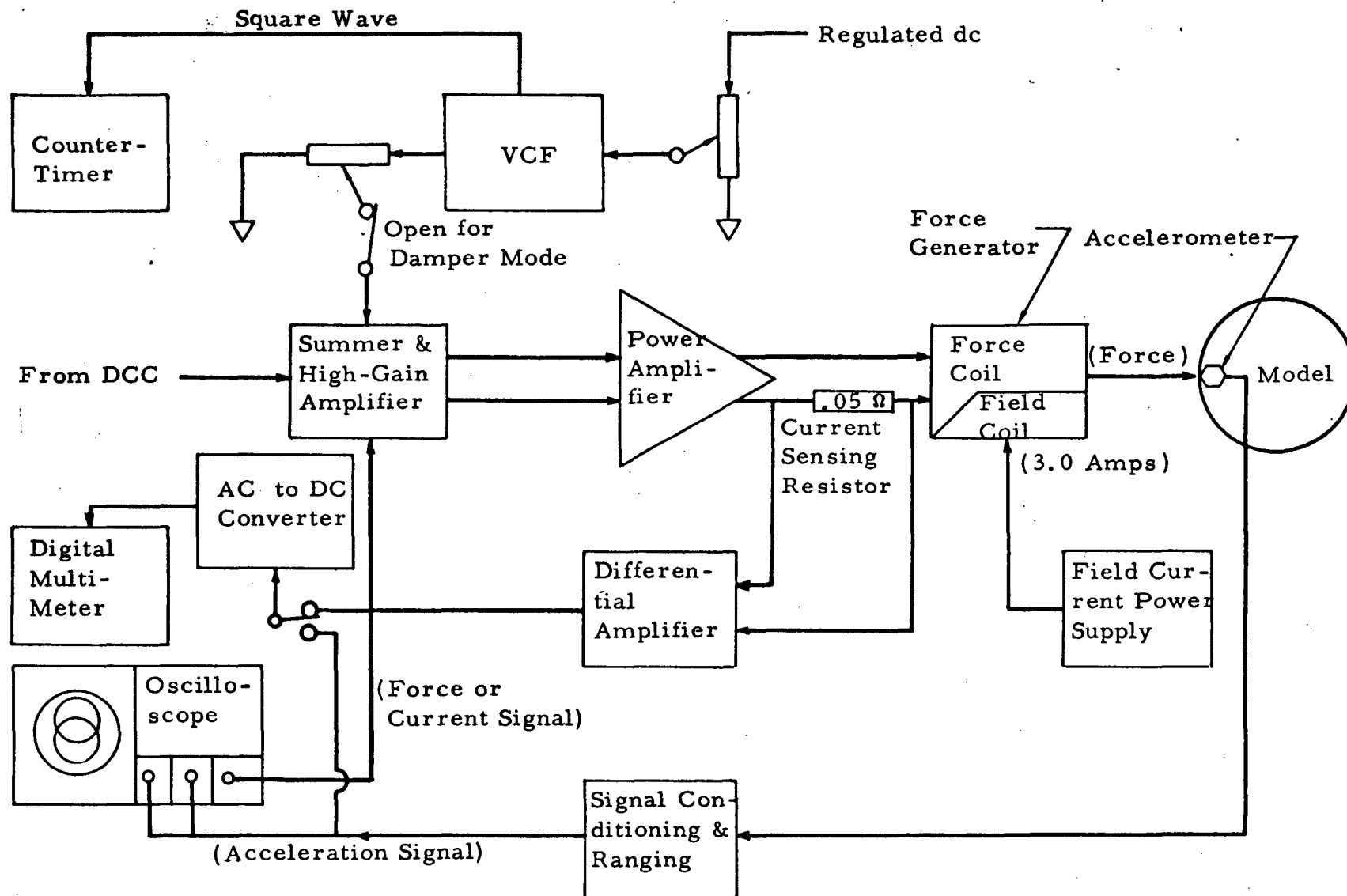


Fig 25 Vibration Test Mode System Block Diagram

## Section 7

## OPERATING PROCEDURES

7.1 Warm-Up and Offset Adjustments

The following warm-up and zero adjustment procedures are recommended before each start-up after prolonged system shut-down.

- (1) Short both inputs of each power amplifier to ground (i.e., ground inputs A and B of each TA100A).
- (2) Connect a 2-ohm power resistor in series with the load (shaker force coil).
- (3) Connect field coils to field power supply (EM Model 160-15) which is to be operating in the Local Control, Local Sensing Mode.
- (4) Turn both front panel controls (current and voltage controls) of the 160 - 15 counter-clockwise to zero. Set Power Switch to OFF position.
- (5) Connect all accelerometers to MB N400 zero Drive Amplifiers.
- (6) Short DCP rear panel jacks (B-1), (B-2), (B-3), (B-8), B-9), (B-10), and (B-11) to ground.
- (7) Patch + 15v op amp power supply output to (B-5) and - 15v output to (B-7).
- (8) Set DCC-X to 349.9 and DCC-Y to 339.1 (null positions).
- (9) Set Excitation Level controls on DCP to 0.000 (zero output).
- (10) Patch TA100A output voltage monitor signals to oscilloscope (both channels, differential mode).

(11) Apply on 115 v ac, turning on Period Counter, DMM, Oscilloscope, N400, VCF, and op amp power supply.

(12) Turn on EM 160-15.

(13) Turn on both TA100A's while monitoring output voltages on oscilloscope. If large dc offset is noticed (above 5 v, either positive or negative) shut off the 208 3-phase immediately and proceed to re-balance them according to trouble-shooting procedures outlined in Section 4.5.

(14) After turning on TA100A immediately switch from monitoring on the oscilloscope to monitoring the front panel collector current meters. If any meter reading exceeds 5 small divisions, turn off the power amplifiers and re-adjust Balance and Bias controls according to Section 4.5.

(15) Wait for a minimum of 30 minutes.

(16) Check and adjust zero reading accuracies of the oscilloscope, the DMM and the True RMS Detector while waiting.

(17) Remove short from (B-2), connect (B-2) to (B-4). The ac to dc converter is now ready for use in further set up tests and zero adjustment of other equipment.

(18) Check zero offset of N400 outputs.

(19) Set up calibration sensitivities for N400.

(20) Verify accelerometers are functioning.

(21) Adjust output voltages of op amp power supply to  $\pm 15$  volts ( $\pm 0.01$  v, balanced to ground).

(22) Null out output voltages of all op amps to within  $\pm 5$  mv.

(23) Minimize input voltages to power amplifiers (B-13), (B-14), (B-12), and (B-15) (to approximately  $\pm 0.5$  v).

- (24) Turn off TA100A's.
- (25) Immediately connect inputs to TA100A's and connect output current signals to (B-8), (B-9), (B-10), and (B-11), and N400 outputs to (B-1) and (B-3).
- (26) Turn on TA100A's while making sure that there is no significant input offset voltage from the DCP.
- (27) Set output of the 160-15 to 3 amps for the field coils.
- (28) The AAD system is now ready for functioning checkout.
- (29) For full power operations, remove or short out the 2 ohm series resistors to the armature coils.

## 7.2 Set Up For Model and Damper Calibration

- (1) Set VCF output to Maximum, adjust front panel control until output sine signal is symmetrical with respect to ground.
- (2) Set VCF output to minimum.
- (3) Patch VCF output to DCP rear connector (B-5).
- (4) Patch between "VCF in" and "To VCF" (on the DCP).

The AAD system is ready for model vibration tests as well as for damper calibrations.

## Section 8

## DAMPER CALIBRATION

The AAD was calibrated extensively in the Saturn IB/GWL model in Building 4619, Marshall Space Flight Center. The primary objective of the calibration tests was to experimentally establish the relationship between damping of the model and the DCC dial for each model configuration to be used during wind tunnel tests.

8.1 Model Configurations

The AAD was calibrated for model configurations outlined in Table IV below:

Table IV Saturn IB/Skylab GWL Model Configurations

Configuration <sup>(1)</sup>		Fuel Configuration	Natural Frequency <sup>(2)</sup> Hz	Generalized Mass <sup>(3)</sup> , #sec <sup>2</sup> /in.
No	Scaling			
1	Primary	Empty	24.13	0.149
2	Primary	Intermediate	21.70	0.1922
3	Primary	Fully Fueled	14.69	0.418
4	60 Knots <sup>(4)</sup>	Empty	17.33	0.1835
5	60 Knots	Intermediate	15.20	0.240
6	60 Knots	Fully Fueled	10.89	0.470
7	70 Knots	Empty	14.29	0.277
8	70 Knots	Intermediate	13.09	0.325

(1) For detailed description of model configuration see Table I, Reference (2).

(2) Measured Natural Frequencies of 1st bending vibration mode.

(3) Measured Generalized Masses of 1st bending vibration mode referenced to Model Station 92.3.

(4) Maximum simulated full-scale wind velocities.



## 8.2 Calibration Methods

Both free vibration and forced vibration test methods were employed to determine modal damping of the Saturn IB model in the first bending mode. For modal damping factors less than 2% of critical damping, the exponential decay rate of a free vibration provides an accurate measurement of the damping. Free vibration tests were used to obtain primary AAD calibrations in that range of damping. At higher damping, the resonant response amplitude provided a more accurate measurement, and was relied upon to supplement free vibration test results.

The first step in a calibration series (for a given model configuration) was to set the DCC dials to the following values:

X-channel: 349.9

Y-channel: 339.1

These are experimentally determined DCC settings for zero gain in the respective channels\*.

In either free or forced vibration tests, the model was sinusoidally excited at the experimentally determined natural frequency of the first bending mode in either the X- or the Y- direction. The AAD was used in the Vibration Test mode for this purpose. Forced

---

\*If all component values of the damper system were exactly according to design, the zero gain DCC settings would be 335.5 for both channels. The noted deviations from ideal design are, however, of no concern because of the end-to-end calibration method used.

vibration data (excitation and acceleration amplitudes and resonant frequency) were recorded.

The condition of free vibration of the model was achieved by suddenly setting the excitation signal to zero after steady-state resonance had been established. Due to the current pumping nature of the power amplifying stage, the only force exerted on the model after removal of the excitation signal is that necessary to maintain the correct damping condition. Free vibration condition was therefore established by the above indicated procedure. The decaying of the free vibration was measured by the accelerometer and recorded on the CRT of an oscilloscope with memory. The display was then photographed as the permanent record of the test result from which the damping factor was to be determined.

For each DCC dial setting for which a free vibration test was run, additional forced vibration tests were conducted to determine the relationship between acceleration and excitation amplitudes at resonance. The resulting forced vibration data were to be used for experimentally establishing linearity of the model-damper combination and for calibrating the DCC dial at high damping values. The dynamic range covered by each forced vibration test series was usually 26 dB.

The above test was then repeated for the other damper channel.

The next step in the calibration was to increase the damping by increasing the gain of both damper control channels, usually by 40 - 70 divisions on both DCC dials (i. e., the second DCC dial setting calibrated was about 400.0). The entire calibration test procedure was repeated for the new DCC condition.

This procedure was repeated until maximum specified damping was reached.

The final test for each model configuration was a check of the accuracy of damper controls for establishing damping in vibrations in planes other than the X- or the Y- planes. This check was conducted with the model vibrating in a  $45^{\circ}$ -plane (with respect to the X- or the Y- plane). An additional accelerometer was employed to measure the response in the plane of vibration. Free vibration only was used for this verification test.

### 8.3 Data Reduction Methods

Photographed free vibration decay records (acceleration signals) were transferred onto semi-logarithmic graph papers by measuring and plotting the successive peaks against a number of vibration periods. Resulting graphs indicate that the model-damper combination was linear for all configurations as the curves connecting the plotted peaks were all straight lines. The slopes of these curves were used to determine damping via the following expression:

$$\zeta = (\ln A_n - \ln A_{n+m})/2m$$

where  $\zeta$  is the modal damping,  $A_n$  is an arbitrarily chosen initial acceleration peak and  $A_{n+m}$  is what remained after  $m$  cycles of free vibration.

Since the model responses were found to be linear, the following relationship is valid among the forcing amplitude  $F$ , the steady-state resonant acceleration amplitude  $A$ , the generalized mass  $m$ , and the modal damping  $\zeta$ :

$$F/A = 2 \zeta M$$

In other words,  $\zeta$  is proportional to  $F/A$ , a ratio which could be determined with good accuracy from forced vibration test records by plotting  $F$  against  $A$  and finding the slope of the best-fit straight line. Furthermore, if  $F'$ ,  $A'$ , and  $\zeta'$  are a set of values determined for the same model configuration corresponding to a low damping condition, and if  $\zeta'$  is known (say from free vibration tests), the generalized mass may be eliminated from consideration because

$$F/\zeta A = F'/\zeta' A'$$

or 
$$\zeta = \zeta' (F/A) / (F'/A')$$

which determines  $\zeta$  from steady-state tests.

#### 8.4 Damper Calibration Results

AAD calibration results are shown in Figures 26 to 33 for the eight model configurations outlined in Table IV. Because of

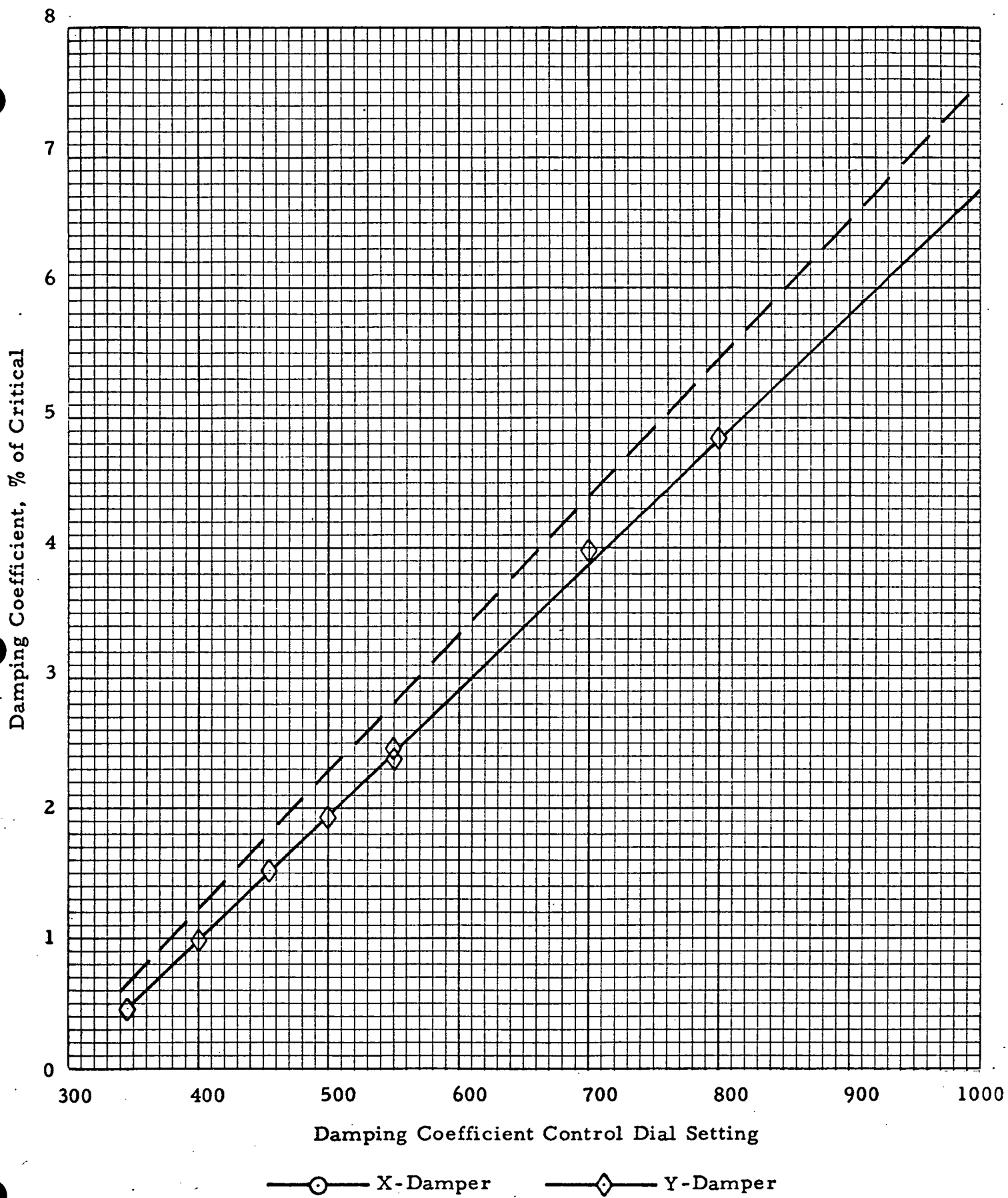


Fig 26 DCC Dial Calibration for Model Configuration 1

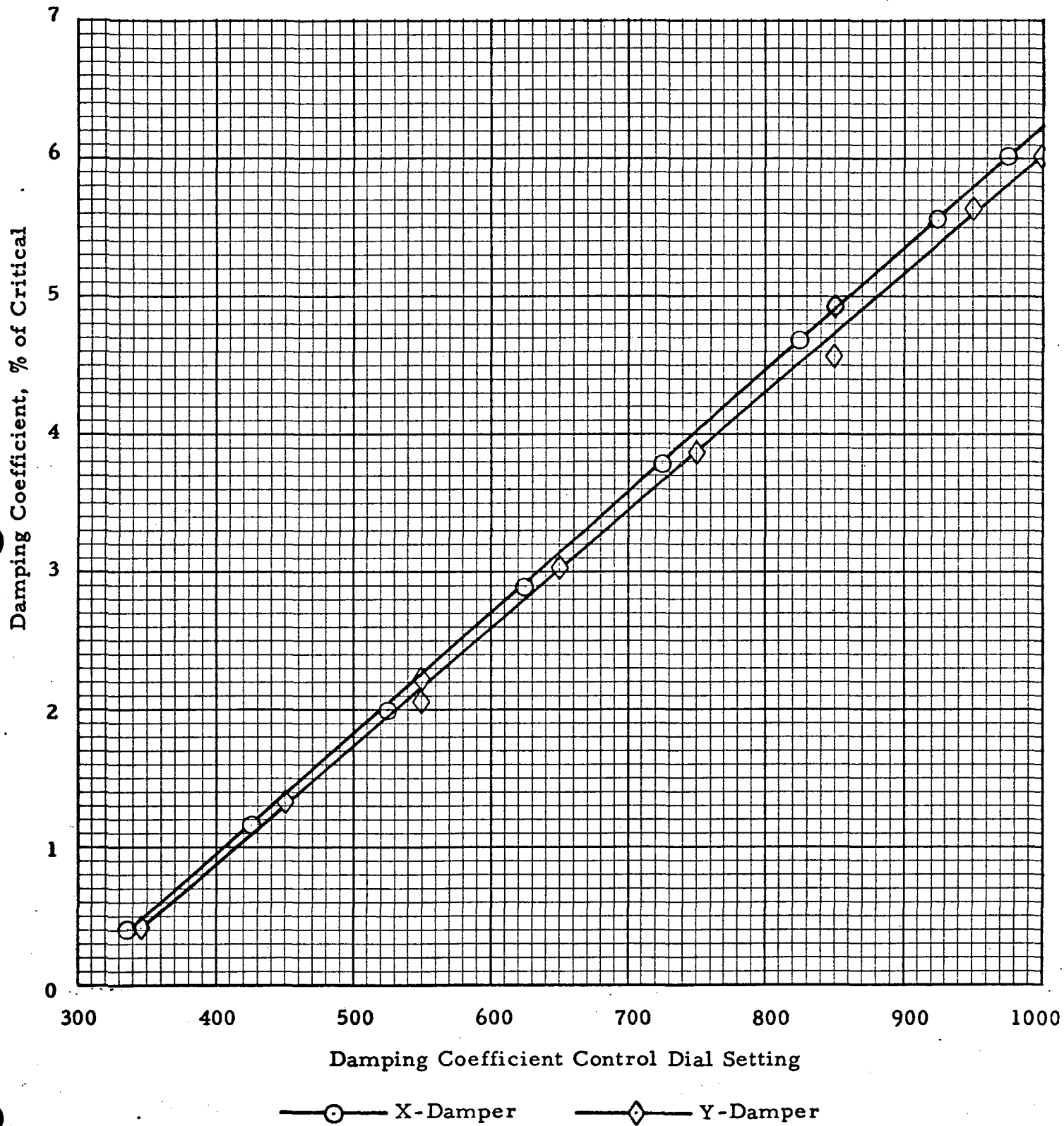


Fig 27 DCC Dial Calibration for Model Configuration 2

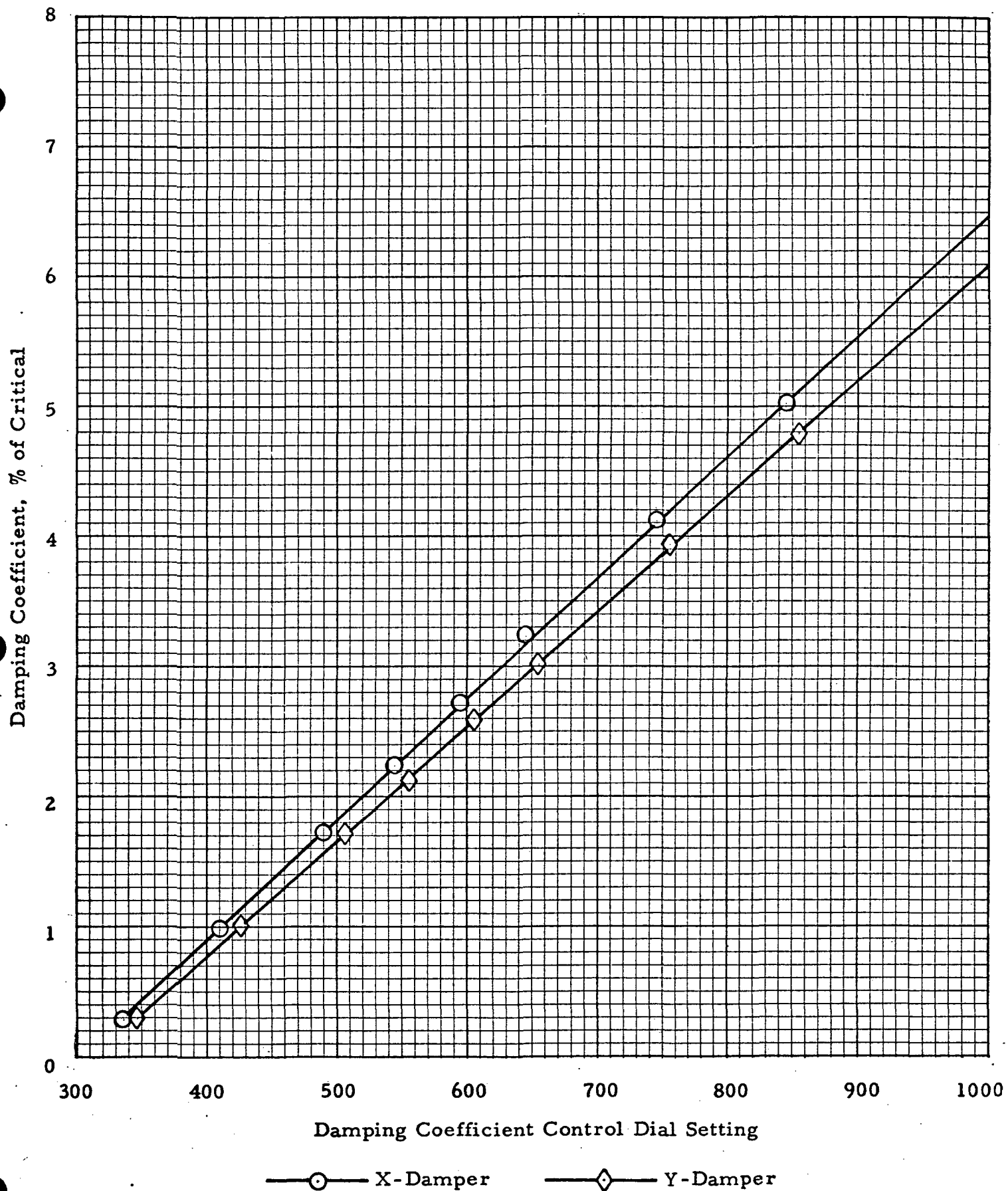


Fig 28 DCC Dial Calibration for Model Configuration 3



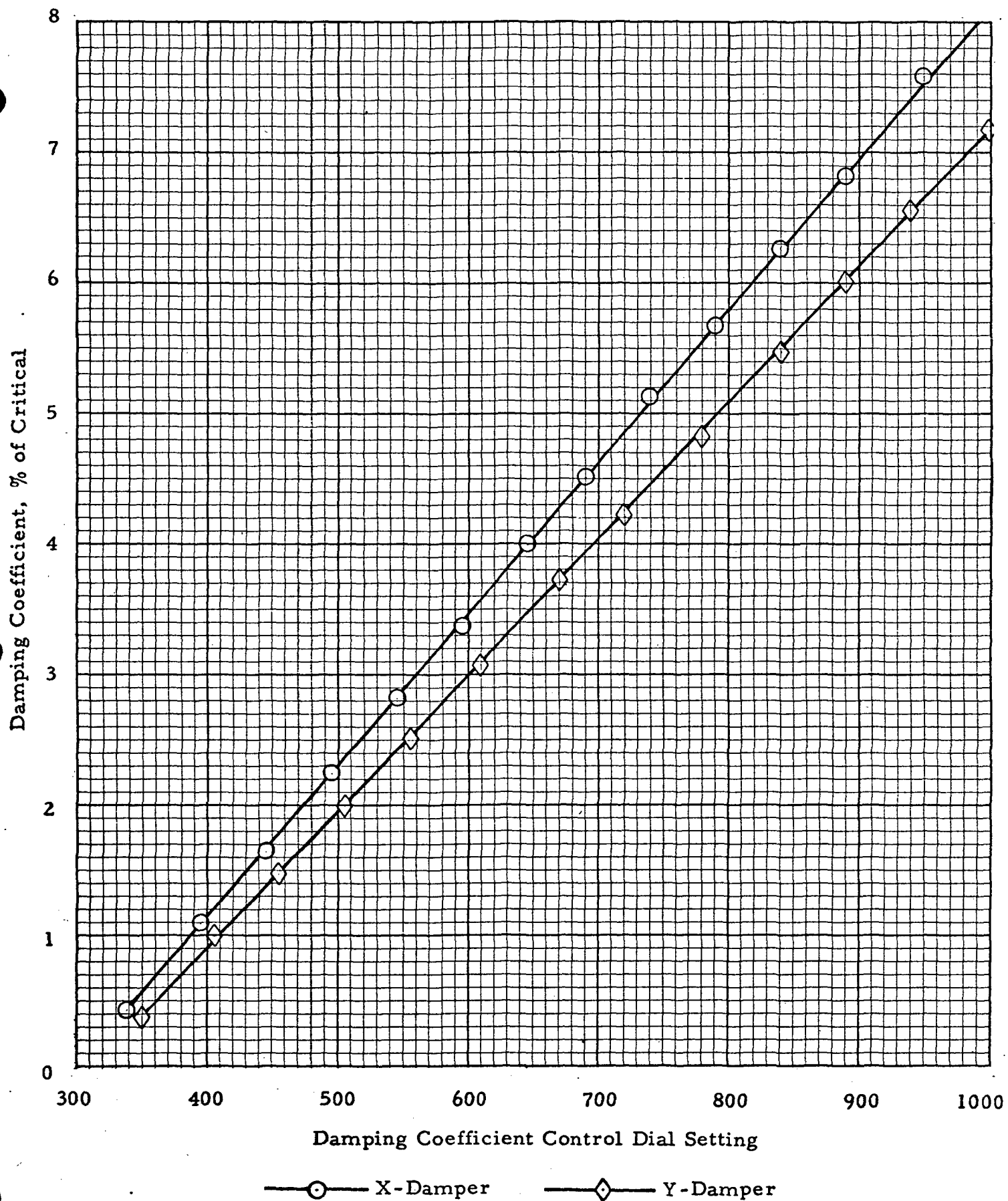


Fig 29 DCC Dial Calibration for Model Configuration 4

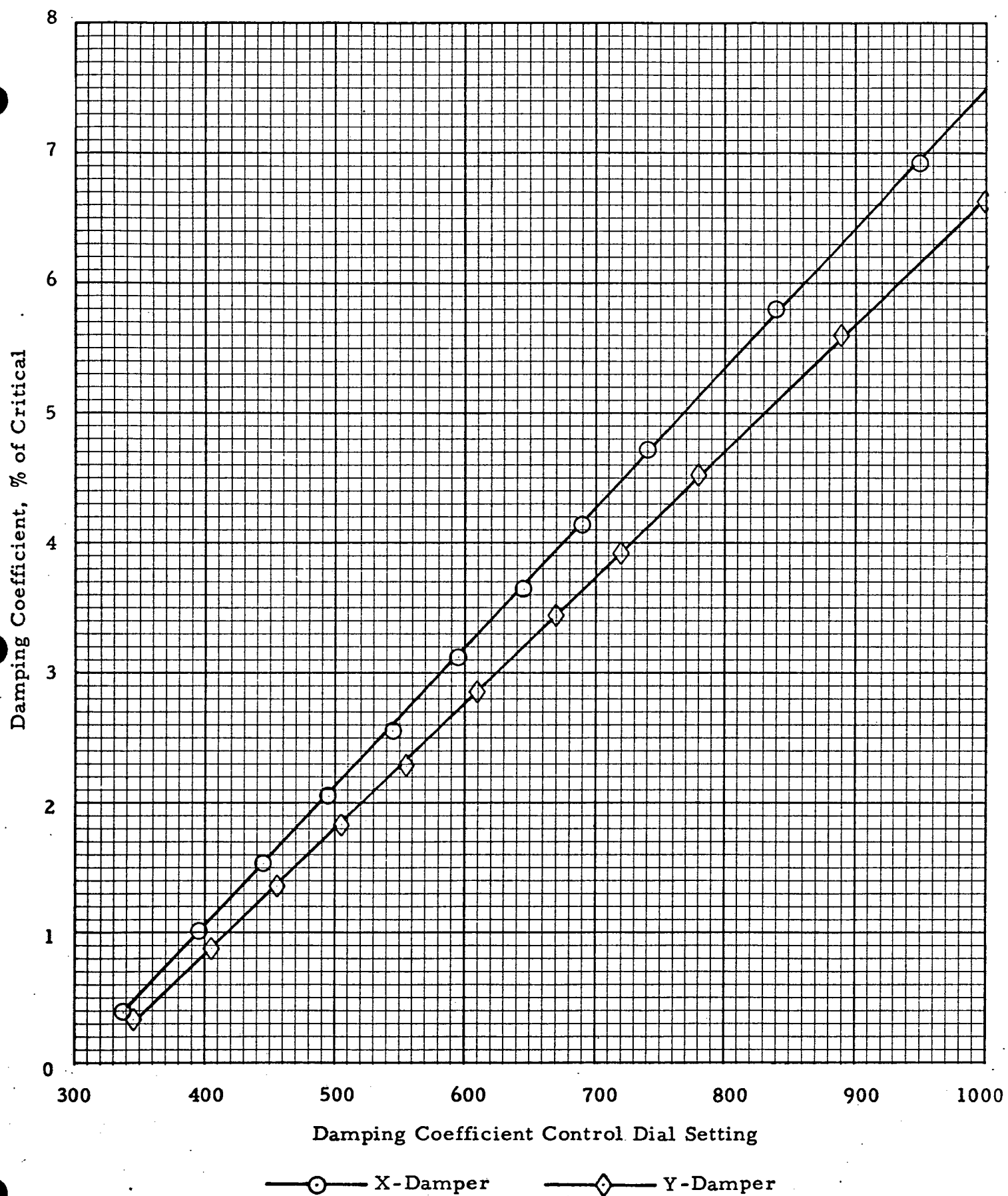


Fig 30 DCC Dial Calibration for Model Configuration 5

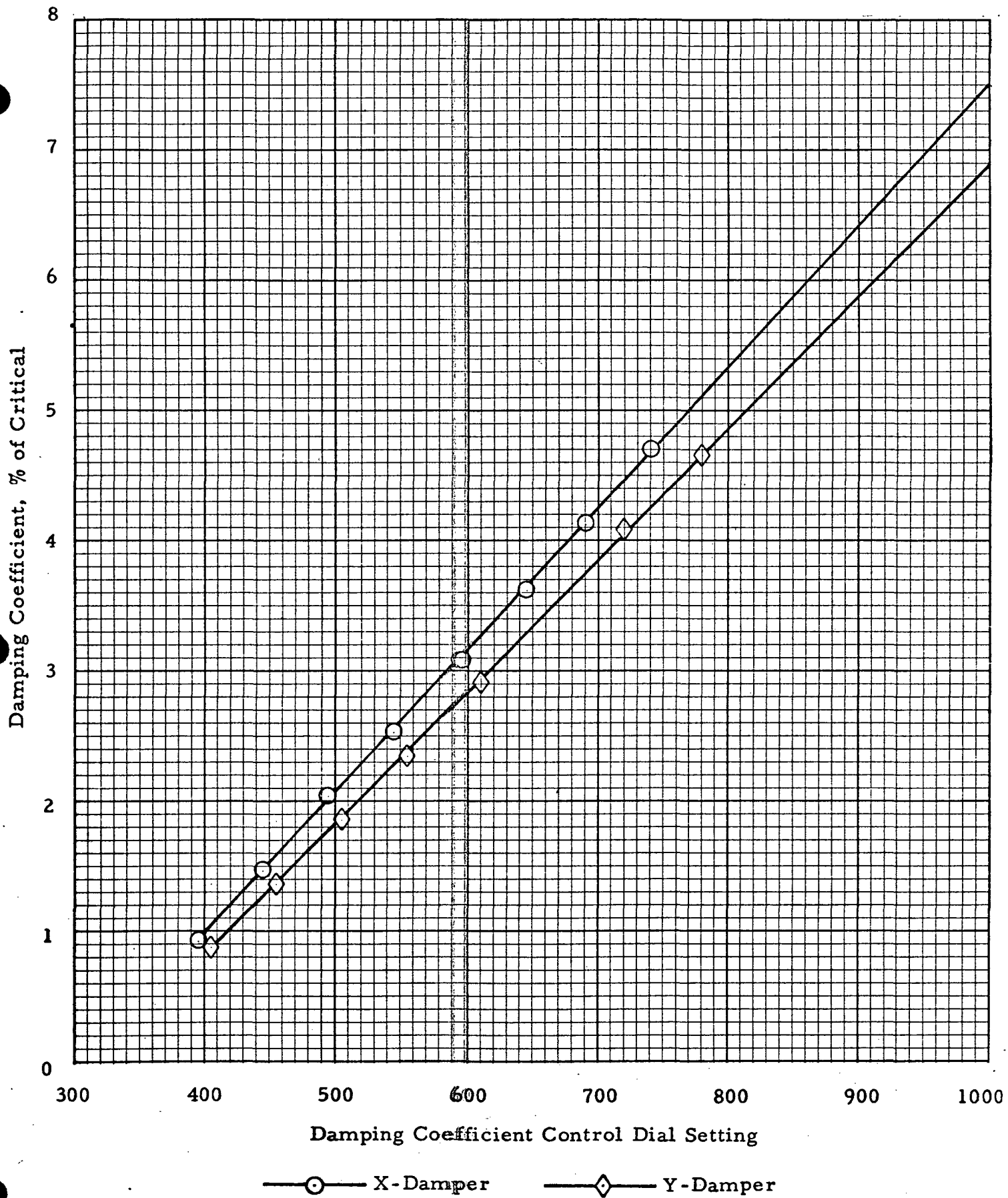


Fig 31 DCC Dial Calibration for Model Configuration 6

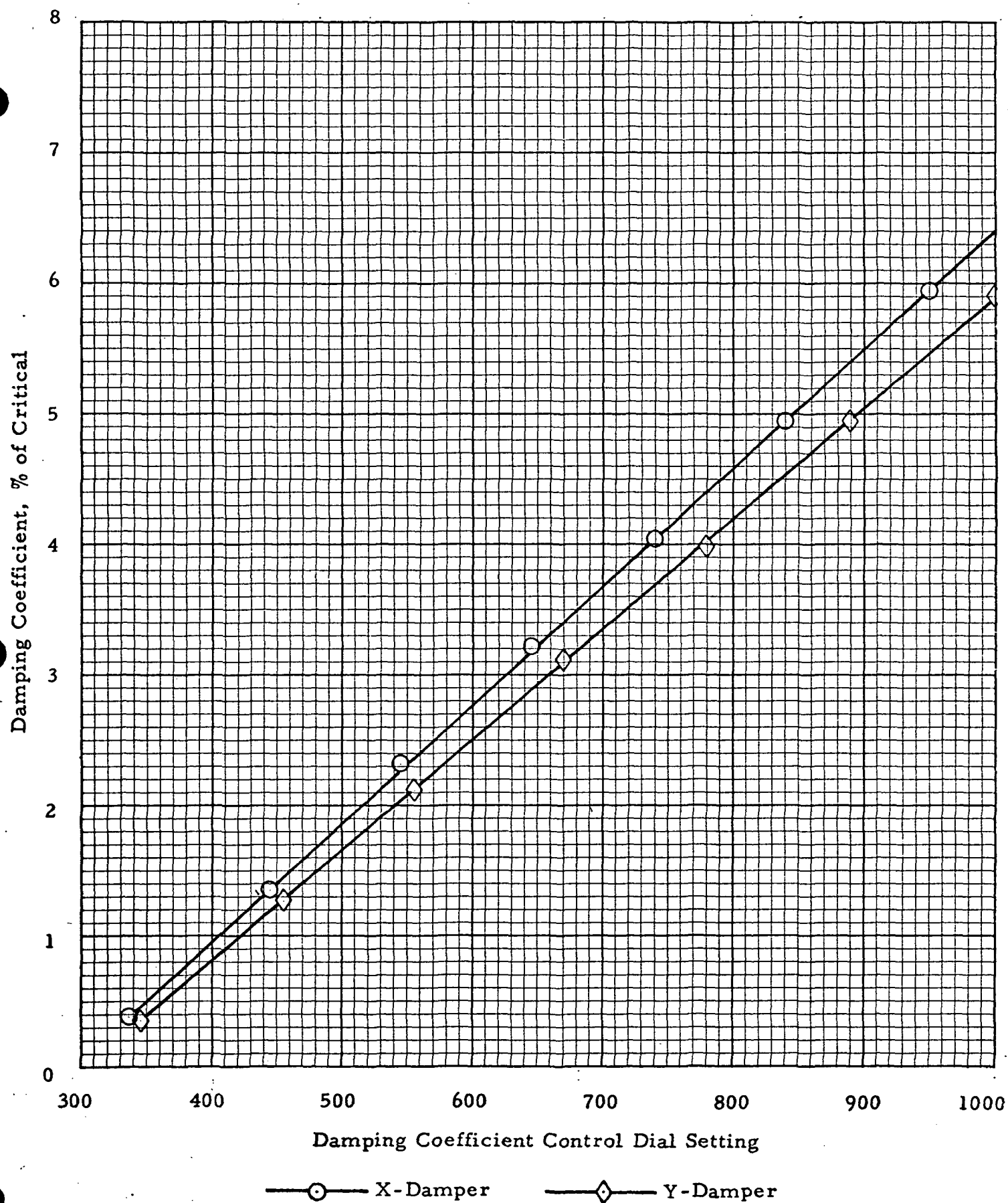


Fig 32 DCC Dial Calibration for Model Configuration 7

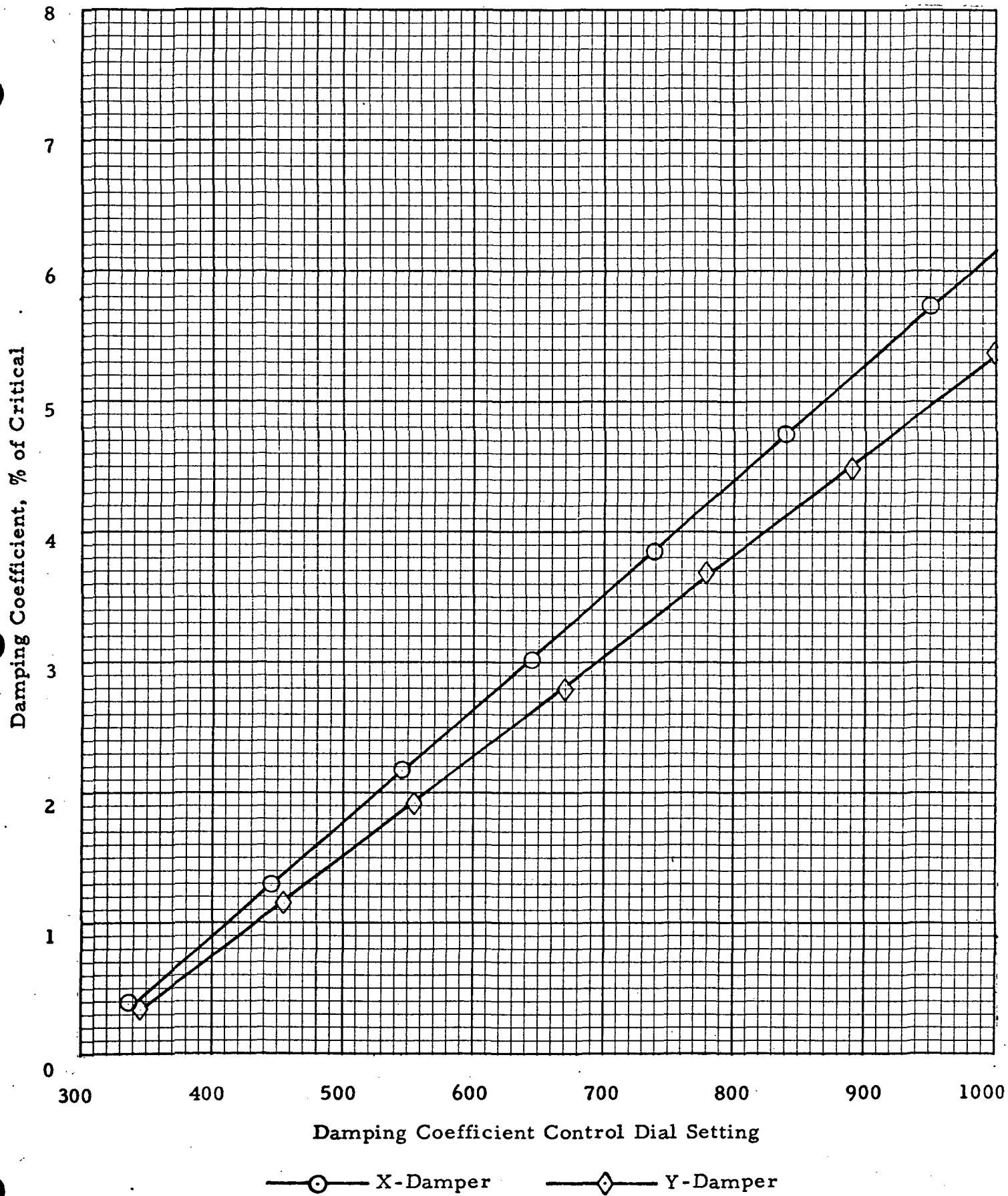


Fig 33 DCC Dial Calibration for Model Configuration 8

the observed linearity between the damping factor and the DCC dial setting, a very simple general relationship may be used to express all results of the entire calibration test series:

$$\Delta \zeta_a = K_a \Delta$$

where the subscript identifies the model configuration and is the incremental change in damping due to an increment of the DCC dial setting  $\Delta$ . The incremental DCC dial settings required to change damping by 1.0% are listed in Table V under the column heading  $\Delta_a$ .

Table V Summary of AAD Calibration Results

Model Configuration			DCC-X	DCC-Y
Scaling		Fuel Condition	$\Delta_a$	$\Delta_a$
1	Primary	Empty	103.0	94.2
2	Primary	Intermediate	116.4	113.8
3	Primary	Fully Fueled	114.4	104.4
4	60 Knots	Empty	96.2	86.2
5	60 Knots	Intermediate	103.4	94.0
6	60 Knots	Fully Fueled	99.4	91.0
7	70 Knots	Empty	118.8	110.0
8	70 Knots	Intermediate	115.2	128.0

The shaker current-to-force conversion factor,  $k$ , can be computed from damping calibration data by the expression

$$k = C/k_1 = \zeta C_{cr}/k_1 = 2\zeta m\omega_o/k_1$$

where  $\zeta$  is the damping added by the AAD, at a given DCC dial setting,  $c_{cr}$ , the critical damping coefficient of the model configuration, and  $k_1$  (in amps/in/sec), the overall sensitivity of the sensor and electronics at the same DCC dial setting.

Using all available damping calibration data,  $k$  was found to be 0.75 lbs/amp for the AAD shakers.



## Section 9

## WIND TUNNEL TEST PROGRAM

9.1 Program Description

The Saturn IB/LC-39 GWL Test Program was conducted by S&E-AERO-AUU, MSFC at NASA/LaRC's 16-foot Transonic Dynamics Tunnel during the period 14 October through 13 November 1971. ADRC supported this test program in the areas of AAD calibration and operations and model dynamic calibrations in the wind tunnel. Materials in this report pertain only to these areas of support.

Five model configurations were tested. They are listed below with first mode natural frequencies and damping values in the wind tunnel test (WTT) conditions.

WTT Config. No.	Description	Natural Freq.(1),Hz	Damping %
1	60-Knot Empty	19.3	1, 3, 5 <sup>(2)</sup>
2	60-Knot Intermediate	16.6	1, 2, 3, 4, 5 <sup>(2)</sup>
3	60-Knot Fully Fueled	10.9	1
4	Primary Fully Fueled	14.65	1
5	Primary Empty	23.97	1

(1) In the X-plane

(2) Not for all azimuths

Some of the listed natural frequencies differ from those obtained during calibration tests conducted at MSFC (Table IV). The differences represent model-scale changes corresponding to changes in predicted fullscale dynamic characteristics between the two test dates.

## 9.2 AAD Calibration

Final AAD calibration tests were conducted in WTT conditions for all WTT configurations and for all azimuths. Several difficulties occurred during these calibration tests which had not occurred previously.

The first and most obvious difficulty was that it was considerably more difficult to obtain repeatable calibrations, be it a model dynamic characteristic or a damper system gain setting. In the wind tunnel calibration test setup, the natural frequencies of all configurations varied with response amplitudes, sometimes by as much as one to two percent. As there was not sufficient time to define the nonlinearities, it was only possible to seek consistency by testing and measuring all properties at consistent response amplitudes.

Since the model and the damper by themselves were known to be linear, the wind tunnel floor structure to which the model was mounted must have been the source of nonlinearity. Coupling was particularly strong for WTT Configuration 5 with a natural frequency of 24.97 Hz. For this configuration, free vibration decay traces exhibited significant "beating" of the two fundamental modes of vibration. Damping calibrations were impossible except for azimuths of 0°, 90°, 180°, and 270°.

A second problem developed when damping above 1% was attempted for WTT configurations 3 and 4. The damper mass had a self-induced oscillation at its natural frequency of 1 Hz. The amplitude of this oscillation became extremely large. It was later concluded that this oscillation was due to a combination of the near-zero damping of this mode of vibration and a 1 Hz excitation of the control system from a yet unconfirmed noise source. The primary suspect was the electronic counter in the system and the noise was picked up through ground loops. The counter input and output are referenced to ground.

Damping Coefficient Control Dial settings used for wind tunnel tests are listed in Tables VI through X.

### 9.3 Miscellaneous Notes

(1) Forced air or Freon cooling of the AAD was employed during calibration and wind tunnel tests. The cooling medium was introduced via a 1/4" tubing. The supply pressure was 12-14 psi. A thermocouple was used to monitor the temperature at the ring structure of the Damper Support Assembly.

Thermal equilibrium (steady-state) was observed when the ring temperature reached 110°F. Under this condition, the field coil resistance was 15.5  $\Omega$  for each shaker and the power supply voltage required to maintain a 3 amp field coil current was 93 volts.

TABLE VI

## Damper Coefficient Control Dial Settings for WTT Configuration 1

Azimuth Degrees	Damping Coefficient Control Dial Settings					
	5%		3%		1%	
	X	Y	X	Y	X	Y
0	706*	775	543	579	380	383
15	678*	778	516	577	355	376
30	682*	775	529	575	370	375
45	680*	769	519	568	367	369
60	677*	760	512	565	349	369
75	703*	770	540	569	376	370
90	705	745	530	567	380	370
105	700*	757	531	565	371	365
120	695*	769	530	564	363	360
135	694	769	530	567	363	366
150	693*	770	530	570	369	372
165	697*	770	535	570	374	370
180	701*	770	541	570	380	368
195	699*	767	536	567	372	368
210	697*	765	532	565	365	367
225	688*	757	513	557	349.5	383
240	679*	750	495	550	349.5	383
255	680*	753	512	558	349.5	383
270	682	756	529	567	375	359
285	688	756	531	562	374	359
300	694	755	533	557	373	359
315	683	757	527	557	373	356
330	672	759	521	557	372	354
345	689	767	532	568	376	369

\* Power amplifier input signal clipping was present due to an error introduced during last-minute modification of control circuit (Y-Channel) to accommodate a substitute power amplifier after the original unit failed. This error was corrected after the  $\phi = 270^\circ$  test on October 29, 1971. A method to correct WTT data was later developed and corrections were forwarded to S&E-AERO-AUU.

TABLE VII

## Damper Coefficient Control Dial Settings for WTT Config 2

Azimuth Degrees	Damper Coefficient Control Dial Settings							
	5%		4%		2%		1%	
	X	Y	X	Y	X	Y	X	Y
0	735	825			480	502	390	390
15							390	390
30	735	825			480	500	390	390
45							390	390
60	735	825			480	500	390	390
75							390	390
90	735	825			480	500	390	390
105							390	390
120	735	825			480	500	390	390
135							390	390
150					480	500	390	390
165							390	390
180					480	500	390	390
195							390	390
210	735	825			480	500	390	390
225							390	390
240	735	825			480	500	390	390
255							390	390
270			650	720	480	500	390	390
285							390	390
300					480	500	390	390
315							390	390
330					480	500	390	390
345							390	390

TABLE VIII

Damping Coefficient Control Dial Setting for WTT Config. 3

Azimuth Degrees	1%	
	X	Y
0	346	400
15	439	370
30	433	339
45	408	375
60	385	416
75	379	432
90	374	453
105	383	430
120	394	412
135	410	388
150	429	370
165	428	380
180	448	390
210	447	338
225	418	365
240	395	395
255	380	425
270	369	456
285	375	442
300	388	432
315	405	390
330	429	356

TABLE IX

Damping Coefficient Control Dial Setting for WTT Config. 4

Azimuth Degrees	1 %	
	X	Y
0	435	370
30	425	404
60	395	465
90	385	480
105	413	474
120	446	468
150	367	339
225	385	415
270	345	462
345	418	354

TABLE X

Damping Coefficient Control Dial Setting for WTT Config. 5

Azimuth Degrees	1 %	
	X	Y
15	361	339
30	358	339
60	330	360
90	282	370
100	293	369
105	299	368
110	310	365
120	330	360
150	367	314
210	367	314
353	374	265
0	374	254



(2) The time required to run an AAD calibration test (one model configuration; 3 damping values for 24 azimuths) was approximately six hours when there were no operational difficulties. If the test data were reduced by manually transferring decay traces of free vibrations from oscillograph records to semilog graph papers, approximately 24 man-hours would be required. The elapsed time is almost inversely proportional to the total number of people working on the data reduction.

(3) The maximum shaker drive current was found to be approximately 10 amps (rms), for WTT Configuration 2 at  $0^\circ$  and 5% damping. The wind was 55 knots, full-scale. The corresponding shaker force was 7.5 lbs. (rms). The total unsteady aerodynamic force component proportional to model velocity was approximately 10% greater on account of the inherent structural damping of the model.

Based on visual observations of oscilloscope displays, the response under this condition could be characterized as a narrow band random process. The response envelope as a function of time was judged to be consistent with the 5% damping and a wide-band excitation. The response amplitude increased gradually with the wind velocity.

(4) On account of various wind tunnel operational constraints, it was observed that once the wind tunnel is sealed, there was very little actual time available to conduct damping or model calibration tests. Some of the restrictions are:

- o Aerodynamic noise during pump-up or pump-down. This noise introduced sufficient unwanted vibrations in the model to prevent calibration.

- o The turn-table usually could not be operated during pump-up or pump-down because the pressure supply to raise the turn-table was almost always of the wrong kind of gas medium. Consequently, it was impractical to conduct extensive calibrations during such transition periods if rotation of the model was required.

## Section 10

## CONCLUSIONS

The AAD System was developed for ground wind aero-elastic model tests. In the present state of development, the electromechanical components (the two-directional force generators and the Damper Support Assembly) performed exceedingly well. The only drawback is that the heat generated by the electromagnets must be removed by forced air cooling.

Functionally, the electronics of the Damper Control subsystem performed satisfactorily. The exception was that of voltage clipping at high gain and high model response conditions due to a wiring error committed during field modification to accommodate a different power amplifier. This problem could be and was eliminated.

Operationally, a significant system improvement is realizable if patching between various pieces of test and control equipment were minimized. (Through the use of more hard-wired circuits and selection switches.)

The major difficulty experienced during the test program was the malfunctioning of the power amplifiers. However, two loan units of the same make performed consistently and reliably throughout the entire test series, indicating that the problems were unique to the specific units and that they could be overcome.

Automatic power amplifier shutdown to protect the amplifier and the load (the shakers) occurred during high damping, high

load operations. This problem can be eliminated by better selection of operating gains of various components.

At high system gain, the net damping for the 1-Hz oscillation of the suspended shaker mass approaches zero. The two contributing causes are: (a) The structural damping of the AAD suspension system is extremely low and (b) The damping added to the model-shaker system is negative in this 1-Hz mode of vibration.\* The problem can be eliminated by increasing the structural damping and by using the relative velocity for control.

\* If absolute velocity of the model is used to drive the power amplifiers.

## Section 11

## RECOMMENDATIONS

11.1 Force Generator Design

Mechanically and electromagnetically, the AAD Force Generators performed exceedingly well. Design modifications are unnecessary.

The heat generated in the electromagnets may, however, be objectionable in future applications. Consequently, the use of permanent magnets (PM's) should be considered. Since most of the force generator design principles are already verified and checked out, a direct substitution of the present electromagnets with PM's should not be too difficult to design. With the exception of the field coils, the core pieces and the top plates, all existing parts of the assembly can be retained. The costs for the new design will, therefore, be a minimum. An added advantage of a PM design is that the 3-amp power supply and the cable can be eliminated, hence eliminating the probability of failure of these components during WTT.

The envelope dimensions of the Force Generator Assembly and the masses of both the armatures and the magnets may be reduced by approximately 50%, if the design is modified to use one common magnetic gap for both armatures. A limited design study in this direction is also recommended, since it will lead to a smaller and lighter system which will undoubtedly be more versatile in future applications.

11.2 Control Principle

The limiting factor for high damping for the present system

was the amount of negative damping being introduced into the 1-Hz vibration mode of the softly suspended magnet assembly. The negative damping characteristic stems from the fact that the absolute velocity of the model was used to operate the damper. The problem can be eliminated by using the relative velocity between the model and the suspended mass as the control signal. In that case, the damper will add positive damping to all modes of vibration, including the 1-Hz mode.

Relative velocity signals may be obtained either by additional accelerometer channels to sense the motion of the suspended mass, or by a moderate amount of positive power amplifier current feedback. The latter approach is exceptionally attractive as it will require no transducer for damper control purposes. Instead, the back emf generated in the armature coils is used. Further investigation in this direction should be fruitful.

### 11.3 Control System Hardware

The reliability of the entire AAD system may be improved by increased use of "hardwiring" and switches which would minimize external patching from component to component. This approach is deemed possible as functional and operational requirements of the system are now thoroughly established after the extensive usage of the system in the two calibration test series and in the WTT program.

Experiences have also indicated that the most time consuming part of electronics trouble-shooting was associated with power amplifier malfunctioning. Even with spare, replacement power amplifiers standing by, a considerable amount of time (four to eight hours) was still required to make the change over. Engineering

work to develop an interface system to allow plug-to-plug interchangeability between the primary unit and the backup unit is, therefore, strongly recommended.

#### 11.4 Full-Power Checkout

A full-power check of the AAD system in the laboratory, using an additional shaker to supply the excitation is recommended to identify potential areas of vulnerability during wind tunnel applications so that corrective procedures may be adopted.

#### 11.5 Model and Damper Calibrations

Considerable difficulties were experienced during model and damper checkout on account of modal coupling. The time and effort required to calibrate the dampers were inversely dependent on how well the modes were isolated by the test engineer. Experience showed that after a mode has been isolated, damping calibrations can be obtained in no more time than required to go through the motions of performing the tests. On the other hand, when a mode has not been isolated, a conclusive damper calibration was nearly impossible to obtain, no matter how many times the tests were repeated. In future applications, such as the Space Shuttle program, modal isolation must be achieved before damper calibrations are permitted to begin. This is recommended to save time and to ensure unambiguous calibration and unambiguous wind tunnel test results.

The method to isolate principal modes with closely spaced natural frequencies has been the subject of many investigations



dating back to 1948. The current consensus is for employment of numerous shakers and iterative procedures to simulate modal force distributions. Once this distribution is determined, the corresponding principal mode is, of course, isolated as the forces are arranged and proportioned in a manner that they are incapable of exciting any other mode on account of orthogonality among the modes. Modal properties can then be measured with standard methods. A two- or three-shaker approach is recommended.

In order to speed up damping data reduction, the analog method shown in Figure 32 is recommended.

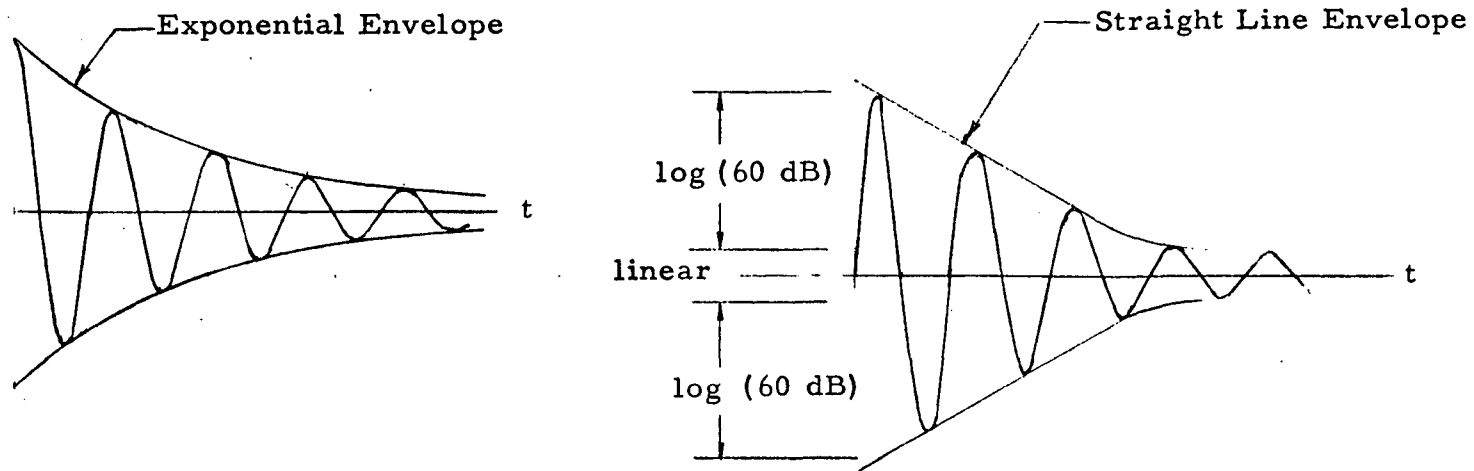
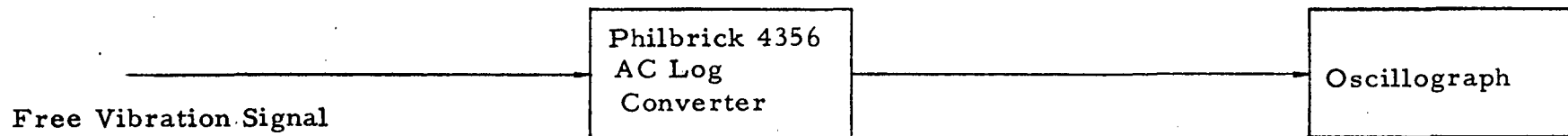


Fig 34 Analog Damping Measuring Approach

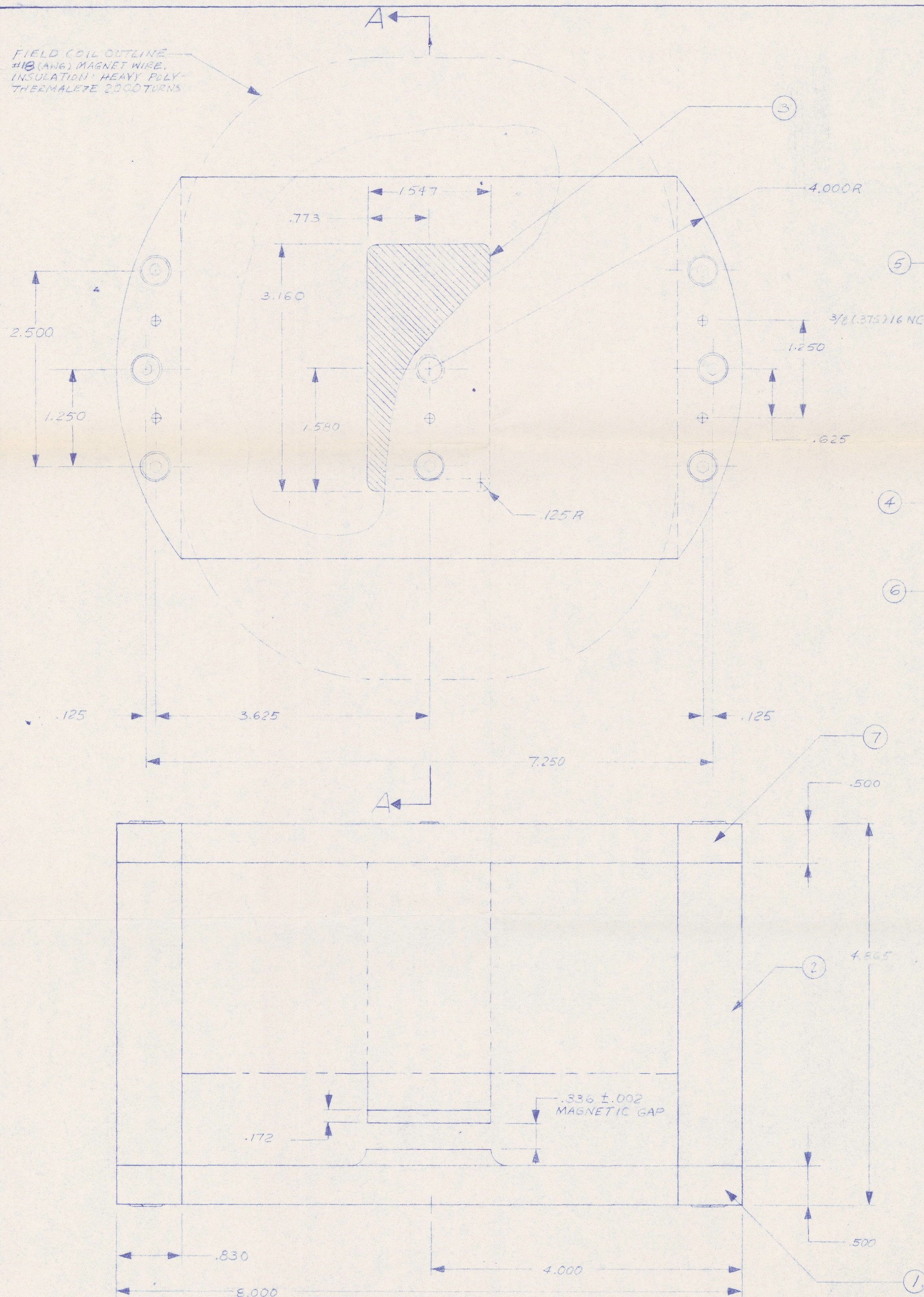
## REFERENCES

- 1: NASA MSFC S&E-AERO-DD-36-70, subject: "Skylab 2 structural data for ground wind load studies". Addressed to R. W. Walker, S&E-AERO-AUE, from Structural Dynamics Section, S&E-AERO-DDS, dated Nov. 25, 1970.
- 2: "Preliminary Analysis of the Ground Wind Effects on Different Saturn IB Configurations Based on Wind Tunnel Data", Contract NAS8-20082, Sub-Contract No. 5-09287, LMSC/HREC A711294, June, 1965.
- 3: Allegheny Ludlum Steel Corp., Blue Sheet, Relay Steels



FIELD COIL OUTLINE  
#18 (AWG) MAGNET WIRE,  
INSULATION: HEAVY POLY-  
THERMALEZE 2000 TURNS

NOTE: ALL (EXCEPT MAGNETIC GAP)  
DIMENSIONS ARE FOR REFERENCE  
ONLY.



VIEW A-A

QTY	DESCRIPTION	MATERIAL	DWG NO.
1	UPPER PLATE (UPPER SHAKER) OR	RELAY 5 SS	20014 B
1	BOTTOM PLATE (LOWER SHAKER)		
1	FIELD COIL - #18 (AWG) MAG WIRE 2000 TURNS		
10	1/8" DIA. ROLL PINS	STAINLESS STEEL	
14	1/4 (250) 20 NC x 75 LG ALLEN SOCKET HD CAPSCRS	STAINLESS STEEL	
1	CORE PIPE	RELAY 5 SS	20016 B
2	SHAKER SIDE PIECES	RELAY 5 SS	20015 B
1	BOTTOM PLATE (UPPER SHAKER) OR	RELAY 5 SS	20013 CA-1
1	UPPER PLATE (LOWER SHAKER)	RELAY 5 SS	20013 CA-2

APPLIED DYNAMICS RESEARCH CORP.  
3313 MEMORIAL PARKWAY, S.W.  
HUNTSVILLE, ALA 35801

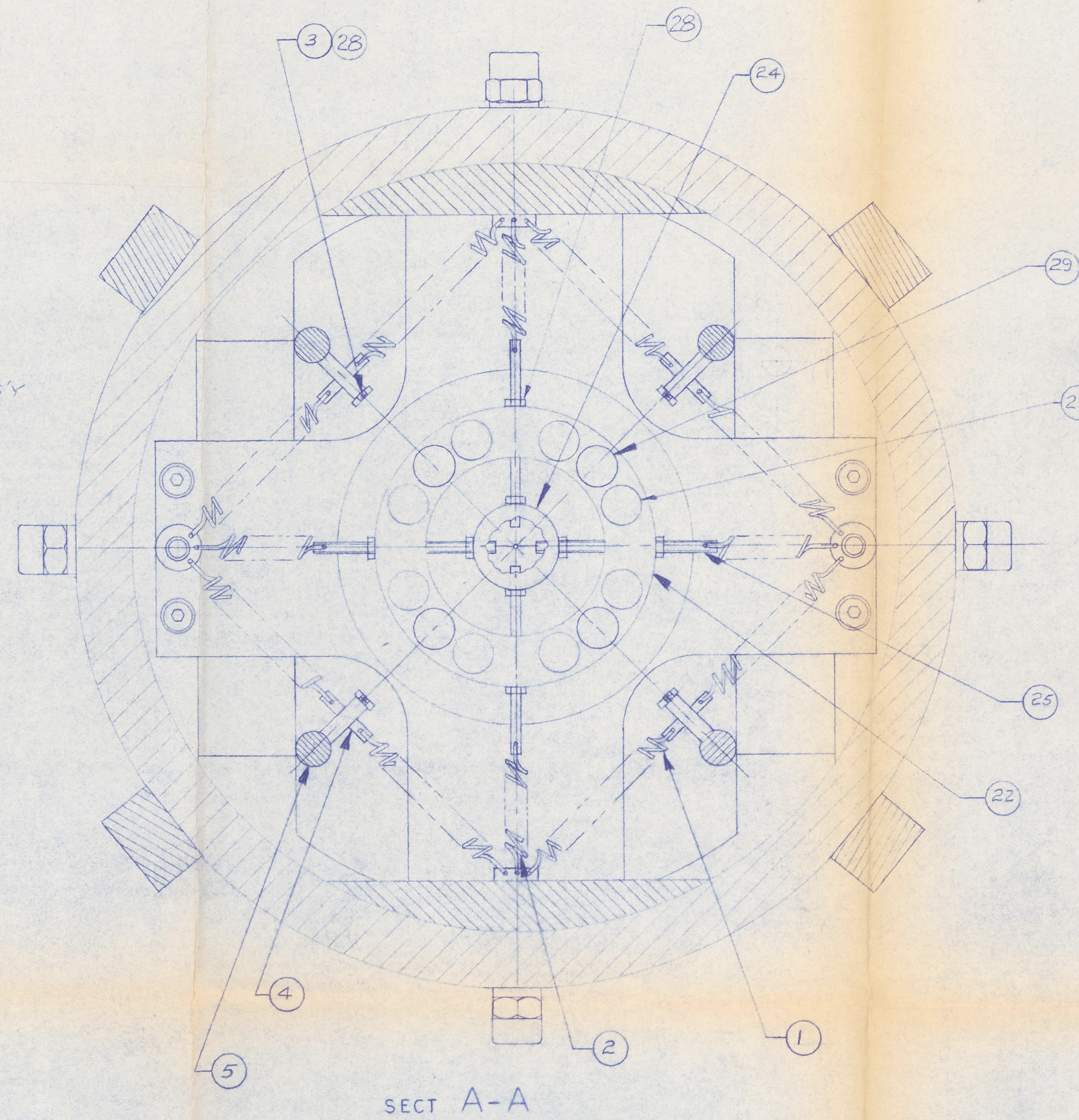
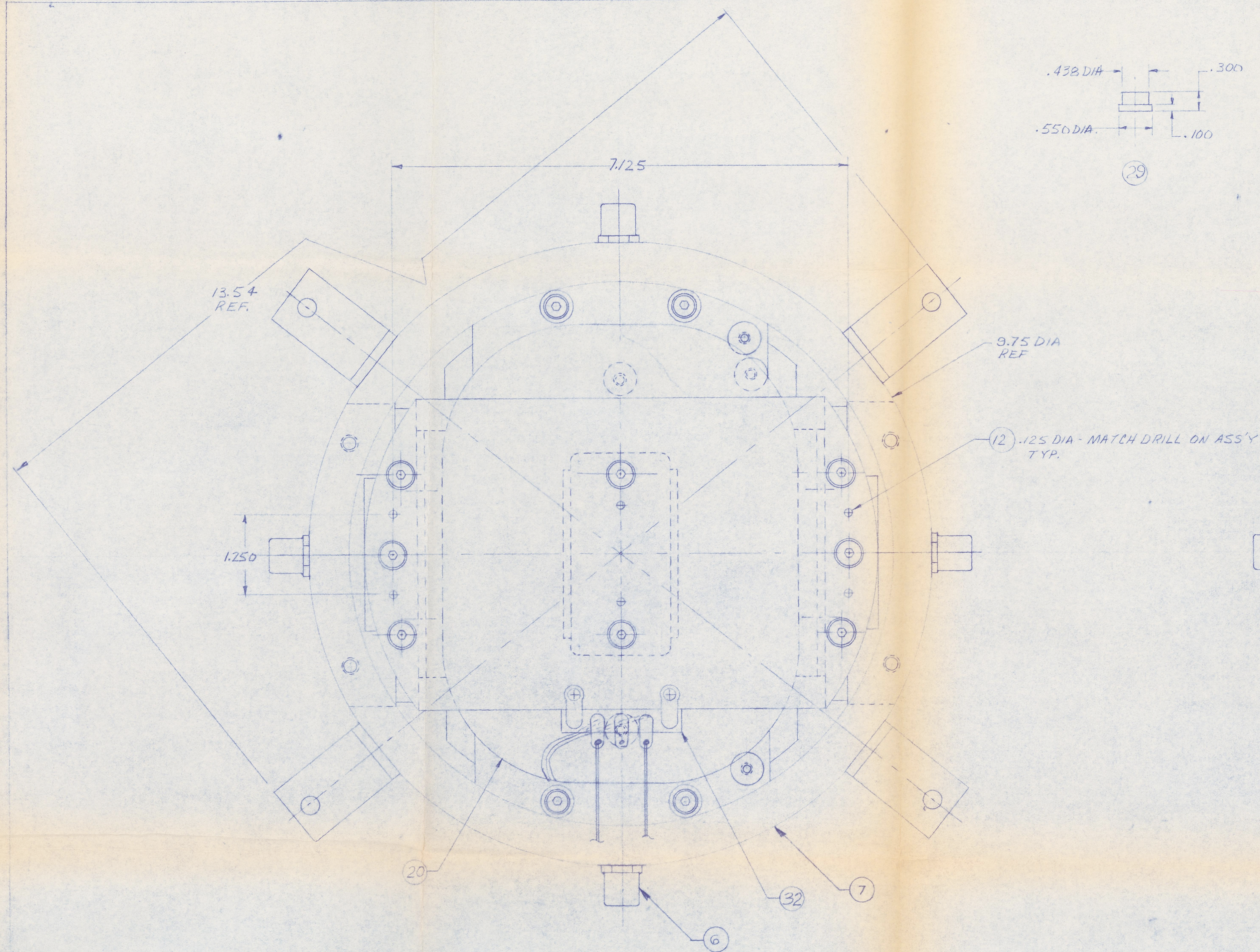
CHK	DATE
SDR	1-14-72
REVE	3/25/71

SCALE = 1/1

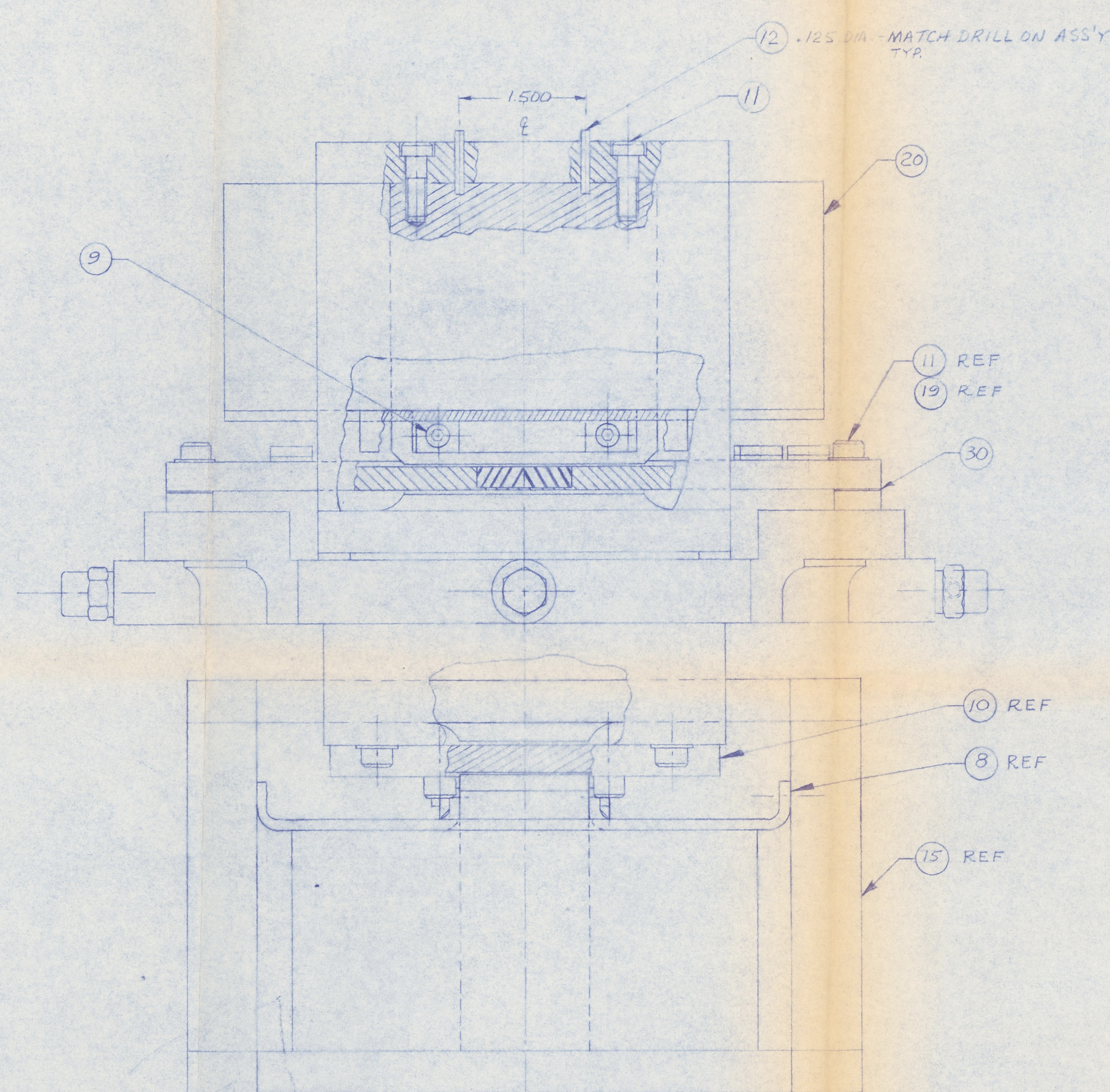
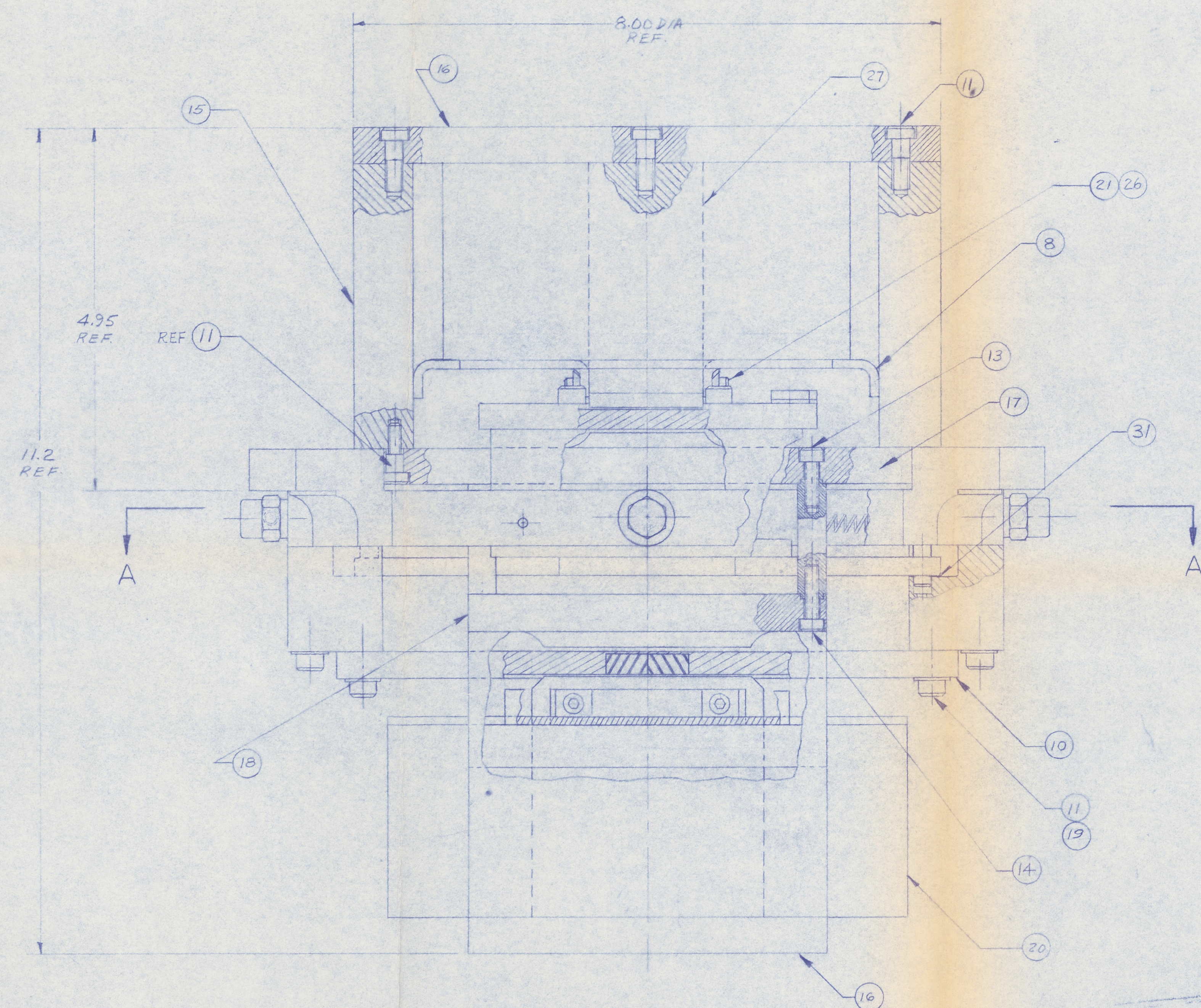
ELECTROMAGNET  
CONFIGURATION

DWG NO 20026CA-





- NOTES:
1. EACH FIELD COIL TO HAVE 2000 TURNS OF #18 BLDEN HEAVY POLYTHANAL LEZE MAGNET WIRE VACUUM IMPREGNATED WITH "ISONEL" VARNISH.
  2. REMOVE AND USE 8 BALLS FROM ANDREWS BEARING CO. BEARING #910



32	2	TERMINAL STRIP H. SMITH MODEL 855		
31	4	SHIM .017 X .25 ID X .50 O.D.	BRASS	-5
30	4	SHIM .020 X .25 ID X .50 O.D.	BRASS	-3
29	4	BRG. RETAINER SUPPORT	TEFLONITE	-1
28	12	4-40 NUT STEEL CAP PLATED		
27	2	CORE PIECE		20016B
26	16	WASHER - SPECIAL 3/16" - 250MM LLS ALUM 6061 T6		
25	4	PIN		20024A
24	1	PIN HOLDER		20025A
23	8	BALL BEARING	STEEL	2
22	1	BEARING RETAINER		20023A
21	8	4-40 UNC X 75 LG. 500 HR. CAP. SCR.	STAINLESS STEEL	
20	2	FIELD COIL		1
19	8	1/4 LIGHT PLAIN WASHER	STAINLESS STEEL	
18	1	UPPER PLATE LOWER SHAKER		20013CA-2
17	1	BOTTOM PLATE, UPPER SHAKER		20013CA-1
16	2	UPPER PLATE (UPPER SHAKER) OR BOTTOM PLATE (LOWER SHAKER)		20014B
15	4	SHAKER SIDE PIECE		20015B
14	4	1/4 (250) 32 NF X 75 LG. SOC. NO. CAP. SCR.	STAINLESS STEEL	
13	4	1/4 (250) 32 NF X 75 LG. SOC. NO. CAP. SCR.	STAINLESS STEEL	
12	20	1/8 DIA ROLL PIN 750 LONG	STAINLESS STEEL	
11	40	1/4 (250) 20-NC X 75 LG. SOC. NO. CAP. SCR.	STAINLESS STEEL	
10	2	FORCE COIL ASSEMBLY		20018C
9	8	#4 (112) 40-NC X 250 LG. FLT. SOC. NO. CAP. SCR.	STAINLESS STEEL	
8	2	FIELD COIL RETAINER		20020A
7	1	DAMPER SUPPORT ASSEMBLY		20009DA
6	4	MB ELECTRONICS ACCELEROMETER		TYPE 303
5	4	SHAKER SPACER DETAILS		20012BA
4	4	PIN SLIDING		20017A
3	4	#4 (112) 40-NC X 250 LG. SET SCR	STAINLESS STEEL	
2	4	LEE SPRING CO. EXTENSION SPRING	MUSIC WIRE	LE-026C-1
1	8	LEE SPRING CO. EXTENSION SPRING	MUSIC WIRE	LE-026C-4
FIND NO.	QTY	DESCRIPTION	MATERIAL	PART NO. OR DRAWING NO.

APPLIED DYNAMICS RESEARCH CORP.  
3313 MEMORIAL PARKWAY S.W.  
HUNTSVILLE, ALABAMA 35801

DATE 1/12/71  
APP. G.S. Chang  
ENG. L.R.  
CHK. L.R.  
DES. L.R.  
DR. L.R.

SCALE = 1/1

DAMPER  
ASSEMBLY

DWG. NO. 20021EA